University of Stavanger

Faculty of Science and Technology

MASTER'S THESIS

Study program/ Specialization: Masters in Construction and Materials/ Offshore Constructions	Spring semester, 2015 Open
Writer: Kåre Edvardsen	…… (Writer's signature)
Faculty supervisor: Sverre K. Haver, University of Stavanger External supervisor(s):	
Thesis title: Forces on simplified offshore structures according to different wave models.	
Credits (ECTS): 30	
Key words: NORSOK N-003, Edition 2 and 3 First and second order wave theory Stokes 5th order wave Comparison Metocean contour methods 100-year wave Regular waves Irregular waves Kinematics Morison equation	Pages: 125 + Front page: 1 + Appendix: 2 Stavanger, 15.06.2015

ACKNOWLEDGEMENTS

I would like to express my greatest gratitude to my advisor, Sverre Kristian Haver for the opportunity as well as the guidance and support provided during the course of my study at the University of Stavanger. A special thanks to Sverre Kristian Haver again, and Professor Ove Tobias Gudmestad, in the help of defining my thesis. This would not have been possible without you. I would also like to thank Ove Mikkelsen, for his help with Matlab. You have been very helpful throughout my studies at the University of Stavanger. A great thanks to all teachers that has not been mentioned here, but has helped me throughout my five-year studies.

Finally, and most importantly, I would like to thank my friends and classmates for their support and encouragement throughout this whole process. Also for all the discussing around my thesis.

ABSTRACT

The reason for creating this thesis was because of the new and revised version of NORSOK N-003 standard. Therefore a comparison between the old and the revised version of NORSOK N-003 standard has been performed. This thesis have been divided in to three main parts. The first part describe how to estimate the 10^{-2} annual probability crest height, $c_{0.01}$ and wave height $h_{0.01.}$ (100-years wave) with the metocean contour lines method. Which resulted in: $h_{0.01.} = 28.61\ m$ and $c_{0.01} = 17.87\ m$ by using $h_s = 14.9m$ and $t_p = 15.8s$

The second part revolves around regular waves. A comparison between the old and new method of calculating the ULS design wave have been discussed. The old method uses a Stokes wave profile defined by the 10^{-2} annual probability wave height, $h_{0.01}$ with an unfavorable period. Where the new method uses the 10^{-2} annual probability crest height, $c_{0.01}$ with a mean wave period to define the ULS design wave. With the same defined wave profiles as the new and old recommendation, one have also compared the Stokes wave with a first order approach. By obtaining the kinematics from all approaches and compared them, one may see that a linear approach has the ability to obtain very close kinematics as the Stokes wave. This depends on the amplitude used and which approximation above mean surface level used. After words, the base shear and overturning moment where calculated by Morison equation. Those results shows that the new method using Stokes wave with $c_{0.01}$ as the amplitude, results in a larger base share and overturning moment for drag and non-dominated forces but a lower overturning moment for a mass dominated case comparing to the old method using a wave height equal to, $h_{0.01}$. The conclusion for this part is that the new N-003 standard is more efficient with time and describe the waves in a more accurate manner.

For the third and last part one have chosen to discuss irregular wave, where the old N-003 standard suggests a first order process to obtain the corresponding kinematics of a time simulation. Where the revised N-003 standard in other hand require a second order process to describe the surface process and a second order theory to obtain the kinematics of the time history. Matlab has been used to create those simulations and calculated all the data for this thesis. By comparing the two different processes, one found out that the:

- Formula used to create the first order irregular surface process follows a Rayleigh distribution for crest heights and the second order surface process follows a Weibull distribution for crest heights.
- Wheeler stretching for a first order process underestimates the kinematics, but a constant value above mean surface level is a very good approximation to a second order process using Standsbergs approached.
- First order process underestimates the crest heights but overestimates the kinematics, which achieves almost the same result as second order process.

Table of Contents

ACKNOWLEDGEMENTS 1
ABSTRACT 2
LIST OF FIGURES 5
LIST OF TABLES 11
LIST OF SYMBOLS 13
1 Introduction 15
1.1 Background of the task 15
1.2 The task itself 15
1.3 Scope of the task 17
1.4 Thesis Outline 18
2 Metocean contour method 18
2.1 Metocean 19
2.2 Wave Data 20
2.3 Worst metocean condition along the 100-year contour line 23
2.4 Extreme wave/crest height value 25
3 Kinematics of regular waves 28
3.1 Linear wave theory 29
3.1.1 Surface Profile 29
3.1.2 Laplace Equation 30
3.1.3 Dispersion Relation 32
3.1.4 Classification of water depth 34
3.1.5 Horizontal water particle velocities and accelerations 34
3.2 Linear wave approximations 35
3.2.1 Horizontal water particle velocities with half the wave height as amplitude 37
3.2.2 Horizontal water particle acceleration with half the wave height as amplitude 39
3.2.3 Horizontal water particle velocities with crest height as amplitude 41
3.2.4 Horizontal water particle acceleration with crest height as amplitude 42
3.3 Stokes 5th order program 43
3.3.1 How to use the program 44
3.3.2 Result of the program 47

3.4 Comparison between linear wave and 5th order Stokes wave....51
3.5 Loads and load effects using linear wave theory and Stokes 5th order 54
3.5.1 Morison equation....54
3.5.2 Drag and mass coefficient....57
3.5.3 Determine mass and drag coefficient used. 59
3.5.4 Load Results from Morison equation.....62
3.6 Summary for regular Waves....68
4 Kinematics of irregular waves....69
4.1 Linear approximation for irregular waves....70
4.1.1 Wave spectrum 71
4.1.2 Simulation of a 3-hours surface process.....74
4.1.3 3-hour extreme values for a generated surface process. 77
4.1.4 Bootstrapping....80
4.1.5 Linear kinematics....83
4.1.6 Verification of linear horizontal particle velocity program....88
4.1.7 Results for horizontal particle velocity compared to Stokes waves 91
4.1.8 Drag dominating forces for simulated maximum crest height compared to Stokes waves 94
4.2 Second order approximation for irregular waves 96
4.2.1 Simulation of a 20-minutes second order surface process....96
4.2.2 Second order kinematics....102
4.2.3 Results for Second order horizontal particle velocity compared to Stokes waves107
4.2.4 Verification of second order horizontal particle velocity program....110
4.2.5 Drag dominating forces for second order simulated maximum crest height, compared to Stokes waves. 113
4.3 Comparison between a 20-minutes simulated first and second order process. 115
4.4 Summary for irregular Waves....121
5 Conclusion and suggestion for further work 122
6 References 124
Appendix A. Attached Matlab and Excel files 126

LIST OF FIGURES

Figure 2.1. Statistical wave distribution of a wave spectrum with definitions. 19

Figure 2.2. Conditional characteristics for the Spectral peak period versus significant wave height with 90% confidence interval and mean value are shown for 3 hour sea state. Obtained from [6]. 21

Figure 2.3. 1, 10, 100 and 10000-year extreme contour lines in the hs – tp plane. Sea state duration 3 hours. Obtained from [6]. 22

Figure 2.4. Showing extreme wave height for an 3-hour period with six different conditions. 24

Figure 2.5. Showing extreme wave height for a 3-hour period with six different conditions zoomed inn. 25

Figure 2.6. Short-term sea state for extreme wave/crest height values. 27

Figure 3.1. Illustrating wave parameters for a surface profile. 30

Figure 3.2. Showing surface profile for t = 0s and t = 1.5s with respect to x. 36

Figure 3.3. Horizontal particle velocity with different time period and estimation methods above surface level. Where amplitude is 14.3m and Tmin = 13.64s, Tmax = 17.74s and Tmean = 15.69s. 38

Figure 3.4. Description of wave profile and orbital path of water molecules. 39

Figure 3.5. Horizontal particle acceleration with different time period. Where amplitude is 14.3m and Tmin = 13.64s, Tmax =17.74s, Tmean = 15.69s. 40

Figure 3.6. Horizontal particle velocity with crest height as amplitude (ζ0=17.81), and Tmean = 15.69s using different estimation methods above the surface level. 41

Figure 3.7. Horizontal particle acceleration with crest height as amplitude (ζ0=17.81), and Tmean = 15.69s. 42

Figure 3.8. Shows the region where each equation fits and the blue X show where our wave would be. 43

Figure 3.9. Stokes velocity plot depending on depth with varying phase angle between Crest and Trough. 100 points between Crest and Trough. (Half a wavelength). Y-axes are Z/d where d is

*depth (100m) and Z is the varying depth position. X-axes is velocity in V/sqrt(g*d), where g is gravity 9.81m/s^2. ..... 46*
*Figure 3.10. Stokes acceleration plot depending on depth with varying phase angle between Crest and Trough. 100 points between Crest and Trough. (Half a wavelength). Y-axes are Z/d where d is depth (100m) and Z is the varying depth position. X-axes is acceleration in A/sqrt(g*d), where g is gravity 9.81m/s^2. ..... 46*
Figure 3.11. Surface profile for four different waves with the use of Stokes program. 48
Figure 3.12. Horizontal particle velocity for four different waves with the use of Stokes program. 49
Figure 3.13. Horizontal particle acceleration for four different waves with the use of Stokes program. 50
Figure 3.14. Comparison of horizontal particle velocity at crest, between linear wave and fifth order stokes wave results. 51
Figure 3.15.Comparison of horizontal particle acceleration at surface level, between linear wave and fifth order stokes wave results. 53
Figure 3.16. Creation of eddy current. Where A has none, B has an increment and C has large eddy currents. 56
Figure 3.17. Wake amplification factor as function of KC-number with dotted line as CDS = 1.05 (rough surface), and solid line as CDS = 0.65 (smooth surface) 58
Figure 3.18. Mass coefficient CM as function of KC, where dotted line is rough and solid line is smooth for tubular members. 58
Figure 4.1. Creation of an irregular sea state by combining four regular waves, figure obtained from [16]. 69
Figure 4.2. Wave spectrum created from a JONSWAP spectrum. 73
Figure 4.3. Raw spectrum. (From Wijaya (2009)) obtained from [17]. 73
Figure 4.4. 3hr surface process created with a JONSWAP spectrum, where hs = 14.9m and tp = 15.8s. 75
Figure 4.5. 3hr surface process with global maxima, which is a 1000s window showing the 3-hour maximum wave. 75

Figure 4.6. 1-hour repeating surface process created with a JONSWAP spectrum, where hs = 14.9m and tp = 15.8s. 76
Figure 4.7. Global maxima versus Rayleigh distribution. 78
Figure 4.8. Extreme crest height values from 80 different 3-hour simulations compared with a Rayleigh distribution and Gumbel distribution. 79
Figure 4.9. Maximum crest height data compared to different distribution function on a Gumbel scale. 81
Figure 4.10. Parametric bootstrapping with 80 values for each samples generated from a surface process with hs = 14.9m and tp = 15.8s. 82
Figure 4.11. 200-second window of a 3-hour linear surface process. Where hs = 14,9m and tp = 15.8s. 84
Figure 4.12. 200 second window of horizontal particle velocity changing with time at mean water level (z = 0m). 85
Figure 4.13. 200 second window of horizontal particle velocity changing with time at depth 30m (z = -30m). 85
Figure 4.14. 400 horizontal particle velocity profiles created from a 200-second surface process with time step 0.5s. 86
Figure 4.15. Horizontal particle velocity profiles for the largest crest height in the time series. Where crest height = 17,23m and period = 14s. 87
Figure 4.16. Largest wave of a 3-hour linear surface process obtained from the same sea state as figure 4.11. Where hs = 14,9m and tp = 15.8s. Simulated from Matlab. 88
Figure 4.17. Largest wave of a 3-hour linear surface process obtained from the same sea state as figure 4.11. Where hs = 14,9m and tp = 15.8s. Calculated from Excel. 89
Figure 4.18. Horizontal particle velocity profiles at time 642s (under crest top) and time 641s. Where crest height = 17,23m and period =14s. Simulated from Matlab. 90
Figure 4.19. Horizontal particle velocity profiles at time 642s (under crest top) and time 641s. Where crest height = 17,23m and period =14s. Calculated from Excel. 90

Figure 4.20. Comparison between different methods to obtain the horizontal particle velocity profiles for the largest crest height in a time series. Where maximum crest height = 17,23m and period = 14s. 91
Figure 4.21. 200-second window of a 3-hour linear surface process. Where hs = 14,9m and tp = 15.8s. Maximum crest height obtained is 14,21m with a period of 12s and wave height = 24.00m.....92
Figure 4.22. Comparison between different methods to obtain the horizontal particle velocity profiles for the largest crest height in a time series. Where maximum crest height = 14,21m and period = 12s with a wave height = 24.00m. 92
Figure 4.23. 200-second window of a 3-hour linear surface process. Where hs = 14,9m and tp = 15.8s. Maximum crest height obtained is 16,11m with a period of 12s and wave height = 26.03m.....93
Figure 4.24. Comparison between different methods to obtain the horizontal particle velocity profiles for the largest crest height in a time series. Where maximum crest height = 16,11m and period = 12s with a wave height = 26.03m. 93
Figure 4.25. 20-minutes second order surface process, created from a JONSWAP spectrum. With hs = 14.9m and tp = 15.8s. 98
Figure 4.26. 20-minutes second order surface process showing global peaks. Created from a JONSWAP spectrum. With hs = 14.9m and tp = 15.8s.....98
Figure 4.27. 100 seconds window, showing maximum crest height of a 20-minutes second order surface process and corrections to achieve a second order process. Created from a JONSWAP spectrum with hs = 14.9m and tp = 15.8s. 99
Figure 4.28. Global maxima versus a 2-parameter Weibull distribution (1).....101
Figure 4.29. Global maxima versus a 2-parameter Weibull distribution (2).....101
Figure 4.30. Illustrating peaks of a surface process, where green peaks are real peaks and red peaks are not valid. 102
Figure 4.31. 100-second window of a 20-minuts second order surface process. Where hs = 14,9m and tp = 15.8s. Maximum crest height obtained is 16,38m with a period of 14s and a wave height = 26.67m. 104

Figure 4.32. Horizontal particle velocity changing with time at mean surface level (z = 0m). For the largest wave in a 20-minuts surface process. 104
Figure 4.33. Horizontal particle velocity profiles for the largest wave in the 20-minutes surface process, where time step = 0.5s. 105
Figure 4.34. Horizontal particle velocity profile for the largest crest height in the time series, where crest height = 16,38m and period = 14s. Showing first order and second order correction to achieve a second order profile. 105
Figure 4.35. Horizontal particle velocity profile for the largest crest height in the time series, where crest height = 16,38m and period = 14s. With linear Taylor expansion above mean water level (z > 0). 106
Figure 4.36. Horizontal particle velocity profile for the largest crest height in the time series, where crest height = 16,38m and period = 14s. Compared to a Stokes wave. 107
Figure 4.37. 100-second window of a 20-minutes second order surface process. Where hs = 14,9m and tp = 15.8s. Maximum crest height obtained is 14,05m with a period of 15s. Where the wave height is 22.65m. 108
Figure 4.38. Horizontal particle velocity profile for the largest crest height in figure 4.37 time series, where crest height = 14,05m and period = 15s. Compared to a Stokes wave. 108
Figure 4.39. 100-second window of a 20.minutes second order surface process. Where hs = 14,9m and tp = 15.8s. Maximum crest height obtained is 17,52m with a period of 13,5s. Where the wave height is 27.19m. 109
Figure 4.40. Horizontal particle velocity profile for the largest crest height in figure 4.39 time series, where crest height = 17,52m and period = 13,5s. Compared to a Stokes wave. 109
Figure 4.41. Example 1, comparison between second order process and Stokes 5th order process. Obtained from, [21]. 110
Figure 4.42. Example 2, comparison between second order process and Stokes 5th order process. Obtained from, [21]. 111
Figure 4.43. Example 3, comparison between second order process and Stokes 5th order process. Obtained from, [21]. 111

Figure 4.44. Example 4, comparison between second order process and Stokes 5th order process. Obtained from, [21]......112
Figure 4.45. 20-minutes first and second order surface process, created from a JONSWAP spectrum. Where hs = 14.9m and tp = 15.8s......115
Figure 4.46. Global maxima from a first and second order surface process versus a Weibull and Rayleigh distribution. 116
Figure 4.47. 200-second window of a 20-minutes first and second order surface process. Where hs = 14,9m and tp = 15.8s. Maximum crest height obtained 17,52m with a period of 13,5s. 116
Figure 4.48. Horizontal particle velocity profile for the largest crest height in figure 4.47 time series, where crest height = 17,52m and period = 13,5 for second and fifth order. First order has a crest height = 15.74m and period = 13s......117
Figure 4.49. 200-second window of a 20-minutes first and second order surface process. Where hs = 14,9m and tp = 15.8s. Maximum crest height obtained is 14,05m with a period of 15s. 118
Figure 4.50. Horizontal particle velocity profile for the largest crest height in figure 4.49 time series, where crest height = 14,05m and period = 15s for second and fifth order. First order has a crest height = 14.64m and period = 13s......118

LIST OF TABLES

Table 2.1. Joint frequency table of spectral peak period (s) (horizontal axis), and significant wave height (m). With a sea state duration of 3 hours for approximately 34 years. Obtained from [6]. 20

Table 2.2. Marginal omni directional extremes for the significant wave height, hs, and corresponding values for the spectral peak period, tp. 3 hour sea states. Obtained from [6]. 22

Table 2.3. hs and tp along the peak of 100-year contour line. Where 14.9 hs and 16s tp is the peak value. 24

Table 3.1. Data input for Data.Dat, showing a wave with wave height 28,61m and a Tmax = 17,74s 44

Table 3.2. Data of the program Convergence.dat.....45

Table 3.3. Data of the program Points.dat 45

Table 3.4. Data used for obtaining surface profile, horizontal particle velocity and acceleration for different waves, with the use of Stokes program. 47

Table 3.5. Mass and Drag coefficients used for different diameters. 61

Table 3.6. Load results for column diameter 1m, drag dominating forces. Where 1GN =10^3 MN = 10^6 kN = 10^9 N. X^o for Stokes waves instead of time for linear waves. Crest top is the x-position when 0^o, mean surface level is approximately 80^o and through is at 180^o. Max value obtained at the crest top. 63

Table 3.7. Load results for column diameter 5m, non-dominating forces. Where 1GN =10^3 MN = 10^6 kN = 10^9 N. X^o for Stokes waves instead of time for linear waves. Crest top is the x-position when 0^o, mean surface level is approximately 80^o and through is at 180^o. The data has been iterated to find max value with time, t or position, X^o. 64

Table 3.8. Load results for column diameter 20m, mass dominating forces. Where 1GN =10^3 MN = 10^6 kN = 10^9 N. X^o for Stokes wave instead of time for linear wave. Crest top is the x-position when 0^o, mean surface level is approximately 80^o and through is at 180^o. Max value obtained at mean surface level of wave. 65

Table 3.9. Comparison between old and new N-003 standard, by comparing load results for column diameter 1m, 5m and 20m. Where 1GN =10^3 MN = 10^6 kN = 10^9 N. X^o for Stokes wave instead of time for linear wave. Crest top is the x-position when 0^o, mean surface level is approximately 80^o and through is at 180^o.....67

Table 4.1. Load results for column diameter 1m, drag dominating forces. Where 1GN =10^3 MN = 10^6 kN = 10^9 N. X^o for stokes data instead of time for linear data. Crest top is the x-position when 0^o, mean surface level is approximately 80^o and through is 180^o. Max value obtained at crest top with a first order process.....95

Table 4.2. Load results for column diameter 1m, drag dominating forces. Where 1MN = 10^3 kN = 10^6 N. X^o for stokes data instead of time for linear data. Crest top is the x-position when 0^o, mean surface level is approximately 80^o and through is 180^o. Max value obtained at crest top with a second order process.....113

Table 4.3. Load results for column diameter 1m, drag dominating forces. Where 1MN = 10^3 kN = 10^6 N. X^o for stokes data instead of time for linear and second order data. Crest top is the x-position when 0^o, mean surface level is approximately 80^o and through is 180^o. Max value obtained at crest top.....119

LIST OF SYMBOLS

α	Method of moments parameter for crest height
α_{F}	Scale parameters in a 2-parameter Weibull distribution by Forristall
α_{H}	Scale parameters in Weibull distribution by Forristall
β	Method of moments parameter for crest height
β_{F}	Shape parameters in a 2-parameter Weibull distribution by Forristall
β_{H}	Shape parameters in Weibull distribution by Forristall
Δf	Frequency solution in Hz
$\Delta\omega$	Frequency solution in radians
ϕ	Velocity potential
γ	Peak enhancement factor
η	Second order surface process, irregular waves
$\eta^{(1)}$	First order surface process, irregular waves
$\eta^{(2)}$	Second order correction for surface process, irregular waves
ρ	Seawater density
σ	Spectral width parameter
σ_{Ξ}	Standard deviation of the surface elevation
σ_{Ξ}^2	Total variance of sea state
ω	Frequency in radians
ω_{Cut_S}	Cut-off frequency in radians, Stansberg
ω_N	Cut-off frequency in radians
ξ_0, ξ, ζ_0, a	Wave amplitude
$\xi(\mathrm{x},\mathrm{t})$	Wave profile
φ	Random phase
$\Psi(K_C)$	Wake amplification factor
A	Horizontal particle acceleration
c	Crest height
$c_{0.01}$	Crest height with annual probability of exceedance of 10^{-2}
$\mathrm{C_D}$	Drag Coefficient
C_{DS}	Drag coefficient for steady flow
C_M	Mass Coefficient
d	Water depth
D	Column diameter
f	Frequency in Hz
$f(z,t)$	Base shear step by step on a column
$F(t)$	Total base shear on a column

F_{Ξ_G}	Rayleigh distribution for crest height
$F_{\Xi_{3h}}$	Rayleigh distribution for extreme crest height
f_{Cut_S}	Cut-off frequency in Hz, Stansberg
$F_{H\|H_s,T_p}$	Weibull distribution for wave height
$f_d(z,t)$	Drag dominated base shear step by step on a column
$F_{C\|H_s,T_1}$	2-parameter Weibull distribution for crest height
$f_M(z,t)$	Mass dominated base shear step by step on a column
f_N	Cut-off frequency in Hz
f_p	Peak frequency
F_{Y_m}	Gumbel distribution, fitted using method of moments
g	Acceleration of gravity
$h_{0.01}$	Wave height with annual probability of exceedance of 10^{-2}
H, h	Wave height
h_s	Significant wave height
k_1	Wave number corresponding to mean wave period
k	Wave number
L	Wave length
$M(t)$	Total overturning moment on a column
N	Number of seconds of time series
N_{KC}	Keulegan-Carpenter number
n_t	Numbers of peaks in a time series
S_1	Measure of steepness
$s\Xi\Xi$	JONSWAP spectrum/ Spectral density
t	Time
T	Period
t_1	Mean wave period
t_2	Zero-up-crossing period
T_{max}	Maximum period for $c_{0.01}$ or $h_{0.01}$
T_{mean}	Mean period for $c_{0.01}$ or $h_{0.01}$
T_{min}	Minimum period for $c_{0.01}$ or $h_{0.01}$
t_p	Spectral peak period
Ur	Ursell number
V_0	Maximum horizontal particle velocity
V	Horizontal particle velocity
x	Wave position
z	Vertical coordinate (zero at mean water surface)

1 Introduction

1.1 Background of the task

When designing a jacket or jack-ups it has been common to adopt a Stokes 5th order wave profile defined by the 0.01-annual probability wave height, $h_{0.01}$, with an associated wave period as the ULS design wave, [1]. This has now been changed in the ongoing revision of the Norwegian standard for loads and load effects (action and action effects), N-003, [2]. Where it states that the ULS design wave shall be defined by having a crest height equal to the 0.01-annual probability crest height, $C_{0.01}$, instead of the wave height, $h_{0.01}$. There has also been some changes on the procedure with time domain for simulating loads and response predictions. Where a second order random process are now needed for modelling the sea surface elevation, and the corresponding kinematics shall also be calculated according to second order theory, [2]. This is why, we will be conducting a master thesis, where a comparison of loads and load effects on a simplified offshore structure will be conducted. By using different approaches recommended from the old and new N-003 version. It is also very interesting to know how hard a second order random process will be to construct, depending on time and programs available. Will this be possible for students in the future?

1.2 The task itself

The following sub-tasks was proposed by Sverre Kristian Haver and has been performed with slightly deviated execution in this thesis.

1. Estimate the 10^{-2} annual probability crest height, c0.01, and wave height, h0.01, and the associated period using the metocean contour lines method summing the sea state above is the worst sea state along the 10^{-2} – annual probability contour line. Guidance regarding this is found in revised N-003. Estimate the associated period following recommendation in N-003.

2. Kinematics of regular waves:

   * Stokes 5^{th} kinematics:
   Determine the horizontal particle speed versus depth under the wave crest based on the old and new recommendation of Stokes 5^{th} order wave profile. Determine also the horizontal fluid acceleration versus depth for the wave phase with maximum horizontal acceleration for the two Stokes 5^{th} implementations.

   * Linear wave approximation:
   Determine the horizontal particle speed and horizontal particle acceleration using linear wave theory and various approximations in order to estimate kinematics above the mean free surface (direct extrapolation above free surface, constant value above surface and Wheeler stretching.

3. Estimate the 10^{-2} – annual probability base shear of the pile structure using the various kinematics models of 2) above. Select 3 diameters: drag dominated case, inertia dominated case and a case with similar contributions from both terms.

4. Establish a simulation tool for Gaussian - and second order surface processes and second order wave induced kinematics. Verify kinematics by comparing with Stokes 5^{th} results for some Stokes 5^{th} like events in the simulated process. It is recommended that the Stansberg approach is applied for the kinematics. The length of the simulation must be decided in view of the times it takes to execute the simulations.

5. Kinematics of irregular waves:
   For the irregular wave investigation, one can focus on the drag dominated. This means that we can assume that we can assume that the 0.01 – annual probability quasi-static loads/load effects are rather well approximated by the values found for the wave event with a crest height equal to $c_{0.01}$.

   * Linear theory: Do a number (20) of 3-hour time domain simulations. Identify the wave event with a crest height corresponding to an exceedance probability of 0.1 for this sea state. If the Gaussian sea state were a correct assumption, this would be a good estimate for the 10^{-2} annual probability crest height. Estimate the particle speed under the wave crest the selected wave event. *(If simulation length 3 hours takes too long time, simulation length can be reduced or we can modify simulation approach by selecting fewer components.)*

*Second order theory: Use too developed in 4) to simulate a number (20) of second order surface processes. Duration of simulation is decided as the time it takes per simulation is known. Identify the wave event with a crest height likely to be exceeded by one out of ten 3-hour simulations. Determine kinematics of the event.

6. Estimate 10^{-2} – annual probability loads/load effects from the kinematic profiles in 5).

7. Compare results and discuss findings.

1.3 Scope of the task

The aim of this thesis is to compare loads and load effects on a simplified offshore structure using the procedures recommended in the 2007 N-003 version, [1] and the revised version, [2].

Regarding the structure a single pile with a fixed support at the sea bed has been adopted. By changing the diameter of the pile, different dominating forces can be obtained, as drag or mass terms. For regular waves a diameter of 1m, 5m and 20m has been controlled and for irregular waves a restriction has been done to focus on the drag dominated forces. Which means only a column diameter of 1m will be controlled.

The depth is taken to be 100m, which case intermediate water depth, which is used and explained under regular waves. For irregular waves, the depth has been classified as deep water to simplify the equations. More explanations for this simplification can be found under irregular waves.

Furthermore, the aim of this thesis is met by restricting the structural analysis to a quasi-static approach. Regarding Stokes 5^{th} order waves, an open code by Fenton is used and obtained from, [3]. Regarding calculations of kinematics on regular 1. order waves and kinematics of irregular processes a proper scripts in Matlab has been used. All loads calculated on the structure has also been done in Matlab. Regarding load effects, the work has been limited to base shear and overturning moment and calculated from Morrison equation.

1.4 Thesis Outline

This thesis consist of 5 chapters, where chapter 1 is an introduction and chapter 2 is about estimating the 10^{-2} annual probability crest height, $C_{0.01}$ and wave height $h_{0.01}$, with an associated period using the metocean counter line method. All the theory used in this thesis, will be introduced along the way at the start of the subchapter. The main part of this thesis can be found in chapter 3 and 4, which divide regular waves in chapter 3 and irregular waves in chapter 4. Each of those two chapters consist of subchapters, where chapter 3 discusses linear methods and 5th order Stokes waves for regular waves. Those methods, will be compared and discussed at the end of chapter 3. For chapter 4, which addresses irregular waves a first and second order approach will be performed in two different subchapters. Where a third subchapter will compare the result of those two method and discussed at the end of the chapter. Finally, chapter 5 will finish the thesis with a conclusion and suggestion for further work.

2 Metocean contour method

In this report, we will be using the metocean contour line method too estimate the long-term extremes. This can be done through short-term sea states. For doing this, we will need to find a good set of metocean data. Then contour lines needs to be established for the metocean data. In our report, we will only be looking at the 100-year extreme wave. Therefore, the only interesting contour line is the 100-year contour line with an 0.01 constant annual exceedance probability for any combinations of h_s and t_p along the contour line. When this is found, it is important to know that the peak of the contour line isn't always the worst case. Therefore, the next step would be to identify the worst condition along the 0.01 probability contour line. To find the worst case, a comparison between the different combinations of h_s and t_p along the peak of the contour line is needed. The comparison can be done with equation 2.2, which is explained under chapter 2.3 and is a Weibull distribution. This is the same formula used later to find the 100 year extreme wave. To satisfy the new N-003 standard the 100-year extreme crest height is also found, this is show in chapter 2.4 along with the estimate of the 100-year extreme wave. Before this, an introduction to what metocean is and what kind of metocean data used here will be explained.

2.1 Metocean

Metocean is a contraction of words from **met**eorology and **ocean**ography. Where meteorology consist of gather data from wind, air temperature, atmospheric pressure, etc. Oceanography includes waves, current, water level and other data, [4]. This means that metocean include most of those data sets. The more data obtained, the better it is for the accuracy of predicting the real environmental conditions affecting offshore operations in the future. In this report, we are only using wave data consisting of the significant wave height and the spectral peak period. The significant wave height and the spectral peak period is found by measuring the height and period of waves from a location. Normally interval of 3 hours for each measurement. Then the spectral peak period, t_p, is the wave period with the highest energy (maximum spectrum spectral density), [5]. The significant wave height, h_s, is the mean value of the 1/3 of the largest waves for the measured 3hr sea state, as shown in figure 2.1. Another method used more in the present is 4 times the standard deviation of the surface process, [5]. Then we have the wave spectrum which is usually estimated from parameters in terms of h_s and t_p. In a year, there will be recorded 2920 h_s and t_p from 2920, 3-hour periods. The reason for 3-hour period instead of a larger period is the change in weather.

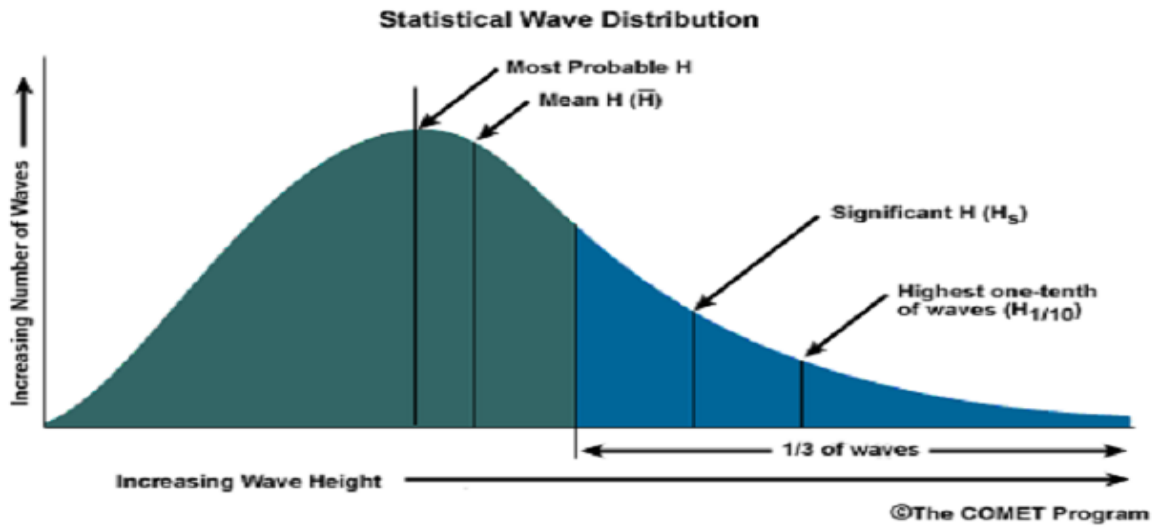

Figure 2.1. Statistical wave distribution of a wave spectrum with definitions.

2.2 Wave Data

The data used is measured from the Northern North Sea between, 1973 and 2002. It include some hindcast data that's only been used to fill in gaps at the measured metocean data set. This comes from DNMI Hindcast Archive, gridpoint 1415, between 1955 and 2001. All the metocean data is obtained from [6].

In table 2.1, you can see all the wave date used for this report. The data here consist of h_s and t_p from 34 years in all directions, and it is used for estimating the 100-year extreme wave of the sea state.

Table 2.1. Joint frequency table of spectral peak period (s) (horizontal axis), and significant wave height (m). With a sea state duration of 3 hours for approximately 34 years. Obtained from [6].

a) All year – omni directional

H_s	SPECTRAL PEAK PERIOD																			SUM
	0-3	3-4	4-5	5-6	6-7	7-8	8-9	9-10	10-11	11-12	12-13	13-14	14-15	15-16	16-17	17-18	18-19	19-20	<20	
0-1	21	179	529	859	977	889	701	503	337	217	135	82	49	29	17	10	6	4	5	5550
1-2	5	141	959	2762	4683	5644	5411	4430	3245	2193	1399	855	507	294	167	94	53	29	36	32909
2-3	0	9	168	956	2604	4359	5230	4964	3980	2819	1822	1099	629	346	185	97	50	25	25	29368
3-4	0	0	9	127	634	1629	2633	3053	2777	2109	1398	835	461	239	118	56	26	12	9	16126
4-5	0	0	0	8	88	397	955	1460	1593	1349	941	566	303	148	67	29	12	5	3	7924
5-6	0	0	0	0	7	66	268	594	838	836	639	397	210	97	41	16	6	2	1	4019
6-7	0	0	0	0	0	6	49	177	352	445	393	263	141	63	25	9	3	1	0	1928
7-8	0	0	0	0	0	0	5	36	111	192	209	159	90	40	15	5	1	0	0	863
8-9	0	0	0	0	0	0	0	5	25	64	93	85	54	25	9	3	1	0	0	363
9-10	0	0	0	0	0	0	0	0	4	16	33	39	29	15	6	2	0	0	0	145
10-11	0	0	0	0	0	0	0	0	0	3	9	15	14	8	3	1	0	0	0	55
11-12	0	0	0	0	0	0	0	0	0	0	2	5	6	4	2	1	0	0	0	20
12-13	0	0	0	0	0	0	0	0	0	0	0	1	2	2	1	0	0	0	0	7
13-14	0	0	0	0	0	0	0	0	0	0	0	0	1	1	0	0	0	0	0	2
14-15	0	0	0	0	0	0	0	0	0	0	0	0	0	0	0	0	0	0	0	1
SUM	25	329	1667	4712	8993	12991	15255	15222	13262	10243	7075	4403	2495	1312	657	322	158	78	81	99280

Simulated observations of h_s and t_p are plotted in figure 2.2. This is to get a better overview of the data and to show the mean value and a 90% confidence interval of the data.

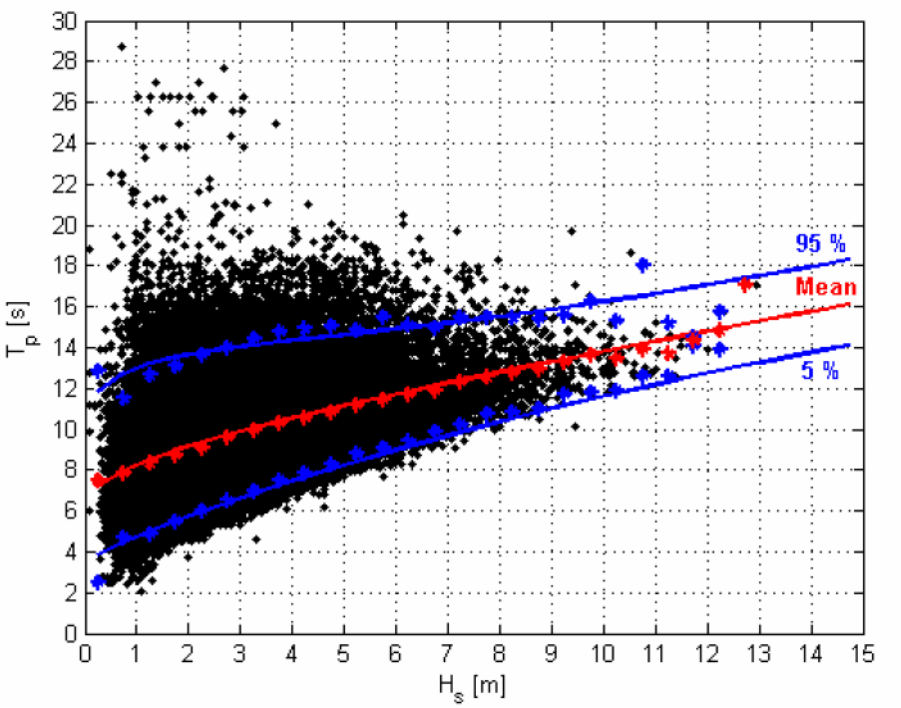

Figure 2.2. Conditional characteristics for the Spectral peak period versus significant wave height with 90% confidence interval and mean value are shown for 3 hour sea state. Obtained from [6].

The next step is to find the 100-year value of the h_s and t_p. To do this we can use figure 2.3, which is obtained from [6]. They have already introduced contour lines that describe the different probability sea states. Contour line is a line consisting of points of equal probability of exceedance. The 100-year contour line will describe all possible combinations of h_s and t_p corresponding to an annual exceedance probability of 10^{-2}. To create contour lines an estimate of the n-probability of h_s along with the conditional average of t_p is needed. Afterword a line can be drawn through all the h_s and t_p obtained from the n-probability. This will make a counter line with n-probability. See [6] and [2] for more guidelines on contour lines.

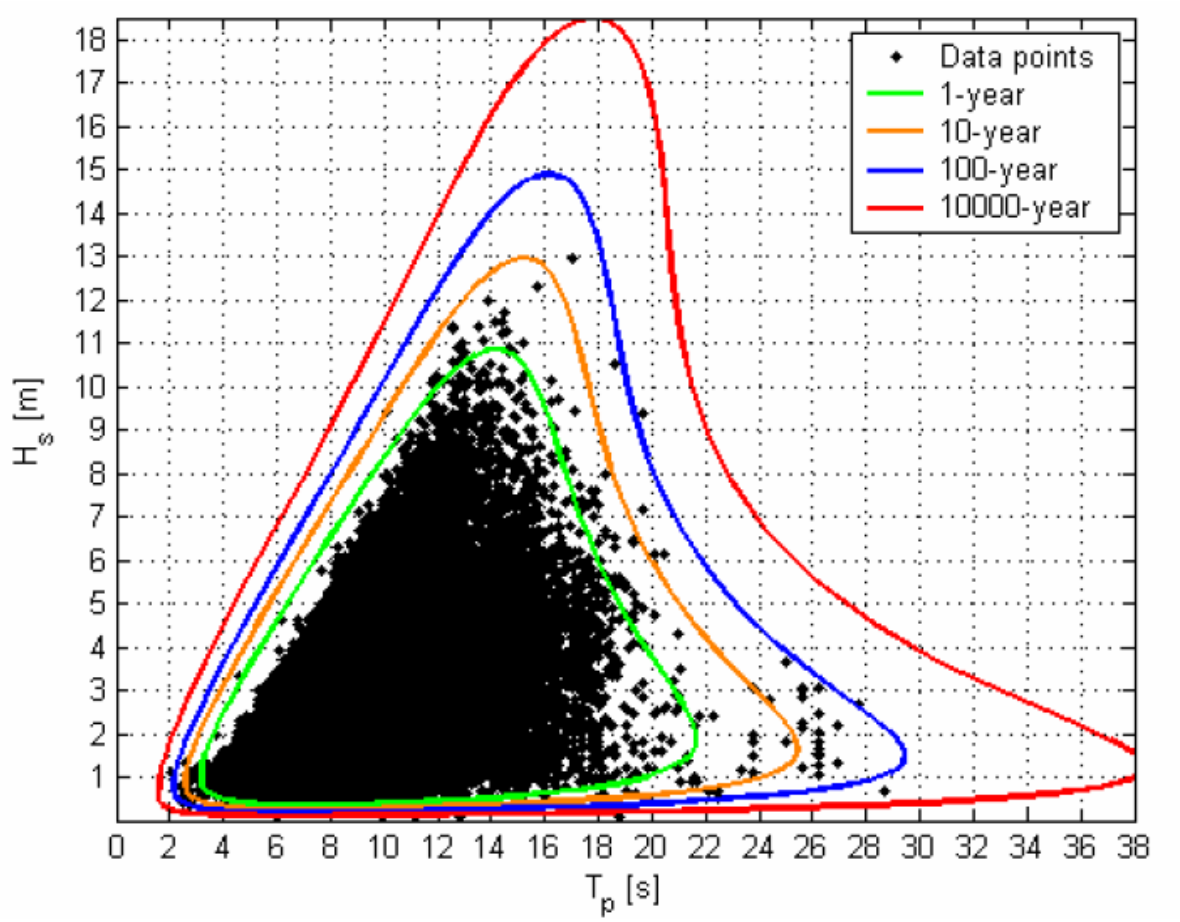

Figure 2.3. 1, 10, 100 and 10000-year extreme contour lines in the h_s – t_p plane. Sea state duration 3 hours. Obtained from [6].

From figure 2.3, we can obtain all the necessary data used lather in our report and table 2.2 shows some exact numbers of different extreme values obtained from figure 2.3.

Table 2.2. Marginal omni directional extremes for the significant wave height, h_s, and corresponding values for the spectral peak period, t_p. 3 hour sea states. Obtained from [6].

Return period (years)	Extreme sea states		
	H_s [m]	T_p [s]	90% range of T_p
1	11.0	14.2	12.1 - 16.5
10	13.0	15.1	13.1 - 17.3
100	14.9	16.0	14.0 - 18.2
10000	18.2	17.5	15.5 - 19.7

2.3 Worst metocean condition along the 100-year contour line

Before estimating the extreme wave or crest height with a 100-year response, we need to identify the most unfavorable sea state for the 100-year contour line. This can be done by looking in to different points along the 100-year contour line. Where those points should be close to the peak of the 100-year contour line and at least five points. Where one point is at the peak and at least two points at the left and right side of the peak, depending on the values. The spectral peak period and the significant wave height will vary along the 100 year contour line and is not depending on each other. By modeling the short term design sea state with those points, we can plot the result and find the most extreme scenario.

First of all, we would need to introduce the formula that can describe the distributions of a short term sea state for wave heights. Later on an estimate of the long term extremes can be found by considering a few short term sea states. This formula is a Weibull distribution that has been verified by a large number of measurements for different environmental conditions. The formula is shown in equation 2.1 and obtained from [7].

$$F_{H|H_s,T_P}(h|h_s,t_P) = 1 - e^{-\left(\frac{h_s}{\alpha_H}\right)^{\beta_H}} \quad \text{Equation 2.1}$$

Equation 2.1 dose not obtain the extreme values for a 3-hour period. For obtaining those, the equation needs to be raised to the power of $\frac{N}{t_2}$ according to [8]. Where N is the seconds in a 3-hour period (10800s) and t_2 is the spectral estimate of zero-up-crossing period. The distribution of the 3-hour maximum wave height is here given by:

$$F_{H_{xhr}|H_s,T_P}(h|h_s,t_P) = \left(1 - e^{-\left(\frac{h}{\alpha_H}\right)^{\beta_H}}\right)^{\frac{N}{t_2}} \quad \text{Equation 2.2}$$

Equation 2.2 will go towards Gumble distribution as $N \to \infty$.
Where the various parameters from Forristall are:

$$\alpha_H = 0.683 * h_s \quad \text{Equation 2.3}$$

$$\beta_H = 2.13 \quad \text{Equation 2.4}$$

The zero-up-crossing period, $t_2 = t_p * 0.77$ according to [8].

Table 2.3 shows the different h_s with the corresponding t_p values around the peak of the 100-year contour line. The peak value of this contour line is $h_s = 14.9m$ and $t_p = 16s$, meaning that two of my points from table 2.3 has to high h_s. The reason for this is to be on the safe side and obtain the worst case that can happen. Those two points has a $h_s = 14.9m$ and $t_p = 16.4s$ or $15.8s$, where h_s should have been reduced a little to follow the contour line. All points are obtained from figure 2.3.
With those data and equation 2.2 a Matlab script has been used to calculate the different 3-hour extreme value distribution of wave heights. This have then been plotted and zoomed inn for a better overview of what the worst scenario is. See figure 2.4 for the different max wave height and figure 2.5 for the zoomed in picture for overview.

Table 2.3. h_s and t_p along the peak of 100-year contour line. Where 14.9 h_s and 16s t_p is the peak value.

Data from peak of 100 year contour line	
Hs (m)	Tp (s)
14.9	16.0
14.9	16.4
14.9	15.8
14.0	14.0
14.0	17,67
14.78	15.5

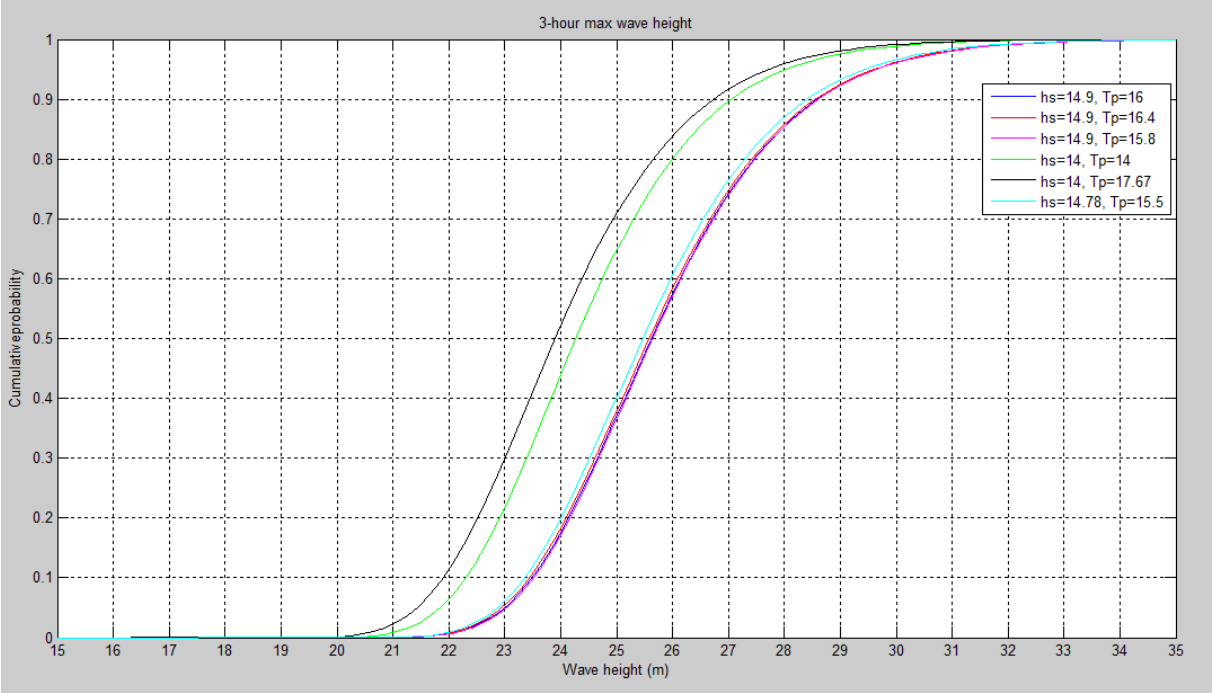

Figure 2.4. Showing extreme wave height for an 3-hour period with six different conditions.

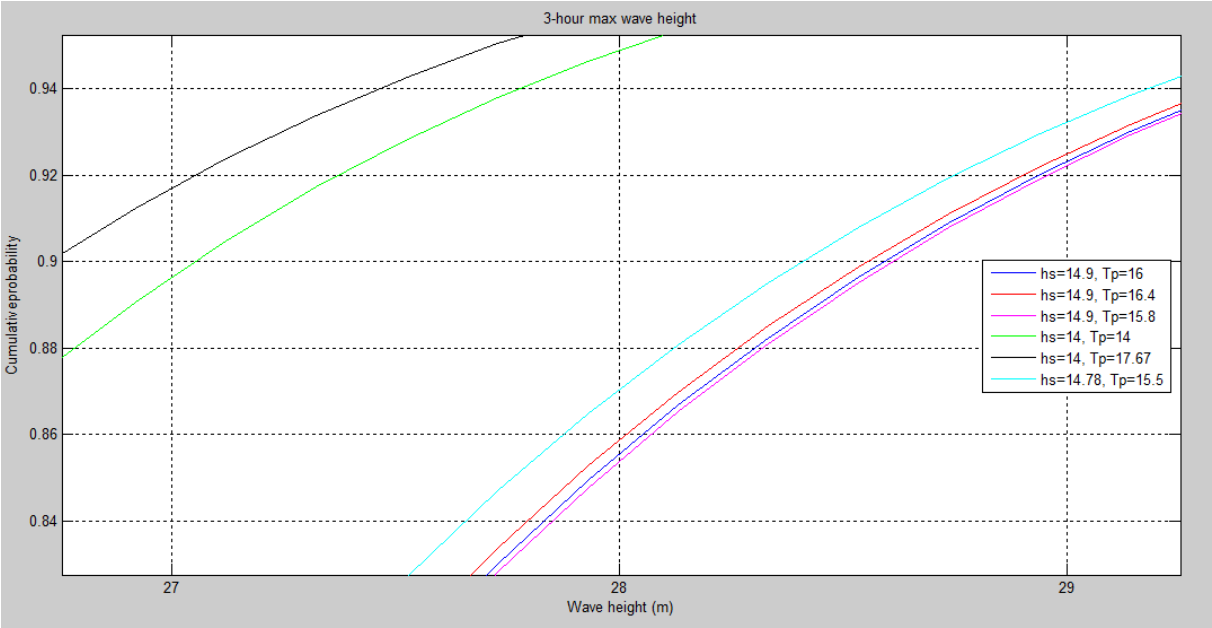

Figure 2.5. Showing extreme wave height for a 3-hour period with six different conditions zoomed inn.

From figure 2.5 we can see that the purple line has the highest wave height value that means that this is the worst scenario for the 100-year contour line. We can also state that from this formula the h_s is the main parameter to increase the extreme wave height distribution. This can be seen from $h_s = 14\text{m}$ compared with $h_s = 14.9\text{m}$, which makes much larger differences than the change in t_p when $h_s = 14\text{m}$.

Another observation from figure 2.5 is that the worst scenario for table 2.3 is with a $h_s = 14.9m$ and $t_p = 15.8s$. Meaning that a reduction in t_p for the same h_s would result in a higher extreme wave height distribution. The reason for this is that a lower t_p in a 3-hour sea state will reduce the zero-up-crossing period and allow more waves to occur. This will increase the probability to obtain the same wave heights as a higher t_p.

2.4 Extreme wave/crest height value

Now that the worst scenario for the extreme wave height distribution is estimated, we will be using hs = 14.9 and Tp = 15.8s for the next step in finding the extreme crest and wave height value. Using the same formula again with those values, the long-term extreme wave height value can be estimated by the 0.90 percentile (cumulative probability), for an annual exceedance probability of 0.01. According to [1] and [2]. The following formula below is used to plot the extreme wave height distribution. This formula where explained under equation 2.1 and 2.2. All the calculations are preform in Matlab and for more details see the Matlab script.

$$F_{H_{3hr}|H_s,T_P}(h|h_s,t_P) = \left(1 - e^{-\left(\frac{h}{10.18}\right)^{2.13}}\right)^{\frac{10800}{12.17}}$$

For the short-term crest height distribution, a 2-parameter Weibull distribution formula is used and obtained from [7]. This distribution has been established by a large number of simulation of a second order Stokes surface model. See the following formula below with description.

$$F_{C|H_s,T_1}(c|h_s,t_1,d) = 1 - e^{-\left(\frac{c}{\alpha_F * h_s}\right)^{\beta_F}} \quad \text{Equation 2.5}$$

And the extreme wave height distribution is:

$$F_{C_{xhr}|H_s,T_1}(c|h_s,t_1,d) = \left(1 - e^{-\left(\frac{c}{\alpha_F * h_s}\right)^{\beta_F}}\right)^{\frac{N}{t_2}} \quad \text{Equation 2.6}$$

Where c is the variable for crest height, t_1 is the mean wave period and parameter α_F and β_F are expressed by measure of steepness S_1 and Ursell number Ur obtained from [7].

$$Ur = \frac{h_s}{k_1^2 * d^3} \quad \text{Equation 2.7}$$

$$S_1 = \frac{2\pi * h_s}{g * t_1^2} \quad \text{Equation 2.8}$$

$$\alpha_F = 0.3536 + 0.2892 * S_1 + 0.1060 * Ur \quad \text{Equation 2.9}$$

$$\beta_F = 2 - 2.1597 * S_1 + 0.0968 * Ur^2 \quad \text{Equation 2.10}$$

k_1 can be found through solving or iterating and the formula is obtained at [9] and explained under chapter 3.1.3.

$$[\ \omega^2 = g * k_1 * \tanh(k_1 * d)\ ] \text{ where } \omega^2 = \frac{2\pi}{t_1} \quad \text{Equation 2.11}$$

k is 0.023 for this case by iterating it in Matlab. The rest of the parameters and values for this case can be seen in the formula below used for plot figure 2.6, which is from equation 2.6.

$$F_{C_{3hr}|H_s,T_1}(c|h_s,t_1,d) = \left(1 - e^{-\left(\frac{c}{0.37*14.9}\right)^{1.88}}\right)^{\frac{10800}{12.17}}$$

We can now plot bout the short-term extreme crest and wave height distribution. This is to find the long-term extreme crest/wave height value at a 0.90 percentile as mentioned earlier. See figure 2.6.

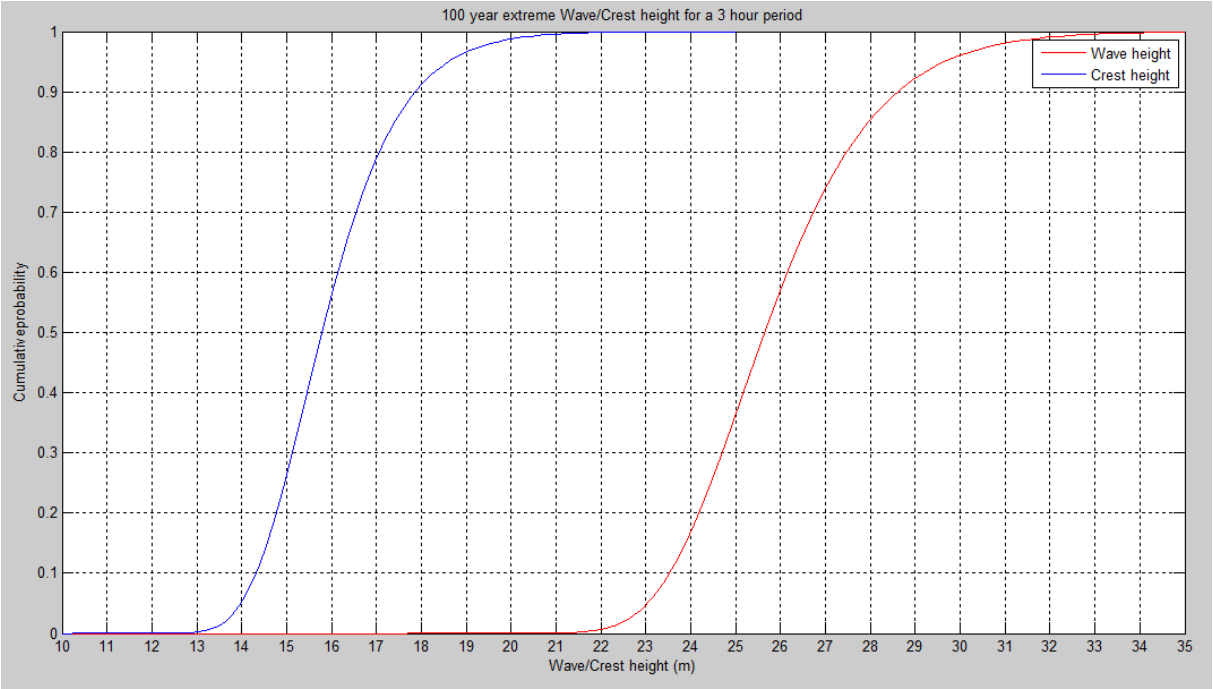

Figure 2.6. Short-term sea state for extreme wave/crest height values.

Figure 2.6 shows that the extreme crest and wave height values are:

$h_{0.01} = 28.61\ m$

$c_{0.01} = 17.87\ m$

Where $H_{0.01}$ is the extreme 100-year wave height and $C_{0.01}$ is the extreme 100 year crest height with and annual probability of 10^{-2}.

[6] also estimated the 100-year extreme crest and wave height with and annual probability of 10^{-2} but they used a different distribution formula. Results in [6], where a wave height of 29 meters. This is a little larger than ours predictions as expected since [6] uses a Forristall distribution, which case higher values than a Weibull distribution. For the crest height, [6] got 17.6 meters from a long-term analyses and that is just below ours. Therefore, we can say that this has been a good estimation for the extreme 100-year crest and wave height with and annual probability of 10^{-2}. This is just an approximate method. For a final design, it has to be confirm by the 0.90 percentile with long-term analysis as the 100-year extreme crest height were.

According to [1] under “6.2.2.4 Design wave”, the period for the extreme 100-year wave can be found by the following formula:

$$\sqrt{6.5 * H_{100}} \leq T \leq \sqrt{11 * H_{100}} \qquad \text{Equation 2.12}$$

Where:

$T_{min} = 13.64\ s$

$T_{max} = 17.74\ s$

$T_{mean} = 15.69\ s$

Another method for estimating T_{mean} is by $0.9 * t_p = 0.9 * 15.8 = 14.22s$, which would have resulted in a much lower period. The method used in this thesis is equation 2.12. Where $T_{mean} = 15.69\ s$.

3 Kinematics of regular waves

In this chapter, we will be looking inn to linear and nonlinear wave theory for regular waves. The object here is to find the horizontal particle velocity and horizontal particle acceleration for the 100-year extreme wave. This will be done in several ways, by using the formulas from first order, and 5thorder wave kinematics. For the first order (liner wave theory) various approximations in order to estimate kinematics above the mean free surface will be used. This can be done by having a constant value above surface, extrapolation of leaner speed above free surface or using Wheeler stretching. For the 5th order Stokes approach, a Stokes 5th order program obtained from [3], will be used to estimate the kinematics.

3.1 Linear wave theory

First, we need to introduce linear wave theory since this is the core theory of ocean surface waves. This theory uses linearized boundary conditions that create regular waves with sinusoidal shape. The reason we can neglect the nonlinear terms at the free surface is because of the small wave height to wave length ratio H/L, this is less than 2% according to [10]. If the wave travels to shore at shallow water or becomes too large a higher order theory would be needed to describe the wave. The sinusoidal shaped waves have the same height for crests and troughs unlike the higher order wave theories that describe the waves more like the real ocean waves. The real ocean waves have higher crests than trough, it also consist of waves with varying wave heights and periods. This is called irregular waves. More about irregular waves can be found at chapter 4. Linear wave theory can be a good approximation to real waves and linear regular waves are the key to describe irregular ocean with the help of Fourier analysis. This kind of Fourier analysis consist of a sum with regular sinusoidal waves.

3.1.1 Surface Profile

The surface profile of a sinusoidal wave can be described as following:

$$\xi(x,t) = \xi_0 * \sin(\omega * t - k * x)$$

Equation 3.1

Obtained from [9]. Where ξ_0 is the amplitude also known as half the wave height or if the higher crest height than trough height is considered then the amplitude will be the crest height. ω is the wave frequency found from $\omega = \frac{2\pi}{T}$, where T is the period, k is the wave number, x is the position and t is the time.

From equation 3.1, we can plot the wave in time and space. This formula can also be used to derive the equation for $k = \frac{2\pi}{L}$ by evaluate the profile's dependence on x when t = 0. Where the wavelength L will be the distance between two wave tops or two wave troughs. See figure 3.1 for an illustration of this.

When evaluate the profile's dependence on t when x = 0, the distance between two wave tops or two wave troughs will be the time period T of the wave. From this, we can derive the equation for $\omega = \frac{2\pi}{T}$.

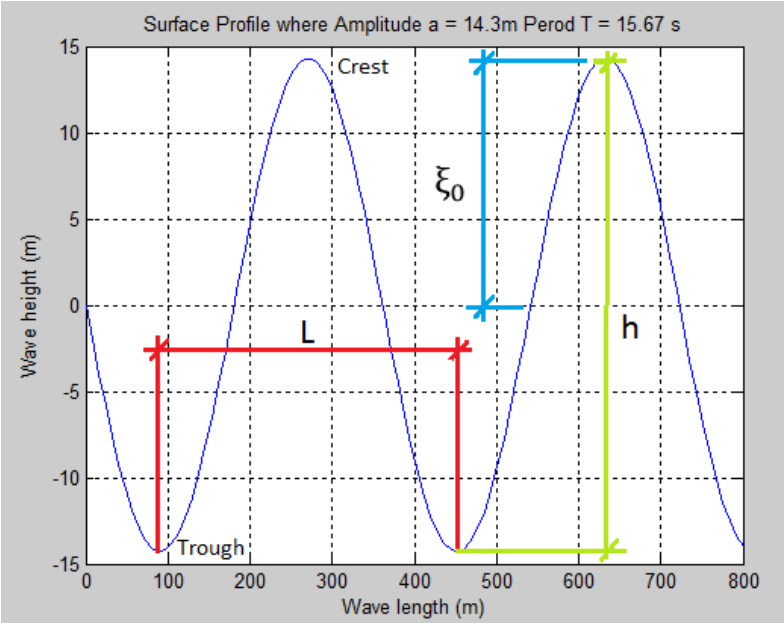

Figure 3.1. Illustrating wave parameters for a surface profile.

To obtain the formula for velocity and acceleration we need to find the velocity potential first by derivation two Laplace exertion. We will not fully show the derivation in this report only the main steps and the entire boundaries used for the derivation of the equations.

3.1.2 Laplace Equation

First of all we need to find the two equation needed. Those can be found by describing the sea with some physical conditions. The first one is that the water need to be incompressible or $\nabla * \tilde{V} = 0$. The next step is to obtain the velocity potential by saying that the sea follows a certain physical condition that the fluid can be considered as irrational. This is because of the effects of turbulence and viscosity are small. From this, we find that the velocities can be described as $(u, v, w) = (\frac{\partial \phi}{\partial x}, \frac{\partial \phi}{\partial y}, \frac{\partial \phi}{\partial z})$ in terms of gradients according to [11] and [12].

Now to set up our Laplace equation, where $-\infty \leq x \leq \infty$ and $-d \leq z \leq \varsigma$

$$\nabla * \phi^2 = \frac{\partial^2 \phi}{\partial x^2} + \frac{\partial^2 \phi}{\partial z^2} = 0 \qquad \text{Equation 3.2}$$

From this we can obtain the following equation by derive it, [9].

$$\begin{aligned}\phi(x,z,t) &= X(x) * Z(z) * T(t) \\ &= (A * \sin(kx) + B * \cos(kx)) * (C * e^{kz} + D * e^{-kz}) * T(t)\end{aligned}$$ Equation 3.3

Where the constants A, B, C and D are depending on our boundaries below.

The boundary's that's needed to complete this derive is the two following below:

To sustain the impermeability of the seabed, we need to have the velocity normal at the seabed zero ($\nabla\phi n = 0$). This is called the bottom boundary condition, and if the seabed is taken as horizontal, the following boundaries are obtained, [11] [12]:

$$\frac{\partial\phi}{\partial z} = 0 \quad when \quad z = -d$$ Equation 3.4

The next boundary needed is the dynamic free surface boundary condition. This states that the atmospheric pressure p_0 is the same as the water pressure on the free surface. Where the formula below is show with nonlinear terms, [11] [12].

$$g * \zeta_0 + \frac{1}{2} * \left(\frac{\partial^2\phi}{\partial x^2} + \frac{\partial^2\phi}{\partial y^2} + \frac{\partial^2\phi}{\partial z^2}\right) + \frac{\partial\phi}{\partial t} + p_0 = p_0 \quad when \quad z = \zeta(\mathrm{x},\mathrm{y},\mathrm{z})$$ Equation 3.5

To simplify this formula and introduce the boundary condition at the surface z = 0 we get, [9]:

$$g * \zeta_0 + \frac{\partial\phi}{\partial t} + p_0 = p_0 \quad \longrightarrow \quad \zeta_0 = -\frac{1}{\mathrm{g}} * \frac{\partial\phi}{\partial t} \quad when \quad z = 0$$ Equation 3.6

From those two boundary's we can obtain the following formula for the velocity potential, [9]:

$$\phi(x,z,t) = \frac{\zeta_0 * \mathrm{g}}{\omega} * \frac{\cosh k(z+d)}{\cosh kd} * \cos(\omega\mathrm{t} - \mathrm{kx})$$ Equation 3.7

Where:

$\cos(\omega t - kx)$ is the term for regular linear wave

and $\frac{\cosh k(z+d)}{\cosh kd}$ is depth dependent.

This means that for deep water when $d \gg 1$ we can write:

$$\cosh(kd) = \frac{e^{kd}+e^{-kd}}{2} = e^{kd} \quad \longrightarrow \quad \frac{\cosh k(z+d)}{\cosh kd} = \frac{e^{k(z+d)}}{e^{kd}} = e^{kz}$$

$$\phi(x,z,t) = \frac{\zeta * g}{\omega} * e^{kz} * \cos(\omega t - kx) \qquad \text{Equation 3.8}$$

And for shallow water:

$$\cosh(kd) = \frac{e^{kd}+e^{-kd}}{2} = \frac{1+1}{2} = 1 \quad \longrightarrow \quad \frac{\cosh k(z+d)}{\cosh kd} = 1$$

$$\phi(x,z,t) = \frac{\zeta * g}{\omega} * \cos(\omega t - kx) \qquad \text{Equation 3.9}$$

According to [9] and see definition of shallow water under 3.1.4, Classification of water depth.

3.1.3 Dispersion Relation

Now that the velocity potential is obtained, another boundary condition can be used to estimate the relation between wavelengths and wave period. This is called the dispersion relation. The boundary condition used here is the combined free surface boundary equation that combines the kinematic and dynamic free surface boundaries and eliminating ζ. The full formula with nonlinear condition can be found below, [12]:

$$-\frac{\partial^2 \phi}{\partial t^2} - g * \frac{\partial \phi}{\partial z} - \left(\frac{\partial}{\partial t} + \frac{1}{2} * \nabla\phi * \nabla\right)|\nabla\phi|^2 = 0 \quad when \quad z = \zeta(x,y,t) \qquad \text{Equation 3.10}$$

To linearize it and set condition for z = 0 we obtain, [9]:

$$\frac{\partial^2 \phi}{\partial t^2} + g * \frac{\partial \phi}{\partial z} = 0 \quad when \quad z = 0 \qquad \text{Equation 3.11}$$

$$\frac{\partial^2}{\partial t^2} * \left(\frac{\zeta_0 * \mathrm{g}}{\omega} * \frac{\cosh k(z+d)}{\cosh kd} * \cos(\omega \mathrm{t} - \mathrm{kx}) \right)\Bigg|_{z=0} + g * \frac{\partial}{\partial z} * \left(\frac{\zeta_0 * \mathrm{g}}{\omega} * \frac{\cosh k(z+d)}{\cosh kd} * \cos(\omega \mathrm{t} - \mathrm{kx}) \right)\Bigg|_{z=0} = 0 \qquad \text{Equation 3.12}$$

By derive equation 3.12 a solution for L and ω can be obtained. The end of this derive is found in equation 3.13 and solution for L and ω is in equation 3.14 and 3.15. According to [9].

$$\frac{\omega^2}{g * k} = \tanh(kd) \qquad \text{Equation 3.13}$$

Where the wave frequency is:

$$\omega^2 = g * k * \tanh(kd) \qquad \text{Equation 3.14}$$

And the wave length is:

$$L = \frac{g}{2\pi} * T^2 * \tanh(kd) \qquad \text{Equation 3.15}$$

Those formulas can be simplified with the condition of deep or shallow water. This is because:

$kd \gg 1$, we get $\tanh(kd) \sim 1$ and the formula for deep water will be, [9]:

$$\omega^2 = g * k \quad and \quad L = \frac{g}{2\pi} * T^2 \qquad \text{Equation 3.16}$$

For shallow water $kd \ll 1$ and $\tanh(kd) \sim kd$ this means that the equation will be, [9]:

$$\omega^2 = g * d * k^2 \quad and \quad L = \sqrt{g * d * T^2} \qquad \text{Equation 3.17}$$

3.1.4 Classification of water depth

For kinematics, the interval classification of water depth, deep, intermediate, and shallow can be found in equation 3.18 according to [9].

Deep water: $d > \frac{L}{2}$

Intermediate water: $\frac{1}{20} < \frac{d}{L} < \frac{1}{2}$ Equation 3.18

Shallow water: $\frac{d}{L} < \frac{1}{20}$

The reason for those intervals is the changes in the depth dependent part of the velocity potential.

3.1.5 Horizontal water particle velocities and accelerations

The last step in our linear theory will be to derive the velocity and acceleration formulas. They can be found by taking the derivatives of the potential function. In our case, the horizontal particle velocity and acceleration is needed for this thesis. Therefore, the potential function needs to be derived with respect to x as shown in equation 3.19. This is to find the horizontal particle velocity:

$$u(x,z,t) = \frac{\partial \phi}{\partial x} = \frac{\zeta_0 * \mathrm{g} * \mathrm{k}}{\omega} * \frac{\cosh k(z+d)}{\cosh kd} * \sin(\omega \mathrm{t} - \mathrm{kx}) \quad \text{Equation 3.19}$$

This formula can also simplify the depth dependent part of the equation, as shown above. Only if it is deep or shallow water. We can also see that the horizontal velocity is on its max at the wave crest. This is when $\sin(\omega \mathrm{t} - \mathrm{kx}) = 1$ and its minimum when $\sin(\omega \mathrm{t} - \mathrm{kx}) = -1$ which is when the wave are at the through. It is also worth mention that the surface profile has the same function as the horizontal velocity function.

The horizontal particle acceleration is found by derivative of the horizontal particle velocity equation with respect to time, t, and obtaining:

$$a(x,z,t) = \frac{\partial u}{\partial t} = \zeta_0 * \mathrm{g} * \mathrm{k} * \frac{\cosh k(z+d)}{\cosh kd} * \cos(\omega \mathrm{t} - \mathrm{kx}) \quad \text{Equation 3.20}$$

Equation 3.20 shows that the acceleration term is zero at the wave crest. This is when the velocity is on its max when sin(w*t* - *kx*) = 1 and cos(w*t* - *kx*) = 0 for this equation. When the surface profile equation is 0, the acceleration function has its maximum value. This is at the mean water surface, where the water particles cross the still water level. Which is when $\cos(\omega t - kx) = 1$

3.2 Linear wave approximations

Now that a theoretical introduction has been done, we can start to find the horizontal particle velocity and acceleration for our extreme 100-year wave. The amplitude will be set to the crest height to satisfy the new N-003 and half the wave height for the old N-003 standard. The interesting part here is to see the deferens of those outcomes. First of all the water depth needs to be categorized as shallow, intermediate or deep water, to choose the formula needed. After words the wavelength can be estimated through the following formula, which were explained above.

$$L = \frac{g}{2\pi} * T^2 * \tanh(kd) \qquad \text{Equation 3.21}$$

For this formula k can be estimated through formula 3.22, but Matlab is required to solve or iterate to a solution for k.

$$\omega^2 = g * k * \tanh(kd) \qquad \text{Equation 3.22}$$

With the help of Matlab, the solution for k is: k = 0.0174, and by using $T_{mean} = 15.69s$ as period the following wave length is obtained:

$$L = \frac{9.81}{2\pi} * 15.69 * \tanh(0.0174 * 100) = 361\ m$$

From here we can find out that $\frac{d}{L} = \frac{100}{361} = 0.28$

This means that this is intermediate water depth since: $\frac{1}{20} < \left(\frac{d}{L} = 0.28\right) < \frac{1}{2}$. Because of this the simplifications mentioned in the linear wave theory, about the wave depth dependent part, can not be used here.

Using half the wave height as amplitude and T_{mean} as the period, the surface profile can be plotted. This gives us figure 3.2 with the use of the following formula when time t is 0s and 1.5s:

$$\xi(x, 0) = 14.3 * \sin(0.4 * t - 0.0174 * x)$$

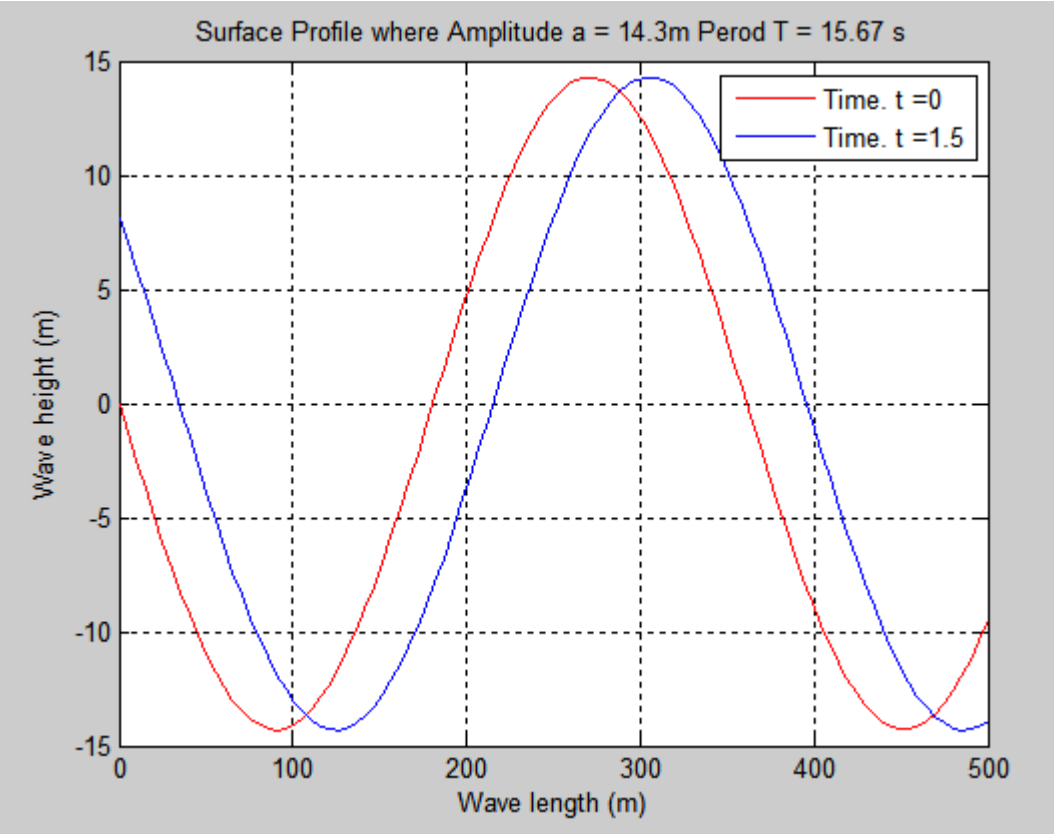

Figure 3.2. Showing surface profile for t = 0s and t = 1.5s with respect to x.

From figure 3.2, one can see that the wave moves in a positive position with time. Since the surface profile function is the same as the horizontal particle velocity function, we can say that max velocity will be at its crest. This means that the horizontal particle velocity will have its maximum at $\frac{3}{4}L$ in t = 0s and the maximum horizontal particle acceleration at 0m. Since the horizontal particle acceleration is maximum at the mean water surface as mentioned before.

3.2.1 Horizontal water particle velocities with half the wave height as amplitude

Next step is to find the horizontal particle velocity for a wave with height = 28.61 meters. With the use of three different periods since this is required of the old N-003 standard, [1]. The three different periods are: $T_{min} = 13.64\ s$, $T_{max} = 17.74\ s$ and $T_{mean} = 15.69\ s$. There are also three different plots for each time period. The reason for this is because of the difficulties on describing the maximum velocity above the mean surface level. The three different approximation methods used here, are constant value above the surface level and up to the crest, extrapolation of leaner speed above free surface or using Wheeler stretching. All the calculations are done in Matlab, and plotted afterwards. For a better understanding for the reader, all the steps with T_{mean} as period and half the wave heights as amplitude will be shown.

The first step is to locate the maximum position of the velocity and this is when $\sin(\omega t - kx) = 1$ (crest top). Since this case has intermediate water depth, the formula used can't be simplified and therefore, the following formula is:

$$u(z) = \frac{\zeta_0 * g * k}{\omega} * \frac{\cosh k(z+d)}{\cosh kd} = \frac{14.30 * 9.81 * 0.017}{0.40} * \frac{\cosh 0.017 * (z+100)}{\cosh(0.017 * 100)}$$

The only value left to specify now is the variable z. For extrapolation of leaner speed above free surface, we can use the formula as it is and use the z value in an interval of:

$$-d \leq z \leq \zeta_0 \ \longrightarrow\ -100m \leq z \leq 14.30\text{m}$$

When constant value from surface level up to the crest is used, the same formula for $-d \leq z \leq 0 \ \longrightarrow\ -100m \leq z \leq 0\text{m}$ can be used, this is up to the surface level. To describe the part from surface level up to the crest, z needs to be 0 (constant value). For the same formula at interval $0 \leq z \leq \zeta_0 \ \longrightarrow\ 0m \leq z \leq 14.3\text{m}$. In Matlab this was done by creating two equations to describe one function with the chosen intervals and z values described here, see Matlab script for more details.

Wheeler stretching is more difficult. This method uses the value at surface level obtained from the equation when z=0 and stretches it up to the crest, making a lower velocity at the surface level than the other approximation methods, [8]. According to [2] this method is not recommended, when operating with extreme value analysis as done here. This is because it underestimates the velocity at surface level.

The same method is also done with T_{min} and T_{max}, see figure 3.3 for the nine different plots.

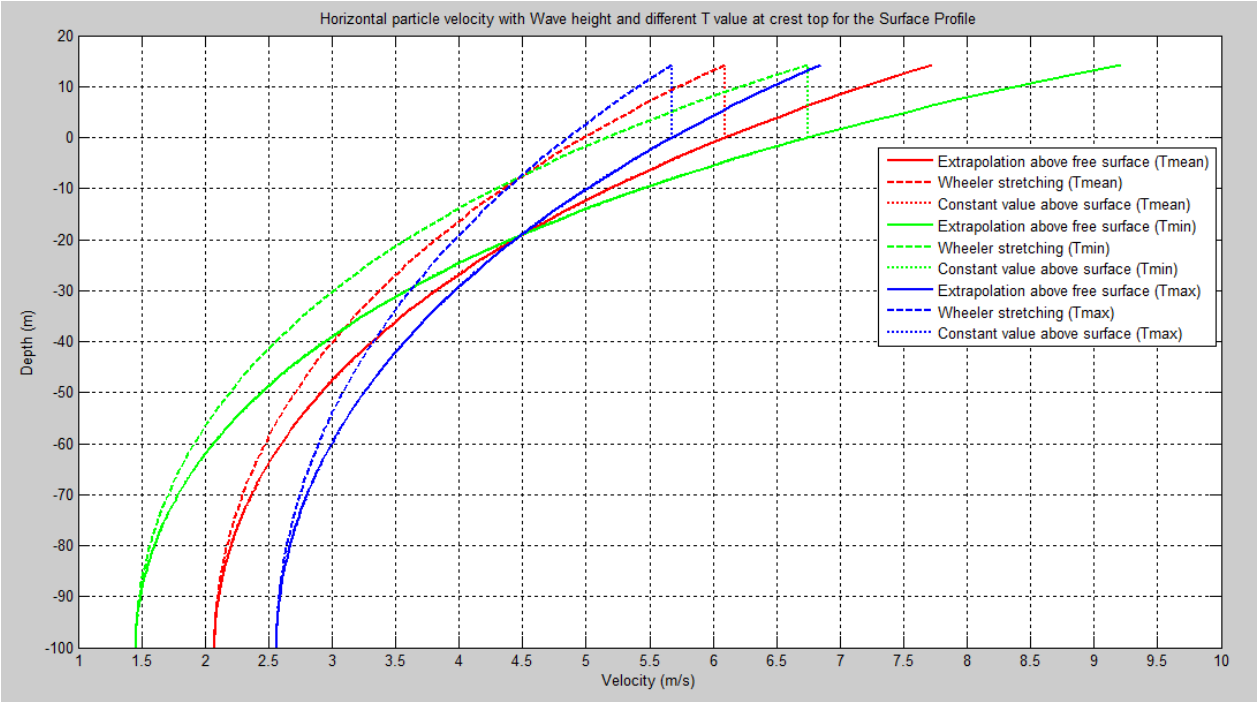

Figure 3.3. Horizontal particle velocity with different time period and estimation methods above surface level. Where amplitude is 14.3m and T_{min} = 13.64s, T_{max} = 17.74s and T_{mean} = 15.69s.

From what we can see of figure 3.3, the extrapolation is giving us an extremely large particle speed at the top of the wave, and wheeler stretching might be producing too low particle speed at the water surface as mentioned before. It will be very interesting to see if the constant value above the surface will be the closes approximation to a 5th order approach. This will be discussed later, when the loads and loads effects are obtained.

Another observation is that the wave with largest period has the most horizontal particle velocity when it approaches the sea bottom. This is because of the phase velocity is proportional to the wave period. This means that the long periodic waves have a waveform that moves faster than a wave with short period when it approaches a certain depth. The reason for an exponential decrement is because of the e^{kz}, where z is negative. We can also state that when $e^{-1000} = 0$ and $e^{-0,001} = 1$. This means that a large k will have larger decrease in horizontal particle velocity by depth than having a small k. The formula for k in deep water is: $k = \frac{(2\pi)^2}{T^2 * g}$ meaning that when we have a large T the k is smaller and we will have a smaller decries in velocity by depth. The last observation we can see is that the shortest period have the largest velocity at the surface. This is because when having an amplitude as 14.3 and changing time period the orbital path of the water molecules will still stay the same but the time they use will increase or decrease. By lowering the time period the water molecules will move faster to travel the same distance as before and that means the wave velocity will increase. See figure 3.4 for description on orbital pat of water molecules.

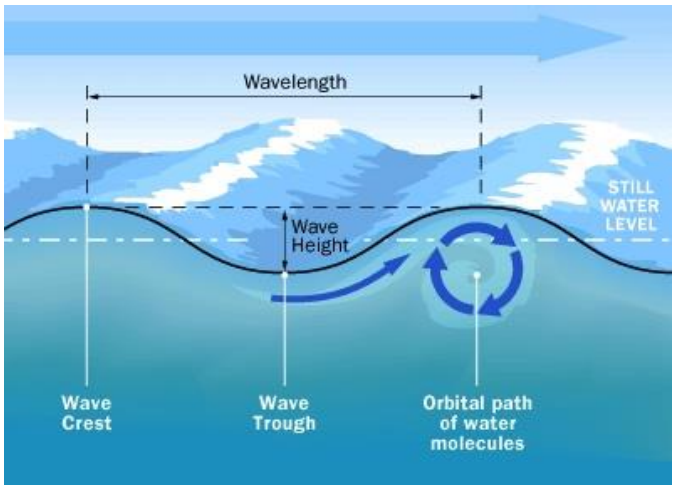

Figure 3.4. Description of wave profile and orbital path of water molecules.

3.2.2 Horizontal water particle acceleration with half the wave height as amplitude

For the acceleration, we know that the maximum value can be obtained at the mean surface level. When the surface profile is 0 and $\cos(\omega t - kx) = 1$ for horizontal particle acceleration. By this the following formula is:

$$a(z) = \zeta_0 * g * k * \frac{\cosh k(z+d)}{\cosh kd} \quad = 14.30 * 9.81 * 0.017 * \frac{\cosh 0.017 * (z+100)}{\cosh(0.017 * 100)}$$

Since the formula with $\cos(\omega t - kx) = 1$ its only valid up to the mean surface level, because the surface profile in this time is at mean water level. Meaning that Wheeler stretching, extrapolation or constant value from mean surface level up to the crest is not needed for maximum horizontal particle acceleration. For any other point in time, it would have been needed to use approximation above mean water level. For example, t = 1.5s when x = 0 as figure 3.2 shows us, an approximation above mean water level would have been needed up to the position in the surface profile, which is approximately 7.5m above mean water level. This is the same case for the horizontal particle velocity profile when time is changed. There will be more info about this when calculating loads for a drag and mass dominating case.

The results of horizontal particle acceleration for the three different periods is shown in figure 3.5.

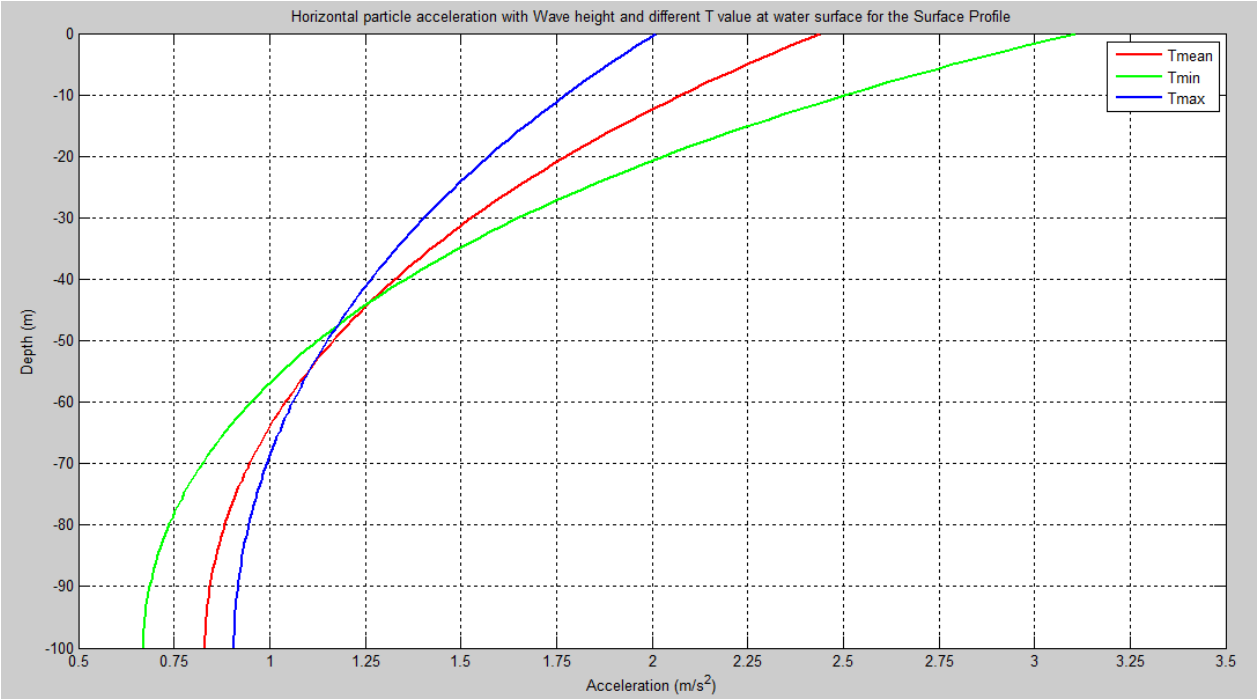

Figure 3.5. Horizontal particle acceleration with different time period. Where amplitude is 14.3m and T_{min} = 13.64s, T_{max} =17.74s, T_{mean} = 15.69s.

From figure 3.5, shows the same theoretical results as seen from figure 3.3. Explaining it more related to the acceleration. We mention that because of k, we can have an influence on e^{kz} that reduces the horizontal particle velocity and acceleration with depth. When having a large k meaning a low period and a faster reduction in horizontal particle velocity. Meaning that the acceleration will be larger for a low period and lower for a higher period. It is also because of the waveform we obtain a larger acceleration when approaching the sea bottom. Since the horizontal particle velocity at the mean surface level is largest with low period, it would need to have a large acceleration to achieve it, because it has the lowest velocity at the sea bottom. That's the reason for obtaining the largest acceleration with a short period at the surface.

3.2.3 Horizontal water particle velocities with crest height as amplitude

Now by changing the amplitude to the crest height ($\zeta_0 = 17.81$) obtained from chapter 2.4, we can see the differences with a larger amplitude and more realistic to a real wave. The same calculations methods are used as above for half the wave height. Except the only period required to check is the T_{mean} period according to [2]. The reason for only T_{mean} is shown are because of this value is sufficient for an approximation on the 100-year extreme crest height value as mention in [2]. T_{min} would have been a to large estimate for the loads later on. Results of this is plot and shown in figure 3.6. Note that the comparison plot between half the wave height and crest height as amplitude can be found at chapter 3.4.

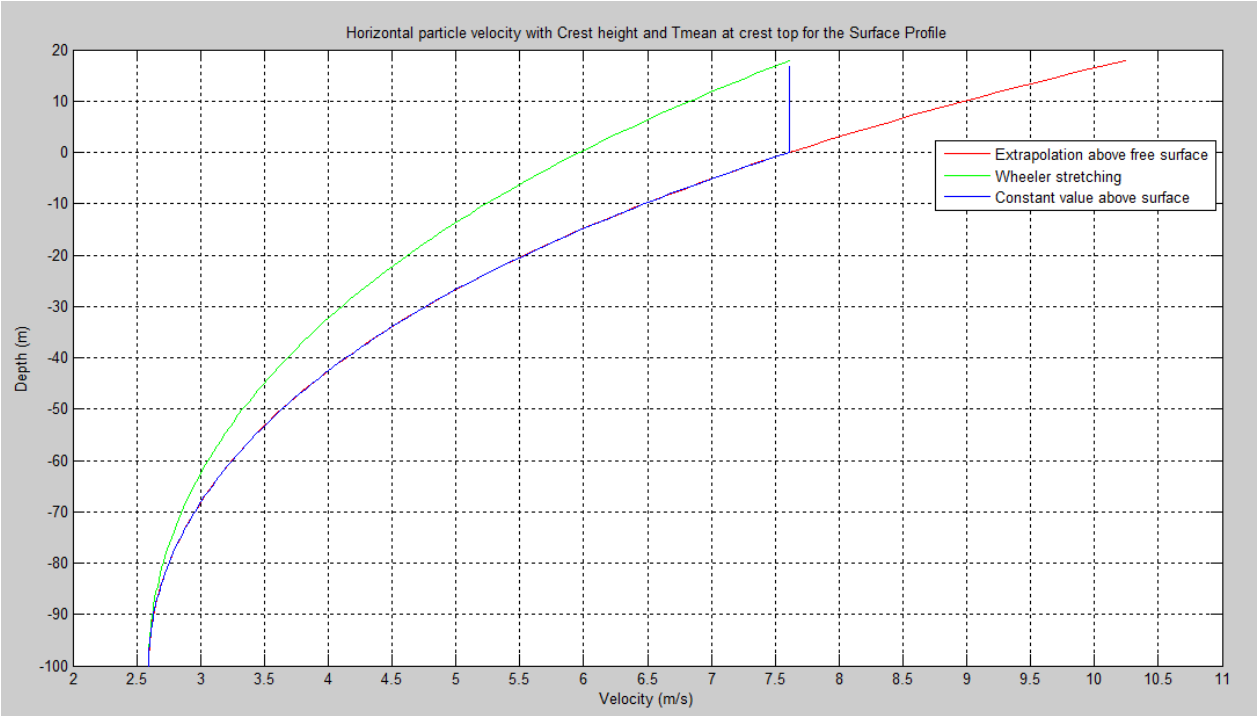

Figure 3.6. Horizontal particle velocity with crest height as amplitude (ζ_0=17.81), and T_{mean} = 15.69s using different estimation methods above the surface level.

We can clearly see from figure 3.6 that a larger amplitude will obtain a larger horizontal particle velocity by comparing with figure 3.4. This is because of the formula of horizontal particle velocity, where an increase in the amplitude the velocity in general will increase. The theoretical solution for this is when an increase in wave height occurs, the distance the water molecules need to travel for one period would increase. The particle velocity has to increase to travel the increased distance on the same time since the time period is the same. This is why we have a larger horizontal particle velocity with a higher amplitude and same period.

3.2.4 Horizontal water particle acceleration with crest height as amplitude

The acceleration for crest height as amplitude is done in the same manner as for half the wave height above except T_{mean} is only plotted and the amplitude is changed. Results of this plot can be seen in figure 3.7.

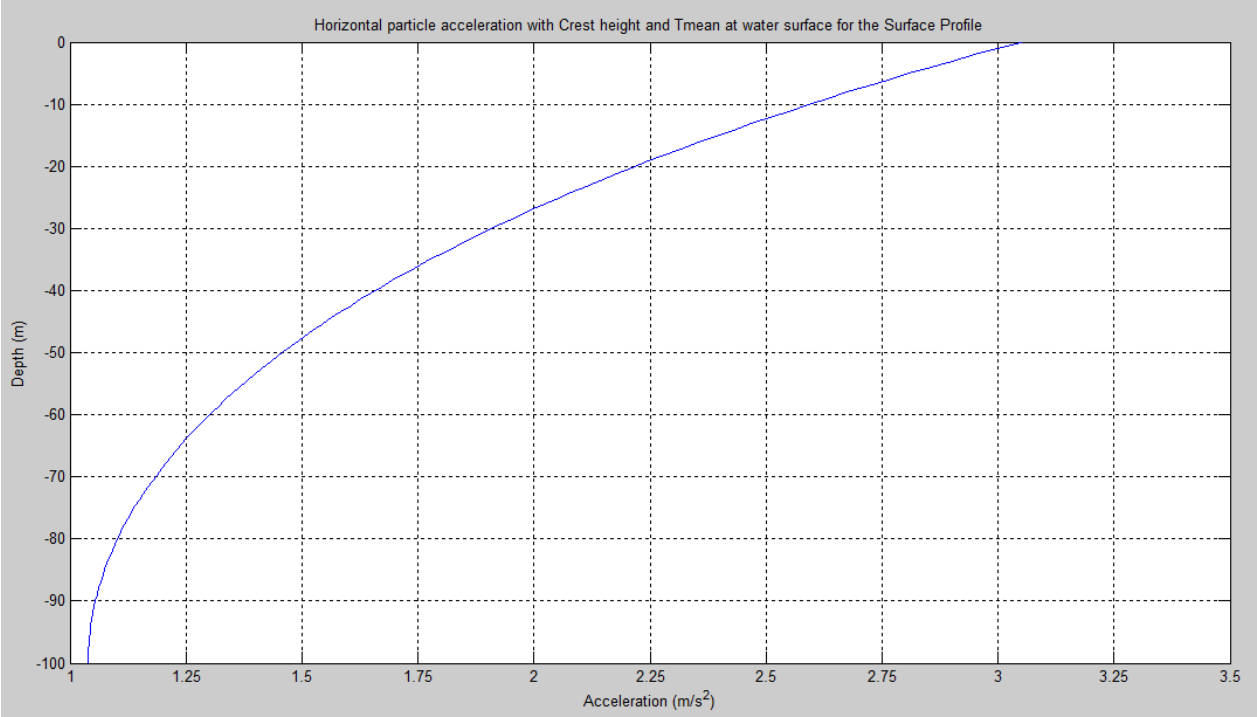

Figure 3.7. Horizontal particle acceleration with crest height as amplitude (ζ_0=17.81), and T_{mean} = 15.69s.

From figure 3.7, we can see that the acceleration is larger with a larger amplitude by comparing it with figure 3.5. The formula of acceleration shows that an increase in amplitude (ζ_0) will results in an automatically general increase all over the acceleration.

3.3 Stokes 5th order program

In this chapter, a Stoke 5th order program obtained from [3], is used to calculate the horizontal particle velocity and acceleration, for the extreme 100 year crest and wave height with an annual probability of 10^{-2}. Stokes 5th order program uses nonlinear term meaning it does not neglect the open elliptical orbit the water particles moves in and other simplification on linear terms. The open elliptical orbit causes a movement for approximately 2% of the phase velocity, [9]. Stokes 5th order program take in to account that the crest height are larger than the trough of a wave. This makes the wave much more realistic compared to real ocean waves. The application for this program are shown in figure 3.8 and is obtained from [13]. Where the worst case used in this thesis is:

$$\frac{H}{d} = \frac{30}{100} = 0.3 \quad \text{and} \quad \frac{L}{d} = \frac{300}{100} = 0.3$$

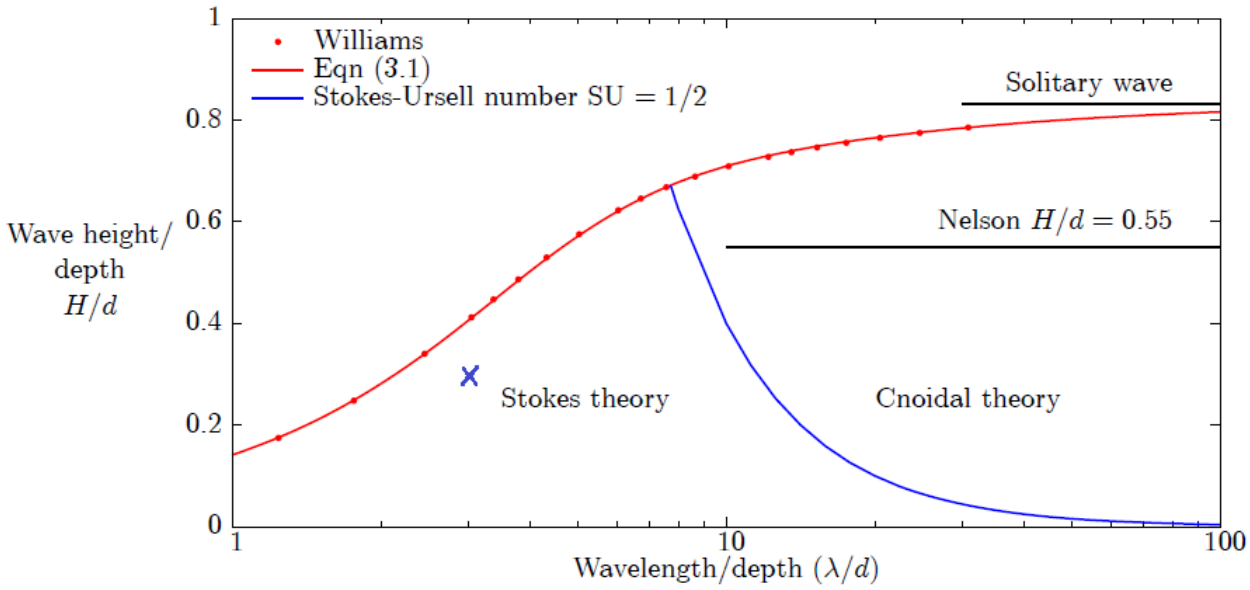

Figure 3.8. Shows the region where each equation fits and the blue X show where our wave would be.

3.3.1 How to use the program

From [3], three different programs can be obtain. They are named Fourier, Stokes and Cnoidal. For this thesis the only program used is the Stokes program, but for Stokes program to work the Fourier program needs to be unpacked at the same folder as the Stokes program. The Fourier program is the main program of those three. This program contains the input files needed to change the data. All data input are to be dimensionless by dividing or multiplying with d, depth and g, gravity. There are three different files that consist of data to be changed. The first one is the Data.Dat, it contains the data set of current and wave properties as the height and time period/wavelength. See table 3.1 for the possible input. As show in table 3.1, there are no current conditions because the magnitude here is set to 0. Current is not taken into account in this thesis.

Table 3.1. Data input for Data.Dat, showing a wave with wave height 28,61m and a T_{max} = 17,74s

0.2861	H/d
Period	Measure of length: "Wavelength" or "Period"
5.5562	Value of that length: L/d or T(g/d)^1/2 respectively
1	Current criterion (1 or 2)
0.0	Current magnitude, (dimensionless) ubar/(gd)^1/2
5	Number of Fourier components or Order of Stokes/cnoidal theory
2	Number of height steps to reach H/d
FINISH	

Next file is the Convergence.dat file, which contains the following shown in table 3.2.

Table 3.2. Data of the program Convergence.dat

Control file to control convergence and output of results	
40	Maximum number of iterations for each height step; 10 OK for ordinary waves, 40 for highest
1.e-5	Criterion for convergence, typically 1.e-4, or 1.e-5 for highest waves

The last data file contains the information of how much data should be computed for the plots. The file name is Points.dat and shown in table 3.3.

Table 3.3. Data of the program Points.dat

Control output for graph plotting	
100	Number of points on free surface
180	Number of velocity profiles over half a wavelength to print out
100	Number of vertical points in each profile

After putting in the correct input data for those three files the Stokes program can be placed in a subfolder of the Fourier program. This allows us to use those data files with stokes program and by starting the program, it will create three more files of result data. Where the first result file is Solution.res. This contains all the properties of the wave, some constants used and other max values. See Solution.res file for more info. The two other files are more interesting, since those are the files used in this thesis. The name of those are Flowfield.res and Surface.res. Surface.res contains data of the surface profile for the wave, and the Flowfield.res file compute all the velocity and acceleration data for bout horizontal and vertical depending on the depth. Flowfield.res file also compute all the data for each phase requested in Points.dat. In this thesis Microsoft Visual Studio is used to open and edit all of those files. All of the result (.res) files can also be opened in excel to later be imported to Matlab. To learn more about the programs see [13] obtained from [3].

For the last file used in Stokes, program, we have Figures.plt. This file can be opened with Gnuplot. The file contains all the plots for surface profile, horizontal/vertical particle velocity and acceleration dependents of depth and time. See figure 3.9 and 3.10 for illustration of the horizontal particle velocity and acceleration plots with some theoretical explanations.

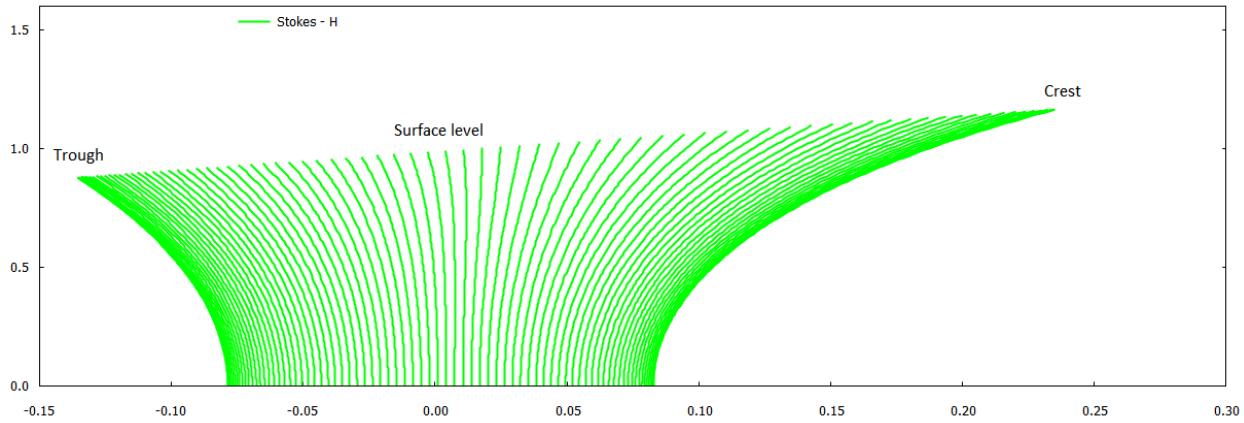

*Figure 3.9. Stokes velocity plot depending on depth with varying phase angle between Crest and Trough. 100 points between Crest and Trough. (Half a wavelength). Y-axes are Z/d where d is depth (100m) and Z is the varying depth position. X-axes is velocity in V/sqrt(g*d), where g is gravity 9.81m/s^2.*

From figure 3.9, we can clearly see that the velocity is at its max at crest as explained earlier. The horizontal particle velocity has a linear decree down to the trough and 0 horizontal particle velocity at the surface level.

Figure 3.10 displays the acceleration plot, which show us that the maximum acceleration point is at the mean surface level as mentioned earlier.

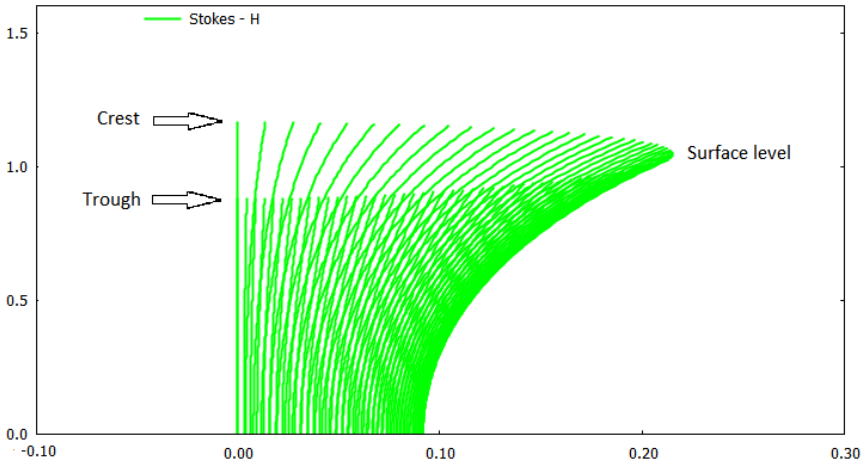

*Figure 3.10. Stokes acceleration plot depending on depth with varying phase angle between Crest and Trough. 100 points between Crest and Trough. (Half a wavelength). Y-axes are Z/d where d is depth (100m) and Z is the varying depth position. X-axes is acceleration in A/sqrt(g*d), where g is gravity 9.81m/s^2.*

3.3.2 Result of the program

We are now going to find the surface profile, horizontal particle velocity and acceleration for four different cases. Where three of them will have the wave height as $h_{0.01}$ = 28,61m with different period as we did for the linear waves. The period used is $T_{min} = 13.64s$, $T_{mean} = 15.69s$ and $T_{max} = 17.74s$. The fourth case is with a crest height equal to $c_{0.01}$ = 17.87m.

To obtain a crest height, equal to $c_{0.01}$ with the Stokes program an iteration needed to be performed. This was done by choosing a wave height and controlling the crest height result until the same crest height equal to $c_{0.01}$ = 17.87m where obtained. The wave height used for obtaining this crest height was 30.14m. The input used are shown in table 3.1, 3.2 and 3.3, except for the period and wave height as shown in table 3.4.

Table 3.4. Data used for obtaining surface profile, horizontal particle velocity and acceleration for different waves, with the use of Stokes program.

Data input for Stokes program, Non dimensions.				
	Wave height with $h_{0.01}$			Wave height with $c_{0.01}$
	T_{min}	T_{mean}	T_{max}	T_{mean}
Wave height = $\frac{h_{0.01}}{d}$ or $\frac{c_{0.01}}{d}$	0.2861	0.2861	0.2861	0.3014
Period = $T * \sqrt{\frac{g}{d}}$	4.27	4.91	5.56	4.91

From those input, all the necessary wave data where obtained. See figure 3.12 to 3.14 for the different plot results. The actually number are stored in the attached files in folder named “2-3. Stokes data for regular waves”.

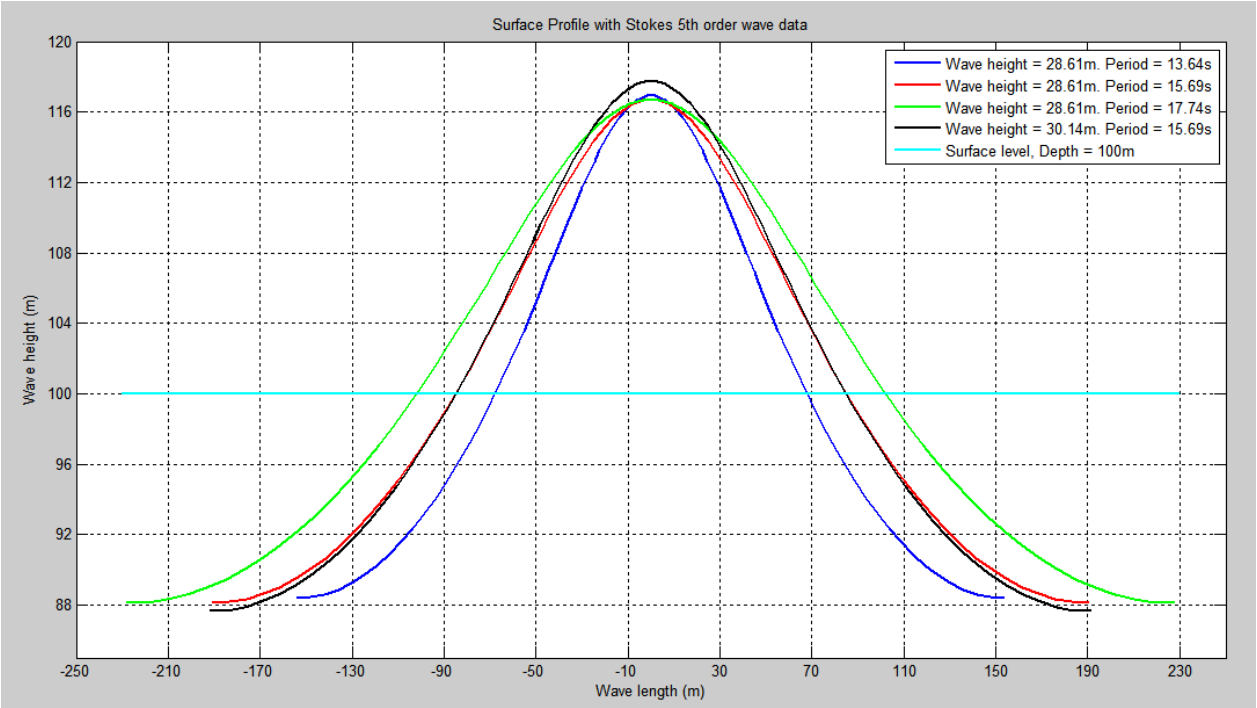

Figure 3.11. Surface profile for four different waves with the use of Stokes program.

Figure 3.11 shows the surface profile for our four different cases. The plot is as expected, since the wavelength is depending on the period, we can see that the shortest wave is the one with the smallest period and the crest height are also larger than the trough. There are also some evidence in the plot that by shortening the period with the same height we will have a higher peak (crest height) and a trough that is closer to mean surface level. This can be seen by looking at the plots which uses $h_{0.01}$ as the wave height and different wave periods.

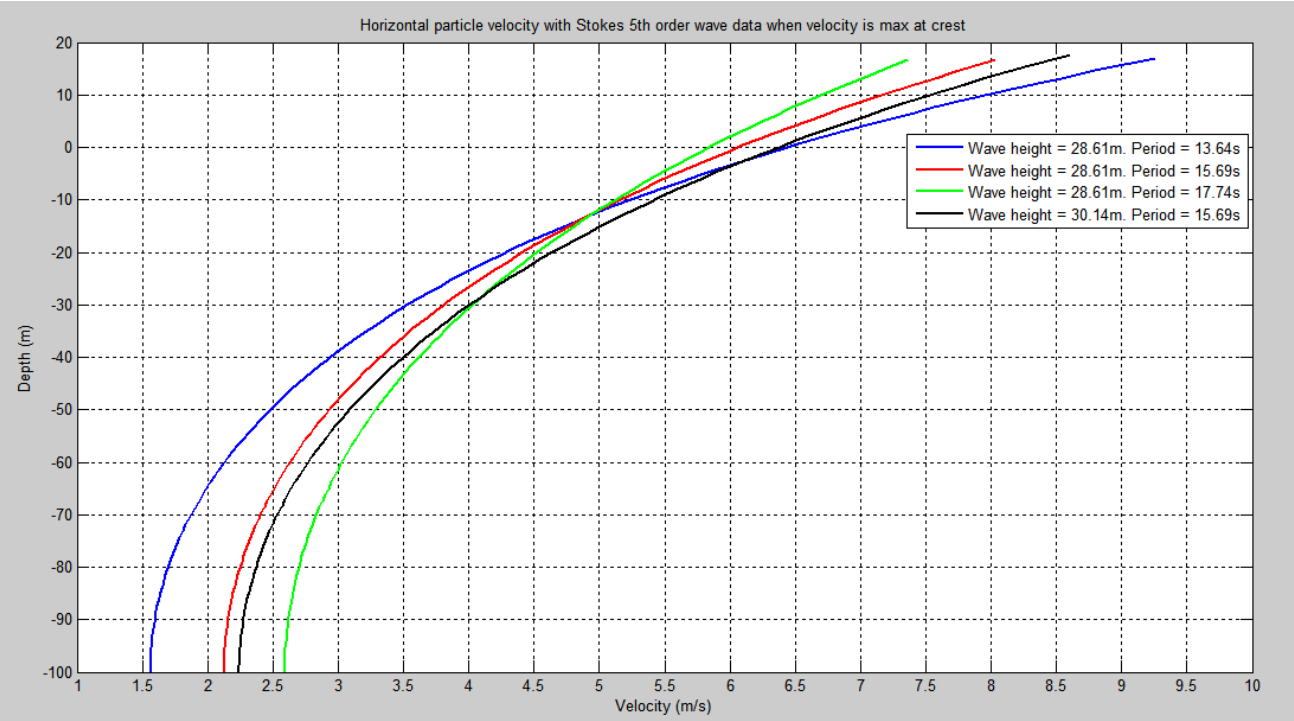

Figure 3.12. Horizontal particle velocity for four different waves with the use of Stokes program.

Results for the horizontal particle velocity at the crest can viewed in figure 3.12. The same theoretical result as discussed under figure 3.3 applies also here. In this plot, there are two waves with different wave height but same period. Which shows us that by increasing the amplitude one will increase the velocity in a parallel manner as the one with lower amplitude.

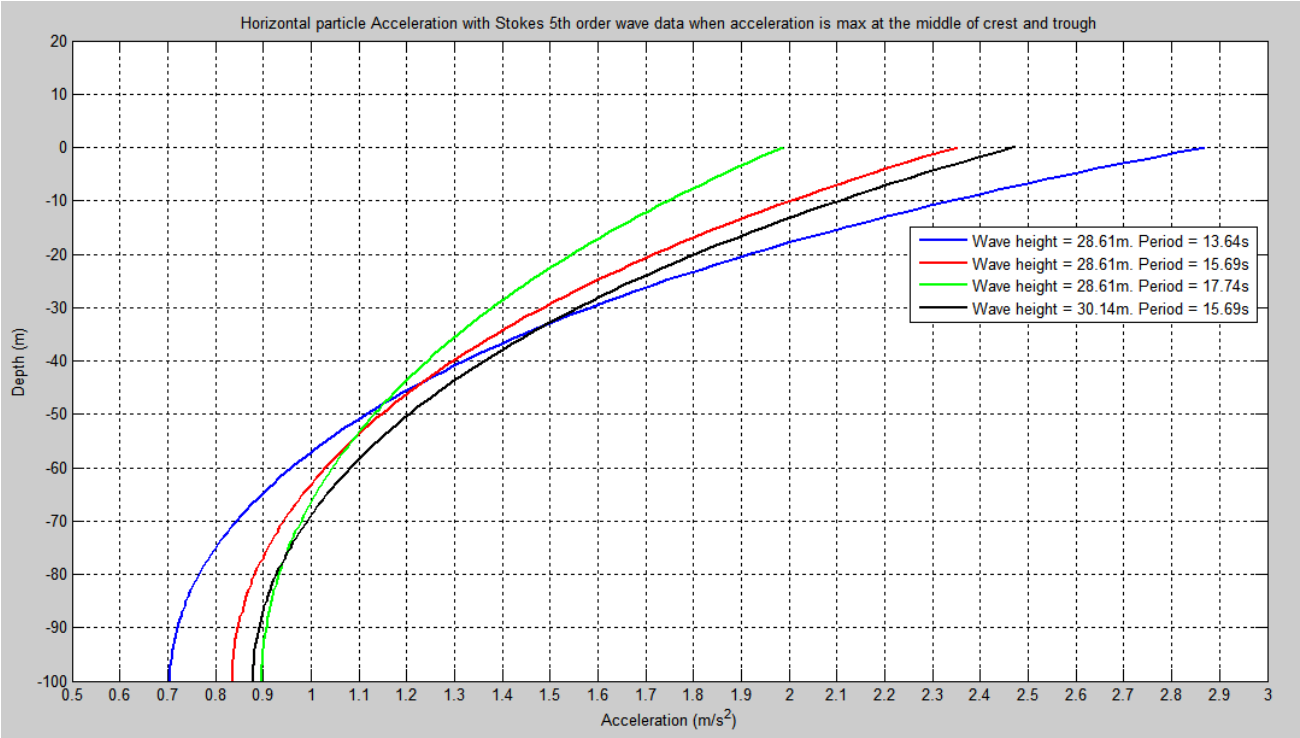

Figure 3.13. Horizontal particle acceleration for four different waves with the use of Stokes program.

Figure 3.13 shows us the acceleration obtained for our four cases at mean surface level. This position is at time and position 0 for surface profile. For comparison between Stokes and linear kinematics see chapter 3.4, which is the following chapter.

3.4 Comparison between linear wave and 5th order Stokes wave

A total of 16 different horizontal particle velocity profile has been obtained. That is why we will shorten down our plots in this comparison. As mentioned in the introduction a comparison of the old and new NORSOK N-003 standard would be performed. Where the old N-003, [1] recommended $h_{0.01}$ as the wave height, for the ULS design wave with the worst associated period. For the new N-003, [2] it recommended to use $c_{0.01}$ as the crest height for the ULS design wave with a mean period value. This means, we would have a higher crest height for the new N-003 than the old N-003 and would result in a larger horizontal particle velocity. An observation done earlier showed that the lowest period is the worst case for the velocity. That is why we are using the lowest period associated with $h_{0.01}$ to compare with a crest height associated with a mean period value as recommended. See figure 3.14 for horizontal particle velocity comparison between the old and new N-003 approach and a 5th order stokes wave. Figure 3.15 shows horizontal particle acceleration for the same comparison.

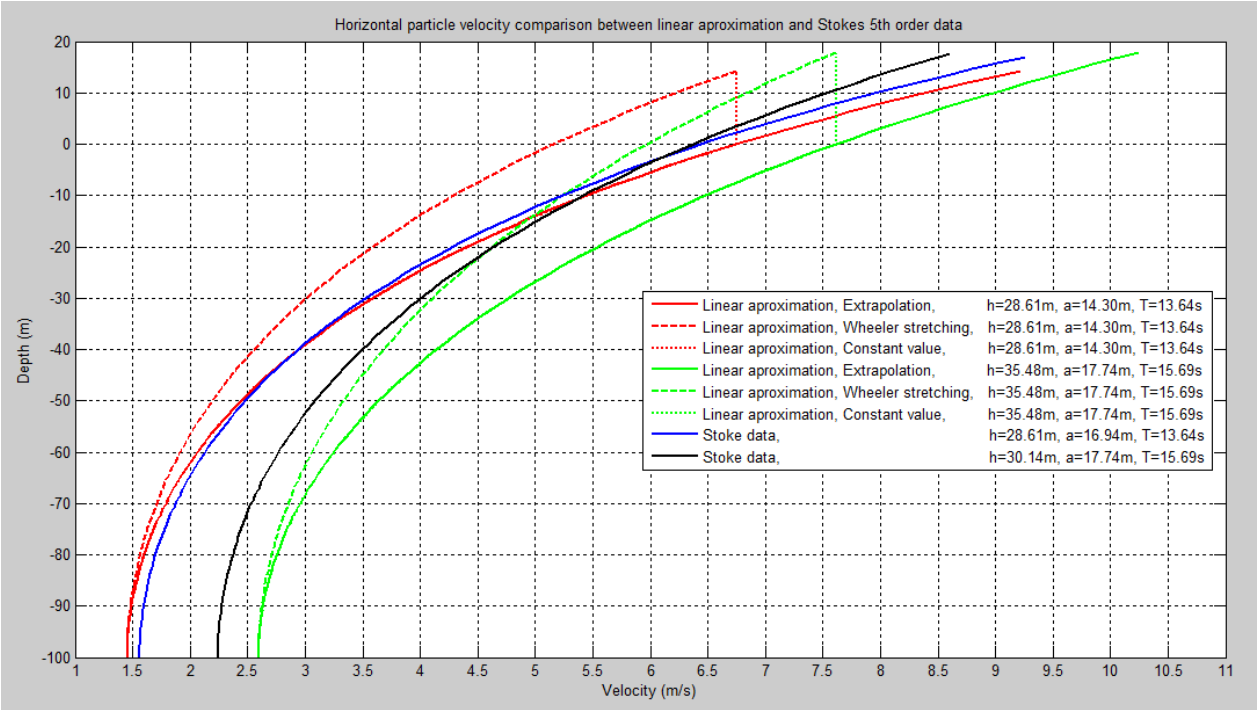

Figure 3.14. Comparison of horizontal particle velocity at crest, between linear wave and fifth order stokes wave results.

Figure 3.14 shows the differences between a linear and a non-linear approach. By look at the linear term with half the wave height as amplitude and T_{min} for period, we can see that the linear term is a good approximation, for both extrapolation as upper value and constant value above mean surface level as a more accurate or right below the approximation for Stokes 5th order kinematics.

The reason we have a good approximation for this term, when linear approach estimates a higher value than a non-linear term is because of the half the wave height is used as the amplitude. This gives us a lower amplitude compared to a Stokes wave, but the linear term calculate a higher kinematic value to make up for the low amplitude. By using the Stokes program, the program calculates a higher crest height (amplitude) like in real ocean, but are more accurate with the horizontal particle velocity profile for that amplitude. Meaning that we achieves a good approximation for the linear term. However, Wheeler stretching does not have a good approximation. This approximation give us a much lower value than expected and we can clearly see why the new N-003, [2] do not recommend the use of Wheeler stretching for extreme waves.

By looking at the comparison between the new recommendations from N-003, we can clearly see that the linear term is giving a much higher value by using the $c_{0.01}$ as the amplitude and T_{mean} as period. This is because what we discussed above does not happen here. Meaning that the linear term will give a much higher approximation, since it does not use a simplification for the amplitude. However, the Wheeler stretching may be a good solution for this, but is a bit lower than the horizontal particle velocity from a Stokes wave. Horizontal particle velocity with constant value above surface level would be a better solution here, since this would be right above the Stokes approximation value and on the safe side. For the extrapolation approach a to large horizontal particle velocity is obtained compared to a Stokes wave, showing that this approach overestimates the kinematics with the crest height as amplitude. More comparison with other values would be needed, to verify that the same case happens each time a crest height is used as the amplitude. This will not be done here, but may be suggested for further study's. Comparing the recommendations from the old and new N-003 standard in figure 3.14 would not give any confirmed answers. Since the horizontal particle velocity is too similar in total for bout cases. Later on there will be more discussions for this subject, when the loads and loads effects has been calculated by Morison equation.

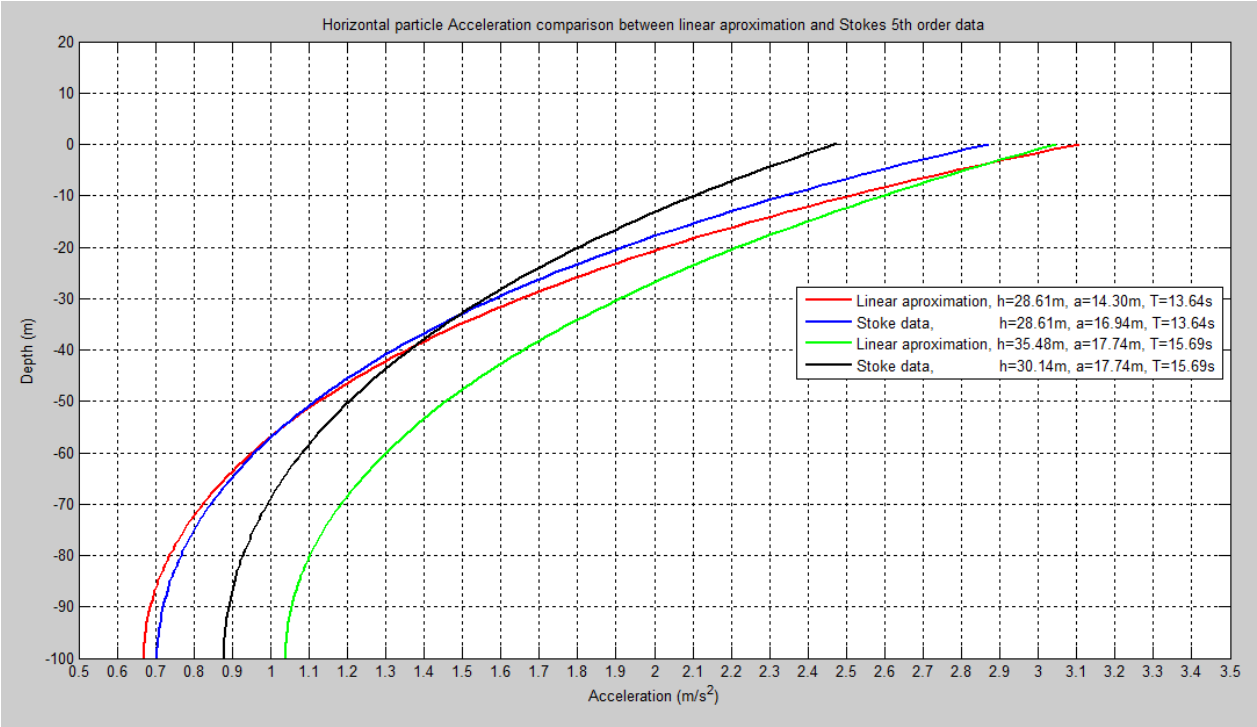

Figure 3.15.Comparison of horizontal particle acceleration at surface level, between linear wave and fifth order stokes wave results.

The acceleration plot shows the same result as mentioned under the horizontal particle velocity plot, but here it displays the consequences for using the crest height as the amplitude in a linear approach much better. Showing that this is a bad approximation to Stokes waves. Therefore, it wouldn't be recommended to use a linear approach with the use of crest height as amplitude, only the use of half the wave height as amplitude is sufficient. Especially for an acceleration case. For half a wave height, we can see that the linear term has a little higher value of the Stokes wave, but still a good and safe approximation.

3.5 Loads and load effects using linear wave theory and Stokes 5th order

The next step is to find the loads and load effects that has been limited to base shear and overturning moment for our 16 different approaches. This is going to be done by three different cases, where those cases are depending on different diameter of the column. Morison equation will be used for this and by having the three different cases, we would be able to find results of a mass, drag or a mass/drag dominating structure. First of all an introduction to Morison equation has to be done and what condition it can be used in.

3.5.1 Morison equation

Morison equation is an equation used to summarize the loads caused by waves on a vertical structure in water. From the equation, base shear and overturning moment can be acquired in an accurate way for the whole structure. It is not a good method to describe the load history on depth dependents in an accurate way, [14]. This is because of a coefficient that varies with depth, but the coefficient usually is a constant for the whole structure, which is divided in two groups. One above surface and one below. More about this coefficient (C_d and C_m) is found in chapter 3.5.2.

Some other limitations are as following, according to [14], [15]:

- Morison equation do not give a good representation on the forces as a function of time when extended to orbital flow. For an example with a horizontal cylinder under waves.
- It does not take in to account the lifting force due to vortex shedding
- It is only valid for relatively small motions of the cylinder, meaning that for Morison equation to be valid it has to be $\frac{a}{D} < 0.2$ where D is the diameter of the cylinder and a is the amplitude of motion for the cylinder. Later on, we will only assume that the column is stiff enough to satisfy this condition.
- This equation is only valid for waves that do not breaks. This is because the equation do not take in to account the forces from slamming waves that hit the structure extended above surface. This means that $\frac{H}{L} < \frac{1}{7} = 0.14$ has to be satisfied or else the wave can break.
- The last limitation discussed here is that the diameter of the cylinder has to be much smaller than the wavelength to satisfy this equation. The reason for this is that the flow acceleration needs to be approximately uniform to the cylinder. If not, then the reflection of the waves from the cylinder has to be taken in to account.

Now that this is known, an introduction to the formula for base shear can be introduced. The name of this formula is Morison equation and obtained from, [14]. The formula can be seen in equation 3.23.

$$f(z,t) = f_M(z,t) + f_d(z,t)$$

$$= \left(\frac{\pi D^2}{4} * \rho * C_M * A\right) + \left(\frac{1}{2} * \rho * \mathrm{C_D} * \mathrm{D} * V * |V|\right) \qquad \text{Equation 3.23}$$

Where $f_M(z,t) = \left(\frac{\pi D^2}{4} * \rho * C_M * A\right)$ is the mass term, and D is diameter of cylinder, A is the acceleration found earlier. ρ is the water density and C_M is the mass coefficient determined from experiments.

For the drag term, $f_d(z,t) = \left(\frac{1}{2} * \rho * \mathrm{C_D} * \mathrm{D} * V * |V|\right)$, V is the velocity found earlier and C_d is the drag coefficient determined from experiments.

Finding the max force one can sum up all the forces using an integral. This is done with the formula shown below. Where ξ is the position of the wave profile in that time when x = 0. For an example if one are, calculating the loads when the velocity is max, the position would be at the crest and ξ would be the crest height. At time zero and x =0 the amplitude ξ would have been 0 acording to figure 3.2.

$$F(t) = \int_{-d}^{Surface} f(z,t)dz = \int_{-d}^{\xi} f_M(z,t)dz + \int_{-d}^{\xi} f_d(z,t)dz \qquad \text{Equation 3.24}$$

This formula can be simplified when having a mass or drag dominating force. To see if one have a dominating force one can use the following equations:

Mass term dominates when: $0{,}5 < \frac{D}{H} < 1{,}0$

Drag term is dominating when: $\frac{D}{H} < 0{,}1$

Meaning that: $0{,}1 < \frac{D}{H} < 0{,}5$ would result in no dominating forces and no simplifications can be performed.

Those simplifications are:

When mass term dominate. Max value can be found at the mean surface level of wave, where the horizontal particle acceleration is max and horizontal particle velocity is 0 meaning that $f_d(z,t) = 0$. Therefore, one can obtain the following formula for base shear:

$$F(t) = \int_{-d}^{0} f_M(z,t)dz = \int_{-d}^{0} \left(\frac{\pi D^2}{4} * \rho * C_M * A \right) dz \qquad \text{Equation 3.25}$$

For a drag dominating case, which is max when the horizontal particle velocity is max. This is at the crest top where the horizontal particle acceleration is 0 and $f_M(z,t) = 0$. From this, one can obtain the following simplification:

$$F(t) = \int_{-d}^{\xi_0} f_D(z,t)dz = \int_{d}^{\xi_0} \left(\frac{1}{2} * \rho * \mathrm{C_D} * \mathrm{D} * V * |V| \right) dz \qquad \text{Equation 3.26}$$

A more theoretical way to look in to a drag or mass dominating case is to understand the eddy currents occurred when water passes the column. When large eddy currents occur, there will be a change in force where an acting force parallel and perpendicular to the current direction occurs. This a drag dominating case. Figure 3.16 shows what eddy current is. The circle in middle shows the column and the others are waves passing the column.

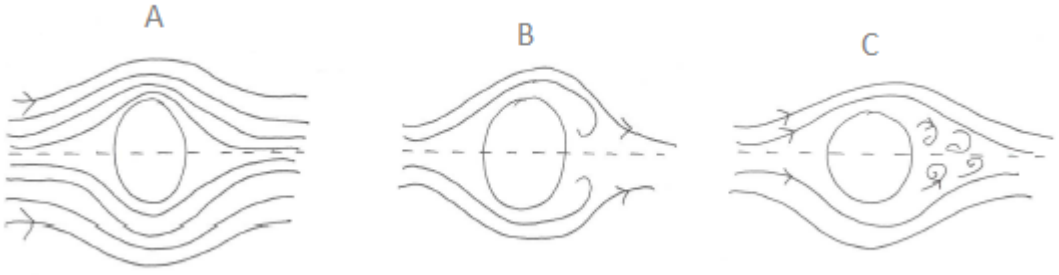

Figure 3.16. Creation of eddy current. Where A has none, B has an increment and C has large eddy currents.

Eddy currents are created when one have rapid flow or small cylinder compared with the wave height. This create a drag dominating case. The roughness of the cylinder may also case more or less eddy currents. If one have a smooth surface on the column it would be harder for eddy currents to occur. The mass dominating case will have the opposite as a drag dominating case. Where flow passes the cylinder slow and the flow term changes before a large number of eddy current would generated, or D is large and few eddy currents would generated.

One can also find the overturning moment by the adding to the Morison equation. The Morison equation finds the forces for each step down to the sea bottom. Therefore one can add multiply the forces for each step with the distance down to the sea bottom to acquire the overturning moment. This is done by adding $(z + d)$ to the Morison equation, see equation 3.27, [14].

$$M = \int_{-d}^{Surface = \xi} (z + d) * f(z, t)\, dz \qquad \text{Equation 3.27}$$

Bear in mind that ξ is the position height from the mean surface level up to the wave position in that time, which changes for each time step. In Matlab, this has been solved by first running a wave profile to determine this position and then used it in the Morison equation. This method is only needed when there are no dominating forces.

3.5.2 Drag and mass coefficient

According to [2] and [8] one can determine those coefficients with the use of the Keulegan-Carpenter number. This formula is shown in equation 3.28:

$$N_{KC} = \frac{T * V_0}{D} \qquad \text{Equation 3.28}$$

Where T is the period and V_0 is the largest water particle speed under the crest.

With Keulegan-Carpenter number (KC > 60 for C_D and KC > 20 for C_M), one can use the following values for tubular structures according to, [2]:

C_D = 0.65 and C_M = 1.6 for smooth members
C_D = 1.05 and C_M= 1.2 for rough members

For a lower, KC<60. One would need to multiply the drag coefficient C_D with a wake amplification factor (KC). According to [8] one can find $C_D$with a low KC from:

$$C_D = C_{DS}(\Delta) * \Psi(K_C) \qquad \text{Equation 3.29}$$

Where $C_{DS} = 0.65$ for smooth and $C_{DS} = 1.05$ for rough cylinder.

And KC < 12:

$$\begin{aligned} \Psi(K_C) &= C_\pi + 0.10 * (K_C - 12) && when && 2 \le K_C < 12 \\ \Psi(K_C) &= C_\pi - 1.0 && when && 0.75 \le K_C < 2 \\ \Psi(K_C) &= C_\pi - 1.0 - 2.0 * (K_C - 0.75) && when && K_C \le 0.75 \end{aligned} \qquad \text{Equation 3.30}$$

Where:

$$C_{\pi} = 1.50 - 0.024 * \left(\frac{12}{C_{DS}} - 10\right)$$ Equation 3.31

For higher value of KC the $\Psi(K_C)$ can be obtained from figure 3.17.

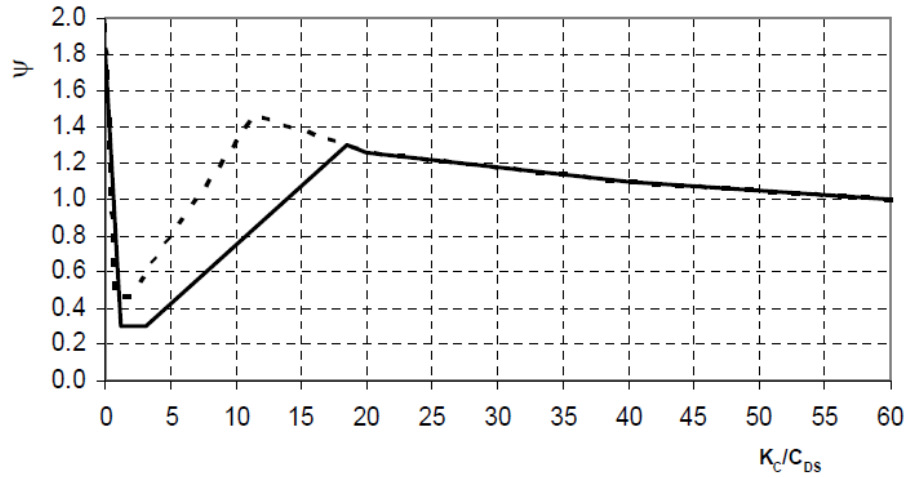

Figure 3.17. Wake amplification factor as function of KC-number with dotted line as CDS = 1.05 (rough surface), and solid line as CDS = 0.65 (smooth surface)

To find the mass coefficient C_M for this case one would need to use the following figure 3.18:

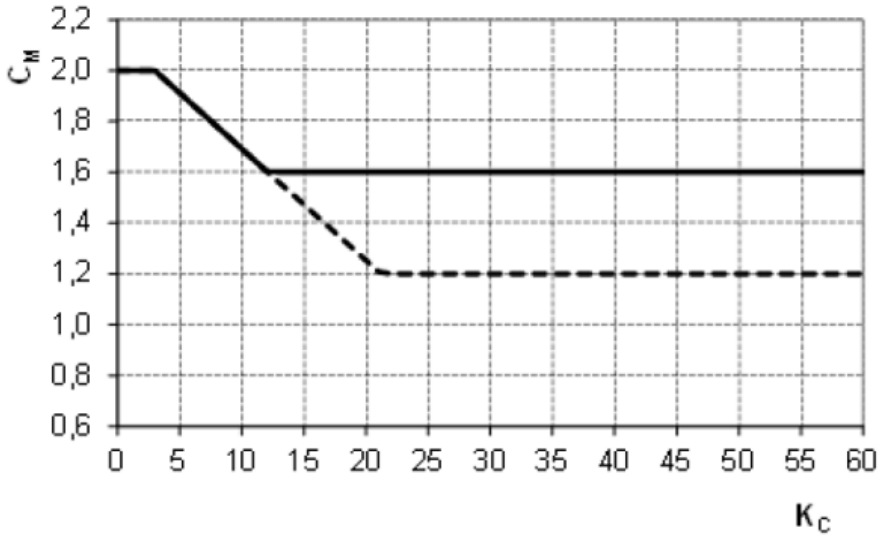

Figure 3.18. Mass coefficient CM as function of KC, where dotted line is rough and solid line is smooth for tubular members.

To obtain the roughness of the cylinder one can use the formula obtained from [8] where:

Smooth for: $\frac{k}{D} < 10^{-4}$

Rough for: $\frac{k}{D} > 10^{-2}$

k is the surface roughness.

3.5.3 Determine mass and drag coefficient used.

First of all we need to determine the mass and drag coefficients and the assumptions use here is that the column has a smooth surface from two meters above mean surface level an upwards. Meaning that below this point the column is rough. Next will be to simplify the work with only one mass/drag coefficient for each column diameter. One could do this more accurate but this is not the point for this theses. This is why simplifications has been used and we also have 48 different load cases. By using 1 meter as the diameter, one will obtain a drag dominating force as shown below.

$\frac{1}{28.6} = 0.03 < 0{,}1 \quad \longrightarrow \quad \text{Drag dominating-}$

D = 1 meter. From this, one can obtain a KC of:

$$N_{KC} = \frac{17.74 * 5.6}{1} = 120$$

Where T_{max} and max horizontal particle velocity from wheeler stretching and constant value above surface level has been used as V_0. For the lowest value T_{min} has been used and max horizontal particle velocity for wheeler stretching and constant value above surface level as V_0:

$$N_{KC} = \frac{13.64 * 6.75}{1} = 92$$

By having a a drag dominated case, we will only need to find C_D because the mass term will be 0 at the crest top, where max drag forces is obtained. This is because the horizontal particle velocity controls the drag term and horizontal particle velocity is max at the crest. With a > 60 for C_D one can obtain a:

C_D = 0.65 for smooth members
C_D = 1.05 for rough members

Doing the same for a D = 20m, we will have that:

$$0{,}5 < \left(\frac{20}{28.6} = 0.7\right) < 1{,}0 \quad \longrightarrow \quad \text{Mass dominating}$$

And:

$$N_{KC} = \frac{17.74 * 5.6}{20} = 6, \qquad N_{KC} = \frac{13.64 * 6.75}{1} = 4.6$$

The average for those two are 5.3 and to be on the safe side we have chosen a KC on 5.5. One will not need to find C_D for this case since mass is a dominating force. To obtain C_M one can use figure 3.18 and see that:

C_M = 1.9 for smooth members
C_M = 1.9 for rough members

The last diameter used is 5 meter. This is going to have a non-dominating force. For this case bout C_M and C_D needs to be obtained.

$$0{,}1 < \frac{5}{28.6} = 0.19 < 0{,}5 \quad \longrightarrow \quad \text{non} - \text{dominating}$$

And:

$$N_{KC} = \frac{17.74 * 5.6}{5} = 19.9, \qquad N_{KC} = \frac{13.64 * 6.75}{5} = 18.4$$

The average KC is 19.2, from this one can obtain the C_M from figure 3.18 and to be on the safe side the following has been obtained:

C_M = 1.6 for smooth members
C_M = 1.25 for rough members

For C_D, one need to use figure 3.17 to obtain the Wake amplification factor $\Psi(K_C)$. The Wake amplification factor $\Psi(K_C)$ is 1.25 for smooth and rough members. The result are as following:

$$C_{D_{rou}} = 1.05 * 1.25 = 1.31$$

$$C_{D_{smo}} = 0.65 * 1.25 = 0.81$$

For a better view of the coefficient chosen, see table 3.5.

Table 3.5. Mass and Drag coefficients used for different diameters.

	Diameter and dominating force		
Coefficient	D=1m, drag	D=5m, drag/mass	D=20m, mass
Cd-rough	1.05	1.31	---
Cd-smooth	0.65	0.81	---
Cm-rough	---	1.25	1.9
Cm-smooth	---	1.6	1.9

3.5.4 Load Results from Morison equation.

The following formula has been used to calculate the forces:

$$F(t) = \int_{-d}^{\xi} \left(\frac{\pi D^2}{4} * \rho * C_M * A \right) dz + \int_{-d}^{\xi} \left(\frac{1}{2} * \rho * \mathrm{C_D} * \mathrm{D} * V * |V| \right) dz \quad \text{Equation 3.32}$$

$$M(t) = \int_{-d}^{\xi} \left(\frac{\pi D^2}{4} * \rho * C_M * A \right) * (z + d) dz + \int_{-d}^{\xi} \left(\frac{1}{2} * \rho * \mathrm{C_D} * \mathrm{D} * V * |V| \right) * (z + d) dz \quad \text{Equation 3.33}$$

Where V is the horizontal particle velocity and A is the horizontal particle acceleration found earlier in chapter 3.2 and 3.3. There are a total of 12 different linear horizontal particle velocity/acceleration profiles and 4 non-linear horizontal particle velocity/acceleration profiles from Stokes program. This gives a total of 48 load cases by having 3 different diameters, (1m, 5m and 20m). ξ is varying since this is the height which is integrated up to. This is decided with the help of surface profile: $\xi = a * \sin(\omega t - kx)$. Where position x = 0 and t is varying. Example, t = $\frac{\pi}{2\omega}$ represents a position at the crest top and t = 0 is at the mean surface level. We have also taken in to account that the C-coefficient is different from 2 meters above mean surface level and upwards compared with below 2 meters above mean surface level. This is not shown in this equation, but has been done in the Matlab files used, Appendix A shows all the Matlab files created for this thesis. Another constant used in those equations are $\rho = 1025\ kg/m^3$, this is the water density for seawater. Results can be seen in table 3.6 to 3.8. Where d = 1m for drag dominating forces and max loads are found at the crest top. For d = 20m, which causes mass dominating forces where maximum loads can be found at the mean surface level of the wave. d = 5m is a non-dominated case, which has to be iterated for each scenario to acquirer the worst case for base shear.

Table 3.6. Load results for column diameter 1m, drag dominating forces. Where 1GN =10^3 MN = 10^6 kN = 10^9 N. X^o for Stokes waves instead of time for linear waves. Crest top is the x-position when 0^o, mean surface level is approximately 80^o and through is at 180^o. Max value obtained at the crest top.

	Forces on simplified offshore structures according to different wave models where: D=1m (Drag dominating force)						
Case name:	Period, T.(s)	Wave height, h.(m)	Amplitude, a.(m)	Height over surface, ξ.(m)	Wave phase (s or ^{o})	Force, F.(MN)	Moment, M.(MNm)
Extrapolation, $T_{min}/h_{0.01}$	13.64	28.61	14.30	14.30	3.41s	0.917	79.40
Constant a.s, $T_{min}/h_{0.01}$	13.64	28.61	14.30	14.30	3.41s	0.833	70.10
Wheeler, $T_{min}/h_{0.01}$	13.64	28.61	14.30	14.30	3.41s	0.590	48.75
Stokes, $T_{min}/h_{0.01}$	13.64	28.61	16.94	16.94	0^o	0.934	81.67
Extrapolation, $T_{mean}/h_{0.01}$	15.69	28.61	14.30	14.30	3.92s	0.898	71.16
Constant a.s, $T_{mean}/h_{0.01}$	15.69	28.61	14.30	14.30	3.92s	0.848	65.71
Wheeler, $T_{mean}/h_{0.01}$	15.69	28.61	14.30	14.30	3.92s	0.671	50.49
Stokes, $T_{mean}/h_{0.01}$	15.69	28.61	16.70	16.70	0^o	0.944	76.14
Extrapolation, $T_{mean}/c_{0.01}$	15.69	35.74	17.87	17.87	3.92s	1.52	124.74
Constant a.s, $T_{mean}/c_{0.01}$	15.69	35.74	17.87	17.87	3.92s	1.39	110.57
Wheeler, $T_{mean}/c_{0.01}$	15.69	35.74	17.87	17.87	3.92s	1.05	81.16
Stokes, $T_{mean}/c_{0.01}$	15.69	30.14	17.74	17.74	0^o	1.07	86.89
Extrapolation, $T_{max}/h_{0.01}$	17.74	28.61	14.30	14.30	4.43s	0.916	67.42
Constant a.s, $T_{max}/h_{0.01}$	17.74	28.61	14.30	14.30	4.43s	0.884	63.83
Wheeler, $T_{max}/h_{0.01}$	17.74	28.61	14.30	14.30	4.43s	0.748	52.42
Stokes, $T_{max}/h_{0.01}$	17.74	28.61	16.94	16.94	0^o	0.993	75.14

Table 3.7. Load results for column diameter 5m, non-dominating forces. Where 1GN =10^3 MN = 10^6 kN = 10^9 N. X^o for Stokes waves instead of time for linear waves. Crest top is the x-position when 0^o, mean surface level is approximately 80^o and through is at 180^o. The data has been iterated to find max value with time, t or position, X^o.

	Forces on simplified offshore structures according to different wave models where: D=5m (Non-dominating force)						
Case name:	Period, T.(s)	Wave height, h.(m)	Amplitude, a.(m)	Height over surface, ξ.(m)	Wave phase (s or ^{o})	Force, F.(MN)	Moment, M.(GNm)
Extrapolation, $T_{min}/h_{0.01}$	13.64	28.61	14.30	13.39	2.63s	6.62	0.552
Constant a.s, $T_{min}/h_{0.01}$	13.64	28.61	14.30	13.15	2.53s	6.15	0.499
Wheeler, $T_{min}/h_{0.01}$	13.64	28.61	14.30	12.21	2.22s	4.81	0.374
Stokes, $T_{min}/h_{0.01}$	13.64	28.61	16.94	15.71	16^o	6.74	0.571
Extrapolation, $T_{mean}/h_{0.01}$	15.69	28.61	14.30	13.44	3.05s	6.38	0.491
Constant a.s, $T_{mean}/h_{0.01}$	15.69	28.61	14.30	13.32	2.99s	6.10	0.459
Wheeler, $T_{mean}/h_{0.01}$	15.69	28.61	14.30	12.81	2.77s	5.09	0.370
Stokes, $T_{mean}/h_{0.01}$	15.69	28.61	16.70	15.57	16^o	6.72	0.529
Extrapolation, $T_{mean}/c_{0.01}$	15.69	35.74	17.87	17.25	3.26s	10.29	0.829
Constant a.s, $T_{mean}/c_{0.01}$	15.69	35.74	17.87	17.09	3.18s	9.55	0.745
Wheeler, $T_{mean}/c_{0.01}$	15.69	35.74	17.87	16.59	2.97s	7.55	0.568
Stokes, $T_{mean}/c_{0.01}$	15.69	30.14	17.74	16.65	15^o	7.51	0.598
Extrapolation, $T_{max}/h_{0.01}$	17.74	28.61	14.30	13.58	3.53s	6.37	0.460
Constant a.s, $T_{max}/h_{0.01}$	17.74	28.61	14.30	13.51	3.49s	6.18	0.438
Wheeler, $T_{max}/h_{0.01}$	17.74	28.61	14.30	13.22	3.33s	5.39	0.371
Stokes, $T_{max}/h_{0.01}$	17.74	28.61	16.94	15.71	15^o	6.94	0.517

Table 3.8. Load results for column diameter 20m, mass dominating forces. Where 1GN =10^3 MN = 10^6 kN = 10^9 N. X^o for Stokes wave instead of time for linear wave. Crest top is the x-position when 0^o, mean surface level is approximately 80^o and through is at 180^o. Max value obtained at mean surface level of wave.

	Forces on simplified offshore structures according to different wave models where: D=20m (Mass dominating force)						
Case name:	Period, T.(s)	Wave height, h.(m)	Amplitude, a.(m)	Height over surface, ξ.(m)	Wave phase (s or ^{o})	Force, F.(MN)	Moment, M.(GNm)
Extrapolation, $T_{min}/h_{0.01}$	13.64	28.61	14.30	0	0	83.83	5.34
Constant a.s, $T_{min}/h_{0.01}$	13.64	28.61	14.30	0	0	83.84	5.34
Wheeler, $T_{min}/h_{0.01}$	13.64	28.61	14.30	0	0	83.84	5.34
Stokes, $T_{min}/h_{0.01}$	13.64	28.61	16.94	0	79^o	81.49	5.10
Extrapolation, $T_{mean}/h_{0.01}$	15.69	28.61	14.30	0	0	80.71	4.82
Constant a.s, $T_{mean}/h_{0.01}$	15.69	28.61	14.30	0	0	80.71	4.82
Wheeler, $T_{mean}/h_{0.01}$	15.69	28.61	14.30	0	0	80.71	4.82
Stokes, $T_{mean}/h_{0.01}$	15.69	28.61	16.70	0	80^o	79.12	4.69
Extrapolation, $T_{mean}/c_{0.01}$	15.69	35.74	17.87	0	0	100.85	6.02
Constant a.s, $T_{mean}/c_{0.01}$	15.69	35.74	17.87	0	0	100.85	6.02
Wheeler, $T_{mean}/c_{0.01}$	15.69	35.74	17.87	0	0	100.85	6.02
Stokes, $T_{mean}/c_{0.01}$	15.69	30.14	17.74	0	79^o	83.26	4.95
Extrapolation, $T_{max}/h_{0.01}$	17.74	28.61	14.30	0	0	76.61	4.37
Constant a.s, $T_{max}/h_{0.01}$	17.74	28.61	14.30	0	0	76.61	4.37
Wheeler, $T_{max}/h_{0.01}$	17.74	28.61	14.30	0	0	76.61	4.37
Stokes, $T_{max}/h_{0.01}$	17.74	28.61	16.94	0	80^o	75.56	4.32

The reason for obtaining the same results for all linear estimation of a mass dominating forces is because of the method used for approximate up to the mean surface level is the same for all linear cases. Those results can be seen in table 3.8.

By comparing the result up against each other, one can clearly see that an increased D produces a larger force than with a smaller column diameter, D. The reason for this is because of the increased column surface, which the wave can slam in to. One would therefore obtain more forces from the waves with a larger D. One can also see that the linear wave kinematics makes a lower base shear and overturning moment compared to the Stokes kinematics with wave height 28.61m, except for mass dominating case. The reason for this is the larger amplitude generated with Stokes program meaning that we integrate higher up for Stokes result than with a lower amplitude. Horizontal particle velocity and acceleration is highest at the top and that's why we get much higher forces with higher amplitude. By comparing the mass dominating case, which has no value above mean surface level we obtain a higher result for linear kinematics. This is because the height of the amplitude doesn't have much of an impact on the result and a linear process usually overestimates the kinematics. Out from the result I would only recommend using extrapolation when half the wave height is used for the amplitude in a linear approach to estimate the wave kinematics. One would also need a safety factor on 1.1 for drag or non-dominating case to be on the safe side. If we assume that the Stokes kinematics are close to a real ocean waves.
With the use of crest height as amplitude, we get a different result for the comparison. We obtain a much larger force with the use of linear kinematics than Stokes kinematics since the same amplitude for both cases has been used. This means that a linear approach gives a higher estimate when the same data are used. A good approximation for this case would be wheeler stretching.

One important thing to mention is that all data obtained is where the forces is at its maximum and the moment in this position in time or position. For mass and non-dominating case one can obtain a larger overturning moment if the calculations where calculated for a higher position at the wave, but then again the base shear would have been lower. This is because of an increased distance from the wave position to the surface bottom. The overturning moment is still not maximum at the crest top for those two cases because the base shear of a mass dominated case is zero at crest top.

As mentioned before, the old N-003 standard state that one should use the wave height, $h_{0.01}$ with an unfavorable value of the period. The horizontal particle velocity and acceleration has an unfavorable value of the period when it is low as we discussed earlier. Now that the mass and drag coefficient is taken in to account for rough and smooth surface one may obtain other unfavorable value of the periods when calculating the forces. This is because the coefficients corrects the values at the different depth heights.

From the base shear and overturning moment data obtained above, one can see that a mass dominating case with a minimum period would be the worst scenario. For linear drag dominating case it is the minimum period as the worst case, but the maximum period has almost as high base shear than the lowest period, where the mean period is the lowest. This is because of the drag coefficient. For Stokes data, the maximum period is the worst case for both drag and non-dominating forces, but there are still not much deferens between them. For a mass term, we obtain a the maximum forces for a small period.

Now to the final comparison between the old and new N-003 standard. This shows that a larger base shear force has been obtained with the use of a mean period and a crest height equal to, $c_{0.01}$ as the amplitude. Instead of an unfavorable period associated with half the wave height equal to $h_{0.01}$ by linear approach or a generated crest height from Stokes program using $h_{0.01}$ as wave height.

This can also be seen in table 3.9, which only shows the worst cases for both N-003 approaches by using Stokes 5th order waves. A very important observation from table 3.9 can be seen in the mass dominating case, where the overturning moment are largest for the Stokes wave with $h_{0.01}$ as the wave height and T_{min} as period. It is still a very small difference, and for all other cases the new N-003 approaches has the largest overturning moment value.

Table 3.9. Comparison between old and new N-003 standard, by comparing load results for column diameter 1m, 5m and 20m. Where 1GN =10^3 MN = 10^6 kN = 10^9 N. X^o for Stokes wave instead of time for linear wave. Crest top is the x-position when 0^o, mean surface level is approximately 80^o and through is at 180^o.

	Forces on simplified offshore structures according to different wave models. Comparison between old and new N-003 standard.						
Case name:	Period, T.(s)	Wave height, h.(m)	Amplitude, a.(m)	Height over surface, ξ.(m)	Wave phase, ^{o}	Force, F.(MN)	Moment, M.(GNm)
Stokes. D=1m $T_{mean}/c_{0.01}$	15.69	30.14	17.74	17.74	0^o	1.07	0.00869
Stokes. D=1m $T_{max}/h_{0.01}$	17.74	28.61	16.94	16.94	0^o	0.993	0.00751
Stokes. D=5m $T_{mean}/c_{0.01}$	15.69	30.14	17.74	16.65	15^o	7.51	0.598
Stokes. D=5m $T_{max}/h_{0.01}$	17.74	28.61	16.94	15.71	15^o	6.94	0.517
Stokes. D=20m $T_{mean}/c_{0.01}$	15.69	30.14	17.74	0	79^o	83.26	4.95
Stokes. D=20m $T_{min}/h_{0.01}$	13.64	28.61	16.94	0	79^o	81.49	5.10

From table 3.9 one can see that the difference between the loads with the use of the old and new N-003 recommendation are not big. With the new N-003 recommendations, we obtain a more realistic value and shape of real ocean waves, because the crest is higher and a more frequent period are used. It is also easier to perform a control with the new recommendations since only one mean period needs to be controlled.

3.6 Summary for regular Waves

We have now looked in to the new and old recommendations for designing the ULS design wave. What have been learned from this is that a linear approach has two different methods giving different results. Those are depending on the amplitude, and if one chose to have a crest height or half the wave height as amplitude, one would need to know which approximation method would give the best approximation to a real wave. Normally a linear approximation is not used for solving this problem, but for further work, it would be interesting to confirm if extrapolation really is the best approximation with half the wave height as amplitude, and wheeler stretching when crest height is used as amplitude. This could be done by comparing result with different waves.

When we observed the horizontal particle velocity and acceleration results of the waves, one could clearly see that the minimum period would be the worst case for the kinematics. This was not the case for the load results when mass and drag coefficients where introduced. This is why it is important not to neglect the higher periods since the maximum period could also be causing greater forces than the minimum period. Those results also shows that there might be a worse load case between minimum and mean period or mean and max period. Further work is needed to confirm this.

In this report, one have assumed that the results from Stokes data program has been the most accurate method for the kinematics. This assumption is good because it is a fifth order approximation and obtained from a reliable source. From those results, we have found the worst case for the ULS design wave defined by the 10^{-2} – annual probability wave height, $h_{0.01}$. By using Morison equation for three different column diameters. Those results have been compared to the results of an ULS design wave defined by a crest height equal to the 10^{-2} – annual probability crest height, $c_{0.01}$ and an associated mean wave period. By comparing those results, one have seen that the new recommendations from N-003 standard gives a little higher value than using the old N-003 recommendations, except for the overturning moment in a mass dominated case. As mentioned before, by using a crest height as amplitude one would generate a more realistic wave. The new method is also much easier to perform since only one period is required to calculate. My conclusion is therefore that the new N-003 recommendation on this subject are better than the old N-003 recommendations.

4 Kinematics of irregular waves

As mentioned earlier, the only waves in the real ocean that looks like regular waves are swells generated from a distant storm. Looking at the sea on a windy day, the waves would be more like Irregular waves with different height and period for each wave generated. That is why we will introduce irregular waves in this thesis, which is random waves. With the use of linear random wave theory, one can model a sea state with the length of our choosing. This theory is basically the same as for regular waves except it uses a random or probabilistic setting. Before one can model this sea state, it is important to select a wave spectrum that fit the area to model. In this thesis a JONSWAP spectrum has been chosen, which is commonly used in the North Sea, according to [16]. Our wave spectrum defines the sea state, and give us the properties needed about the waves. To generate an irregular sea state, one can summarize all the waves obtained from the wave spectrum with a random phase. An example of this is shown in figure 4.1, where one combine the smaller waves obtained from the wave spectrum to generate an irregular sea state.

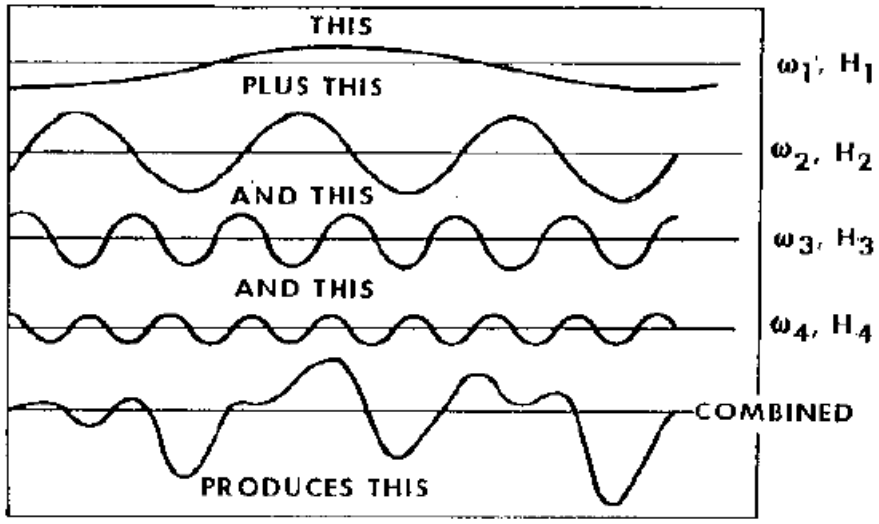

Figure 4.1. Creation of an irregular sea state by combining four regular waves, figure obtained from [16].

After generating a 3-hour sea state the kinematics under the largest wave will be obtained and then compare those results up against waves created from Stokes program. At the end, only the loads for a drag dominating case will be found and therefore only need to find the horizontal particle velocity for the kinematics in this chapter of irregular waves. To complete this task a random linear and second order process will be created.

4.1 Linear approximation for irregular waves

To simulate an irregular sea state, we have chosen to use deep-water formulas. The reason for this simplification is to decrees the work time for Matlab. There are only small differences between deep and intermediate water depth for this case. The formula of surface process is:

$$\xi(t) = \sum_{i=1}^{\infty} \xi_{0,1} * \cos(\omega_i t - \varphi) \qquad \text{Equation 4.1}$$

This formula is obtained from [17], and creates a Fourier series of the time history of the sea. To do this one need to assume that the time history is analogue. Where t is time, ω_i is the frequency in radians per seconds and φ is a random phase between 0 and 2π to generate a random sea state. The amplitude $\xi_{0,1}$ may also be a random process, but with a large number of frequency components (n >1000) there will be small deference's between the random process and a non-random process according to [17]. Large numbers of frequency components can be obtained through small steepness of the wave spectrum. That is why a random amplitude in this thesis will not be used. The largest period that this formula can identified is the length of the time history, T which is 3 hour and the shortest period is 2* Δt. Where Δt is the steepness of time. The reason it can't identify a lower period than 2* Δt, is because of the need for three values within the wave period of the component to identify a sinusoidal component. This is called the cut-off frequency, which is:

$$f_N = \frac{1}{2\Delta t} = \frac{\omega_N}{2\pi} \qquad \text{Equation 4.2}$$

The time steepness Δt will be 0.5s in this theses, meaning that we will have an upper limit of:

$$f_N = \frac{1}{2 * 0.5} = 1\ Hz$$

The last part one need to define is the frequency resolution to avoid the Fourier series to repeat itself before 3 hours. If 1/T is used for the steepness, where T is the seconds of a 3hr period the Fourier series will repeat itself for each 3-hour period. Therefore, the frequency resolution needs to be:

$$\Delta f = \frac{\Delta\omega}{2\pi} < \frac{1}{10800} \qquad \text{Equation 4.3}$$

For a 3-hour period.

4.1.1 Wave spectrum

The wave spectrum is a very important parameter to define the amplitude in a sea state and below we have chosen to use the JONSWAP spectrum. This spectral model is very good to define a pure wind sea state. If there was a swell system as well, which may have generated a double peaked spectrum, another spectrum may be optimized for this solution. An example of this is the Torsethaugen model, which is also parameterize in terms of significant wave height, h_s and spectral peak period, t_p. For comparison of those two spectrums, see [17]. The formula for the JONSWAP spectrum and its parameters is found below and obtained from [17].

$$s\Xi\Xi(f) = 0.3125 * h_s^2 * t_p * \left(\frac{f}{f_p}\right)^{-5} \exp\left(-1.25 * \left(\frac{f}{f_p}\right)^{-4}\right)(1 - 0.287 \ln\gamma) * \gamma^{\exp\left(-0.5\left(\frac{f-f_p}{f_p*\sigma}\right)^2\right)}$$

Equation 4.4

Where $f_p = \frac{1}{t_p}$ is the peak frequency, f is the wave frequency in Hz and the spectral width parameter (σ) can be found in equation 4.5.

$$\sigma = 0.07, \ \ if \ \ f \leq f_p$$
$$\sigma = 0.09, \ \ if \ \ f > f_p$$

Equation 4.5

The peak enhancement factor is:

$$\gamma = 42.2 * \left(\frac{2\pi * h_s}{g * t_p^2}\right)^{\frac{6}{7}}$$

Equation 4.6

Where $g = 9.81\ m/s^2$ and is the acceleration of gravity.

According to [17], one can change the spectral density formula from frequency in Hz to radians by the following formulas:

$$s\Xi\Xi(\omega)d\omega = s\Xi\Xi(f)df \Rightarrow s\Xi\Xi(\omega) = s\Xi\Xi\left(f = \frac{\omega}{2\pi}\right)\frac{df}{d\omega} = \frac{s\Xi\Xi\left(f = \frac{\omega}{2\pi}\right)}{2\pi}$$

Equation 4.7

This means that the spectral density formula with frequency in radians is:

$$s_{\Xi\Xi}(\omega) = \frac{0.3125 * h_s^2 * t_p * \left(\frac{f}{f_p}\right)^{-5} \exp\left(-1.25 * \left(\frac{f}{f_p}\right)^{-4}\right)(1 - 0.287 \ln \gamma) * \gamma^{\exp\left(-0.5\left(\frac{f-f_p}{f_{p*\sigma}}\right)^2\right)}}{2\pi}$$

Equation 4.8

We also have that the total variance of a sea state is the following:

$$\sigma_\Xi^2 = \sum_{i=1}^{N} \sigma_{\Xi,i}^2 = \sum_{i=1}^{N} s\Xi\Xi(\omega_i) * \Delta\omega \Rightarrow \int_0^\infty s\Xi\Xi(\omega) d\omega$$

Equation 4.9

Where the spectral density = variance density:

$$s\Xi\Xi(\omega_i) = \frac{\sigma_{\Xi,i}^2}{\Delta\omega}$$

Equation 4.10

As known from earlier, the significant wave height can be written as, $h_s = 4\sqrt{\sigma_\Xi^2}$. This can be used to control the Matlab script later on.

Now that we have introduced all the parameters and defined our interval, one can plot the results of our wave spectrum. This is done by the following formula and can be seen in figure 4.2.

$$\gamma = 42.2 * \left(\frac{2\pi * 14.9}{9.81 * 15.8^2}\right)^{\frac{6}{7}} = 2.57$$

$$s_{\Xi\Xi}(f) = 0.3125 * 14.9^2 * 15.8 * \left(\frac{f}{\frac{1}{15.8}}\right)^{-5} \exp\left(-1.25 * \left(\frac{f}{\frac{1}{15.8}}\right)^{-4}\right) * (1 - 0.287 \ln 2.57) * 2.57^{\exp\left(-0.5\left(\frac{f-\frac{1}{15.8}}{\frac{1}{15.8}*\sigma}\right)^2\right)}$$

Where frequency, f is the variable and spectral width parameter (σ) is:

$$\sigma = 0.07, \ \ if \ \ f \leq \frac{1}{15.8} = 0.06$$

$$\sigma = 0.09, \ \ if \ \ f > \frac{1}{15.8} = 0.06$$

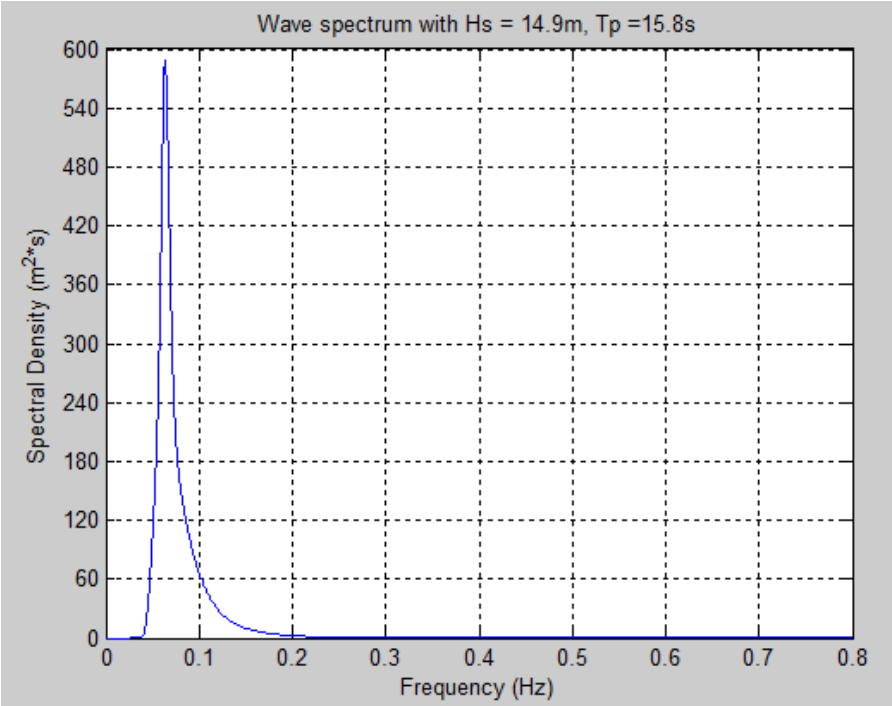

Figure 4.2. Wave spectrum created from a JONSWAP spectrum.

Since we have a theoretical wave spectrum, the line is very smooth and not irregular. A real wave spectrum obtained from the ocean would have been very noisy, see figure 4.3 for illustration purposes of a raw spectrum gathered from Wijaya.

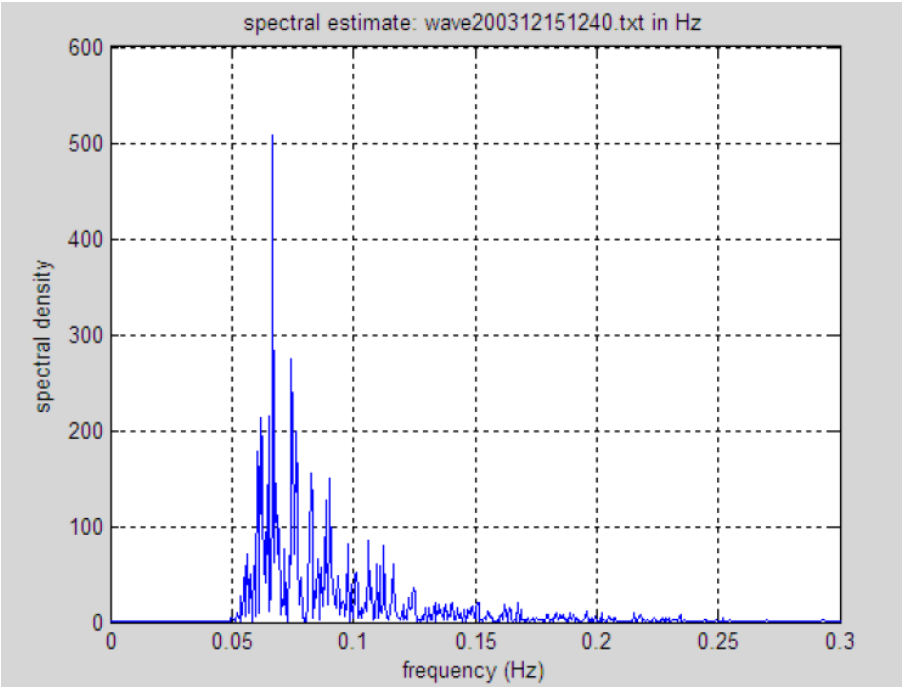

Figure 4.3. Raw spectrum. (From Wijaya (2009)) obtained from [17].

4.1.2 Simulation of a 3-hours surface process.

From formula 4.1, one can simulate the surface process, but first the amplitude needs to be determined. After defining the wave spectrum above the wave amplitude can be defined as:

$$\xi_{0,i} = \sqrt{2 * s\Xi\Xi(\omega_i) * \Delta\omega} \qquad \text{Equation 4.11}$$

By introducing this amplitude to the surface process, one can obtain the following equation:

$$\xi(t) = \sum_{i=1}^{\infty} \sqrt{2 * s\Xi\Xi(\omega_i) * \Delta\omega} * \cos(\omega_i t - \varphi_i) \qquad \text{Equation 4.12}$$

Where:

$$\Delta\omega_{3hr} = 2\pi * T_{3hr} = 2\pi * 11000 > 2\pi * 10800 \qquad \text{Equation 4.13}$$

The generated process will not repeat itself within a 3-hour period by using, $\Delta\omega_{3hr}$. φ_i is a random number between $0 - 2\pi$ for each i, where each i generate a new frequency of ω and then summarize all the small components in to one sea state. A 3-hour surface process generated from Matlab can be seen in figure 4.4. Where figure 4.5 show the location of the maximum wave amplitude in a 1000s span.

To verify the Matlab script used, we changed the frequency resolution to $\Delta\omega = 2\pi * 3600s$ and observed that the time series repeated itself every 3600s. This can be seen in figure 4.6. A second method to control the process is to control the significant wave height. With an input of $h_s = 14.9m$, we obtained $h_s = 14.89m$ with an f interval of $0 - 0.5$ and with and interval of $0 - 0.8$ we obtained $h_s = 14.90m$. with the use of the following formula described earlier.
Where:
$\Delta\omega = 2\pi * 11000$ for this case.

$$h_s = 4\sqrt{\sigma_{\Xi}^2} = 4\sqrt{\sum_{i=1}^{N} s\Xi\Xi(\omega_i) * \Delta\omega} \qquad \text{Equation 4.14}$$

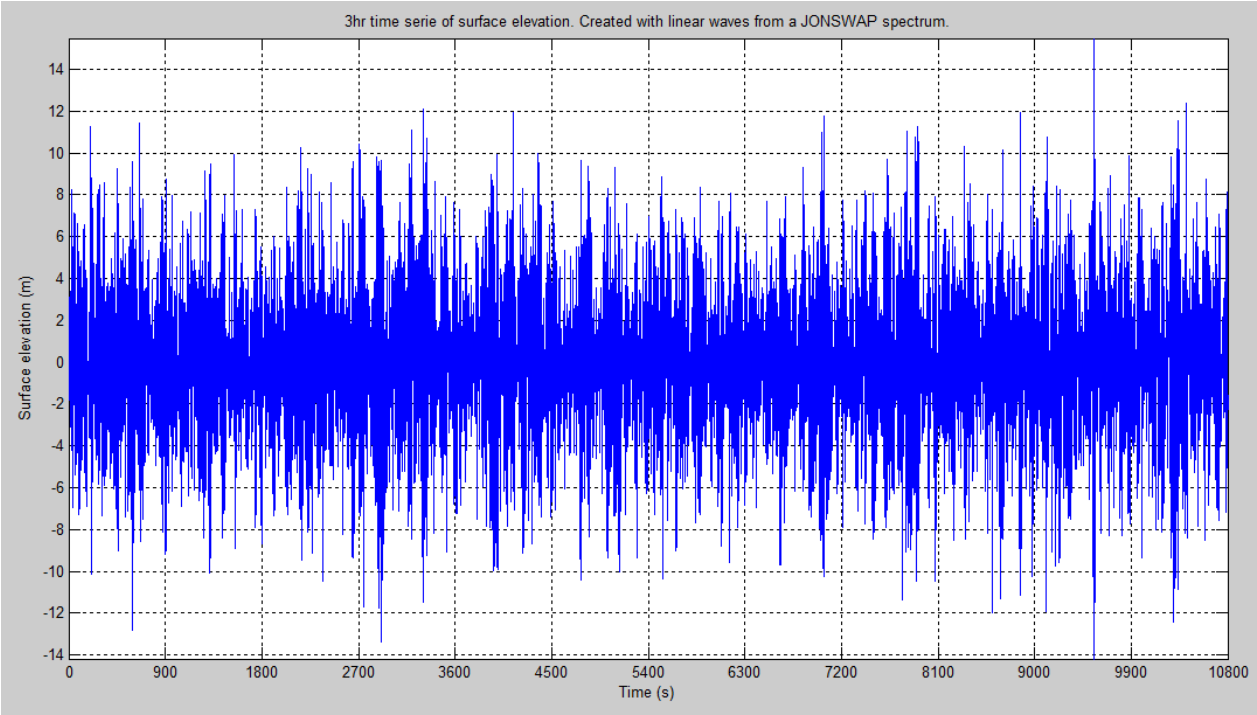

Figure 4.4. 3hr surface process created with a JONSWAP spectrum, where h_s = 14.9m and t_p = 15.8s.

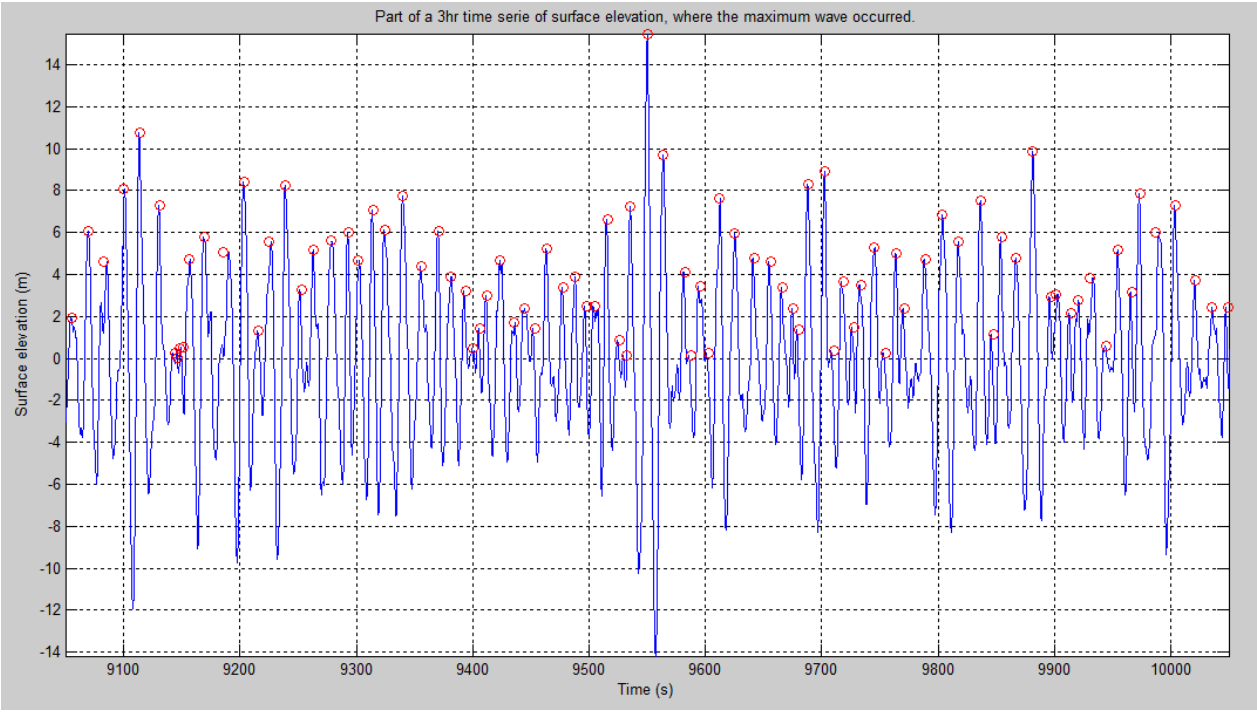

Figure 4.5. 3hr surface process with global maxima, which is a 1000s window showing the 3-hour maximum wave.

For this 3-hour surface process, we obtained an amplitude of 15.46m in time position 9550s, where the period of this wave was 14.5s. In the whole 3-hour time series a total of 906 peaks where obtained, using zero up crossings to identify the largest crest height for each zero up crossings. All those data changes each time the program runs, since the phase changes for each frequency when φ_i changes.

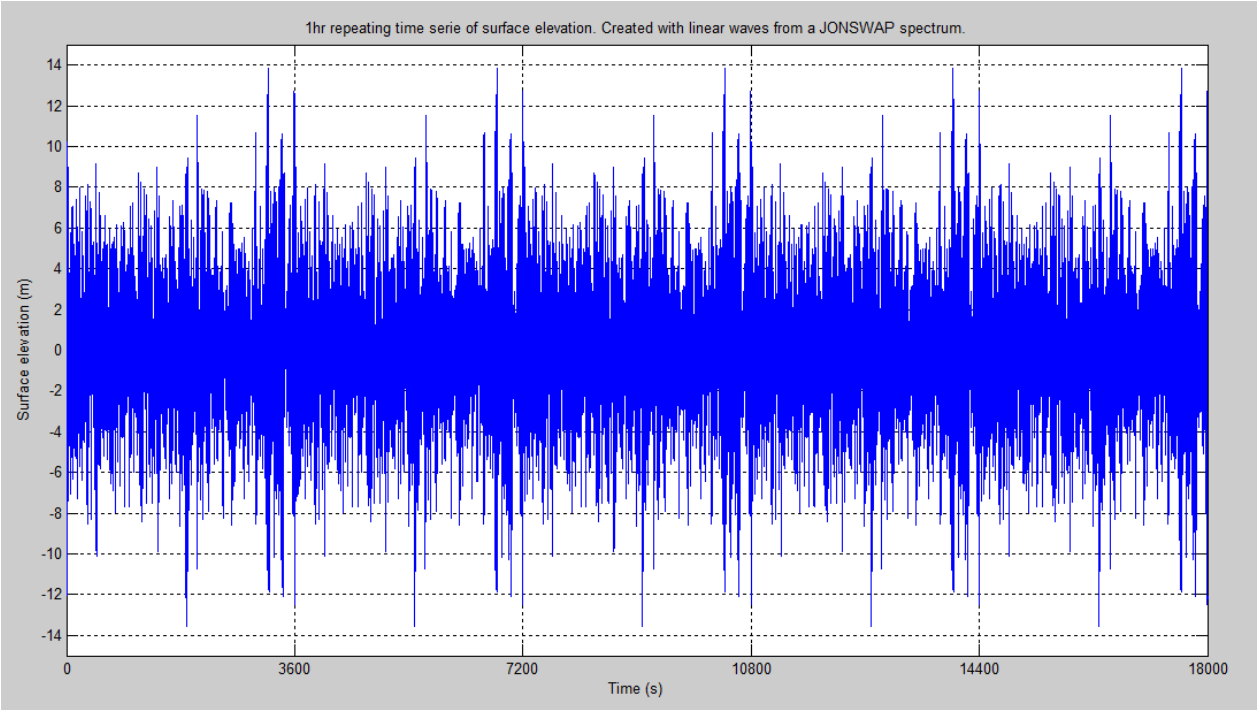

Figure 4.6. 1-hour repeating surface process created with a JONSWAP spectrum, where h_s = 14.9m and t_p = 15.8s.

4.1.3 3-hour extreme values for a generated surface process.

When we have a reasonably narrow wave spectrum one can assume that the Rayleigh distribution is a sufficient model for global maxima in a stationary, Gaussian process, [17]. We will now test this by plotting the Rayleigh distribution up against global maxima gathered from our surface process. Where:

The Rayleigh distribution formula is, [17]:

$$F_{\Xi_G}(\xi) = 1 - \exp\left(-\frac{1}{2} * \left(\frac{\xi}{\sigma_\Xi}\right)^2\right) \quad \text{Equation 4.15}$$

$$\sigma_\Xi = \frac{h_s}{4} \quad \text{Equation 4.16}$$

The global maxima crest height obtained from our surface process will be sorted from the lowest value to the highest. Crest height data will be plotted up against the cumulative probability chance. Finding the cumulative probability chance for each crest height can be done with the following formula.

$$F(\xi) = \frac{n_{c.i}}{N+1} \quad \text{Equation 4.17}$$

Where N is the total numbers of crest heights (906 in this case), and $n_{c.i}$ is the number position of the crest height used. Where the lowest crest height of global peaks are $n_{c.i} = 1$ and the second lowest $n_{c.i} = 2$ meaning that the largest crest height will have, $n_{c.i} = 906$. The results of those two plots can be seen in figure 4.7.

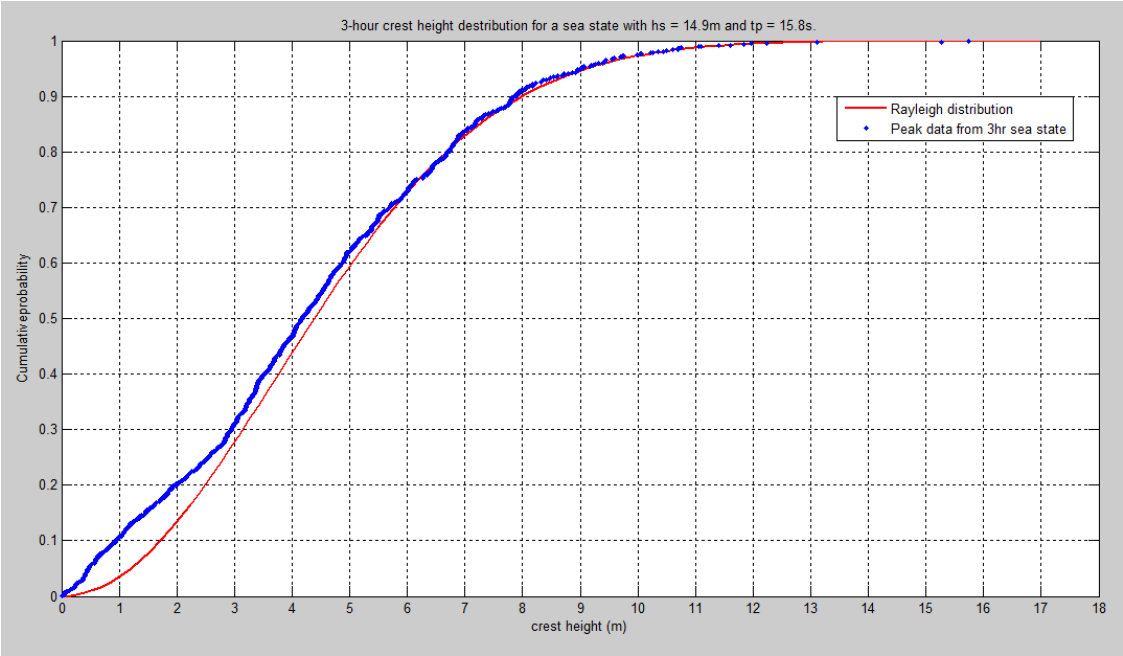

Figure 4.7. Global maxima versus Rayleigh distribution.

From figure 4.7, one can see that the Rayleigh distribution fits the global maxima very well, except for the smallest crest heights. For the smallest crest heights, we can see some deviating away from the Rayleigh distribution. The reason for this may be because of the zero up crossing, which may cause some extra global peaks with low crest height.

For obtaining the extreme crest height value with the Rayleigh distribution, one can exalt the formula with n_t. Where n_t is the mean numbers of global maxima for the surface process. This formula can also be used to estimate the crest height corresponding to an exceedance probability of 0.1 for this sea state, [17]. We can also verify this distribution with the same meted used in figure 4.7, but instead of using the global maxima for one sea state, we simulate 80 different sea states and uses the maximum crest height for the whole sea state. Then we sort the crest height from low to high and use formula 4.18 to plot against the data.

Rayleigh distribution exalted in n_t.

$$F_{\Xi_{3h}}(\xi) = [F_{\Xi_G}(\xi)]^{n_t} \quad = \left[1 - \exp\left(-\frac{1}{2} * \left(\frac{\xi}{\sigma_\Xi}\right)^2\right)\right]^{n_t} \qquad \text{Equation 4.18}$$

Later on, this formula will be changed to fit a Gumbel scale to perform bootstrapping. The result can be found in equation 4.19 and is called “exact distribution with Rayleigh”.

$$-\ln\left(-ln\left(F(\xi)\right)\right) = -\ln\left(-n_t * ln\left(1 - exp\left(-\frac{1}{2} * \left(\frac{\xi}{\sigma_\Xi}\right)^2\right)\right)\right) \qquad \text{Equation 4.19}$$

According to [17], if n_t becomes large in the Rayleigh distribution it will approaches the asymptotic extreme value distribution, which is called the Gumbel distribution. This formula can be found in equation 4.20.

$$F_{\Xi_{3h}}(\xi) \Rightarrow \exp\left(-\exp\left(-\frac{\xi - \sigma_{\Xi}\sqrt{2\,ln(n_t)}}{\frac{\sigma_{\Xi}}{\sqrt{2\,ln(n_t)}}}\right)\right) \qquad \text{Equation 4.20}$$

This formula can also be fitted to a Gumbel scale and will be used later under bootstrapping. The result of this is found in equation 4.21 and the formula is called “Gumbel approximate”:

$$-\ln\left(-ln\left(F(\xi)\right)\right) \Rightarrow \frac{\xi - \sigma_{\Xi}\sqrt{2\,ln(n_t)}}{\frac{\sigma_{\Xi}}{\sqrt{2\,ln(n_t)}}} \qquad \text{Equation 4.21}$$

Now that the formula has been introduced one can plot the Rayleigh distribution exalted in n_t and the Gumbel distribution it goes towards up against the maximum crest height values from 80 different simulations. See figure 4.8 for the results.

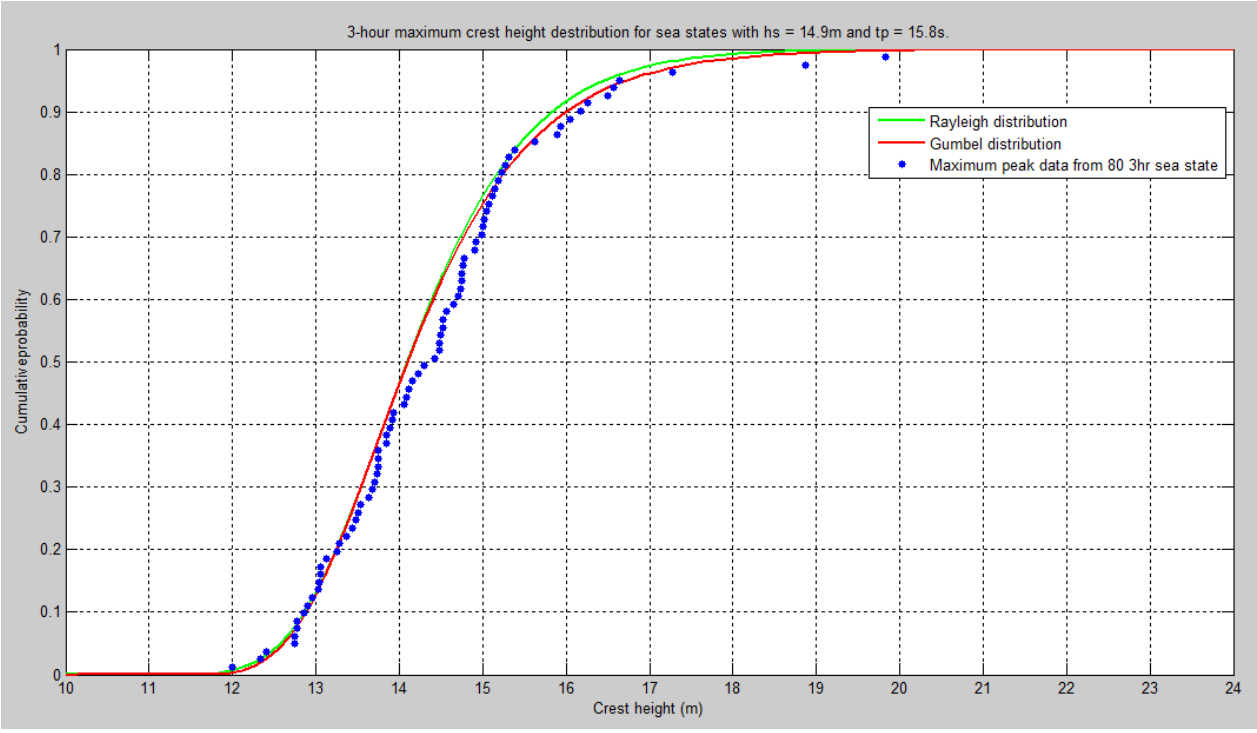

Figure 4.8. Extreme crest height values from 80 different 3-hour simulations compared with a Rayleigh distribution and Gumbel distribution.

From figure 4.8, one can see that the Gumbel distribution is the best-fit, meaning that an increased n_t in the Rayleigh distribution would create a better fit here. It still doesn't deviate much. Therefore, the extreme crest height data follows a Rayleigh distribution. To identify the wave event with a crest height corresponding to an exceedance probability of 0.1 for this sea state, one can obtain the values when the cumulative probability is 0.9. This means that the $c_{0.01} = 15.84\ m$ for the Rayleigh distribution and $c_{0.01} = 16.00\ m$ for the Gumbel distribution. This is smaller than $c_{0.01} = 17.87\ m$, which we predicted in regular waves, but larger than half the wave height of $h_{0.01} = 28.61\ m$ which also where predicted in regular waves. The reason we get a much lower $c_{0.01}$ with Rayleigh distribution is that the Rayleigh distribution follows the distribution from a first order process. In the regular waves, we used a Weibull distribution to predict the maximum crest height distribution of a second order process, which will result in a much larger value since higher order waves have larger crest than trough. Later on, this will be confirmed by comparing first and second order surface process.

4.1.4 Bootstrapping

Bootstrapping can be used to illustrate the uncertainty of the data, when fitting a probabilistic model to a limited number of observations by using method of moments. In this report, we are using a generated maximum crest height set with 80 crest heights obtained from 80 different simulations. They are stored in an excel file and used in Matlab to plot the following figures below. Before one can plot the crest height data, one would need a probabilistic model to compare those with. A good probabilistic model for estimating the 10^2 – annual probability crest height is the Gumbel distribution fitted using method of moments. All the figures below will be on a Gumbel scale to insure that the data collected follows a straight line. If it follows a straight line, the data follows a Weibull distribution. Formula 4.22 insures that the probability data plotted against crest height data is set on a Gumbel scale.

$$F_B(\xi) = -\ln\big(-ln\big(F(\xi)\big)\big) \qquad \text{Equation 4.22}$$

Where $F(\xi)$ is the same as above.

The Gumbel distribution, fitted using method of moments is shown in equation 4.23, and is obtained from, [18].

$$F_{Y_m}(\xi) = \exp\left(-exp\left(-\frac{\xi - \alpha}{\beta}\right)\right) \qquad \text{Equation 4.23}$$

By transforming the formula to a Gumbel scale one can obtain the following formula:

$$-\ln\left(-ln\left(F(\xi)\right)\right) = \frac{\xi - \alpha}{\beta}, \quad Fitted\ Gumbel \qquad \text{Equation 4.24}$$

The method of moments parameters obtained from, [18] are as following:

$$\beta = 0.7797 * s \qquad \text{Equation 4.25}$$

$$\alpha = \xi_{Average} - 0.57722 * \beta \qquad \text{Equation 4.26}$$

Where s is the standard deviations from the crest heights and $\xi_{Average}$ is the mean value of all crest heights.

The Gumbel distribution fitted to the original sample using method of moments and also compared with two other distributions are shown in figure 4.9.

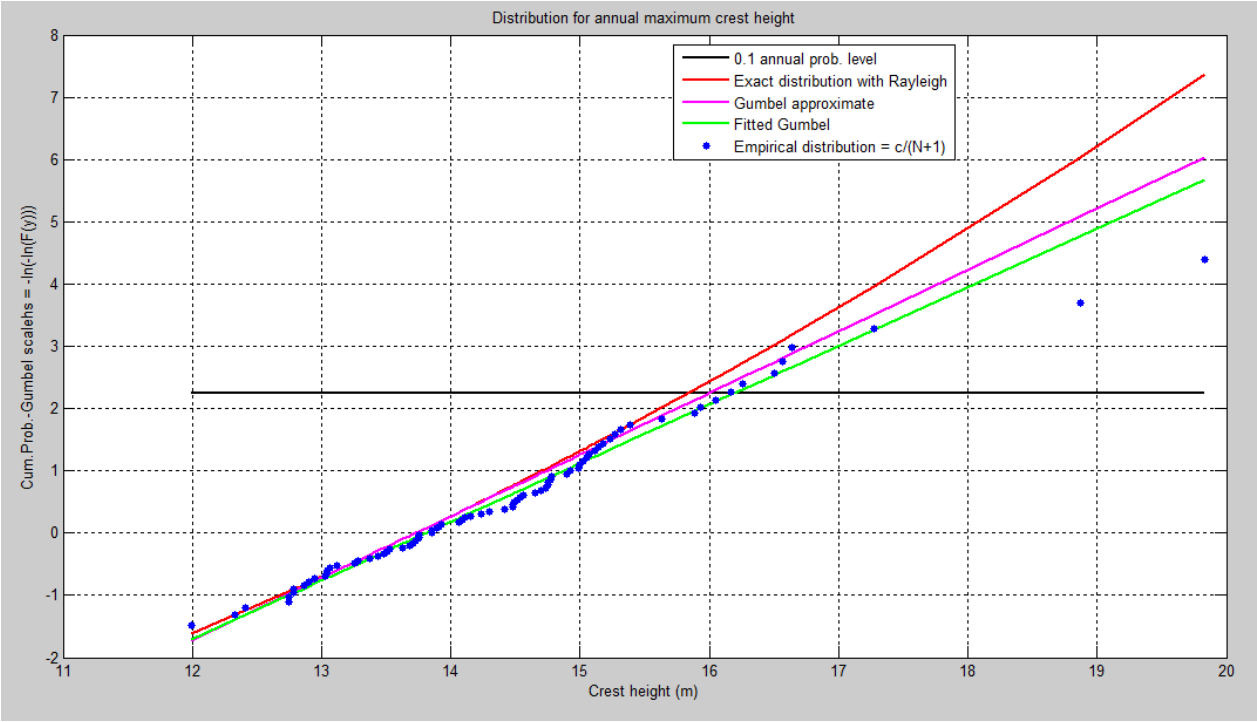

Figure 4.9. Maximum crest height data compared to different distribution function on a Gumbel scale.

From figure 4.9 one can see that the crest height data follows a straight line and fits the distribution function very well. The best fit of those three distributions are the fitted Gumbel distribution and can therefore assume that this is the true distribution. Figure 4.9 also shows that the 10^2 – annual probability crest height is between 15.8m and 16.3m depending on the distribution.

From here on, we need to generate more samples of size 80 since this sample are only one way that the nature could generate a distribution of crest height, [19]. To generate more samples, one can use Monte Carlo simulation from the Gumbel distribution used earlier to fit the data. From [19] one can obtaining the formula 4.27.

$$\xi = \alpha - \beta * \ln(-ln(F_{rand})) \qquad \text{Equation 4.27}$$

Which is the Gumbel distribution (Equation 4.23), fitted using method of moments equation where it is solved for crest height instead of probability. Now F_{rand} is a random number from 0-1 and by generating 80 different values we obtain one data sample. Doing the same procedure 40 times will generate 40 different samples that can be plotted up against the true Gumbel line and the first set of data collected earlier to verified them. If the first data is inside the distribution of the 40 samples, we will have a good fit and valid data. This method are called the parametric bootstrapping according to [19]. From figure 4.10 one can see the results of our parametric bootstrapping with 40 samples.

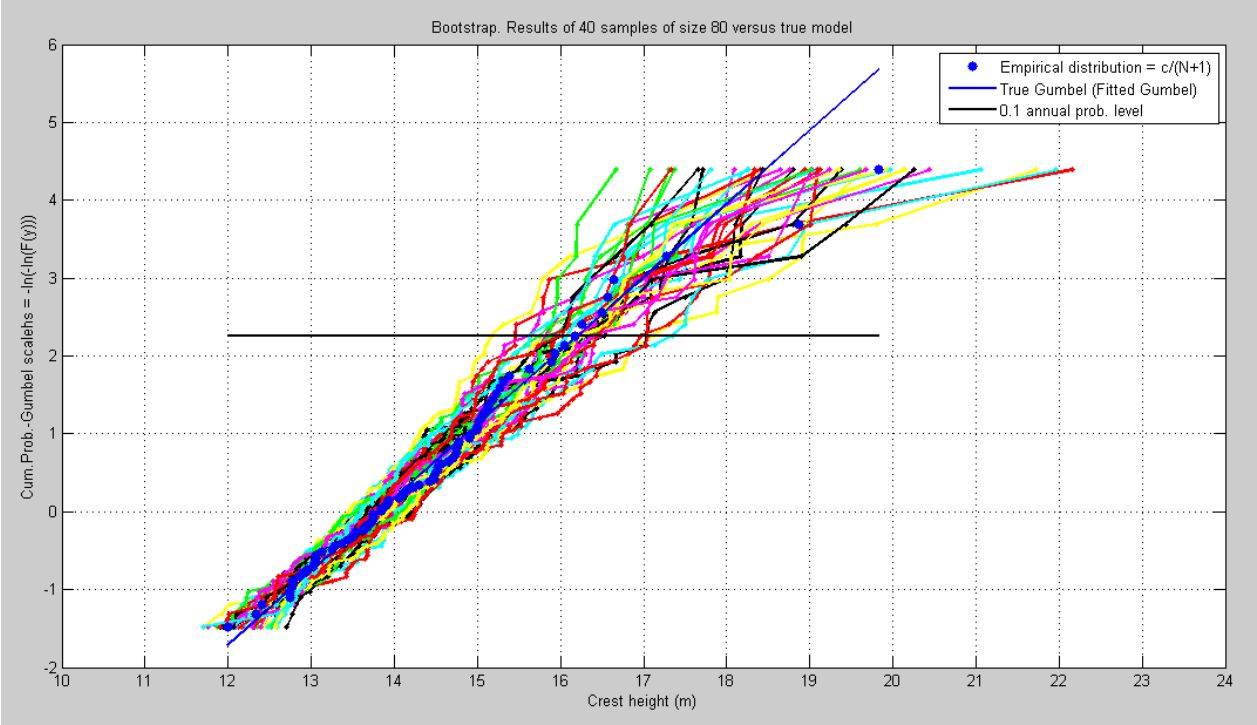

Figure 4.10. Parametric bootstrapping with 80 values for each samples generated from a surface process with h_s = 14.9m and t_p = 15.8s.

Figure 4.10 shows that our data are not out side of our generated samples, this means that the data is valid. The data may still be a rare sample that might have been a high value or low.

This is why it's not wise to have few values inside a sample because more data insures more accuracy. That's why 80 values inside the first sample was chosen. For the 10^2 – annual probability crest height, we have a large range and it shows that the value are between 15,2m to 17,4m.

4.1.5 Linear kinematics

The focus in irregular waves are drag dominated forces as mentioned earlier. To calculate the loads and loads effect from a drag dominated case one would only need to obtain the horizontal particle velocity profile. Because of this, we are shortening the work to only calculate the horizontal particle velocity. There has been some changes for the horizontal particle velocity formula used earlier and those changes are as following: The reason for our first change in the horizontal particle velocity formula is because of the surface process. As mentioned earlier that the surface process and the horizontal particle velocity has the same phase. This means that by using "cosine" for our surface process, one would need to use "cosine" for our horizontal particle velocity profile as well to insure that they have the same phase. The formula obtain is shown in equation 4.28.

$$V^1(z) = \sum_{n=1}^{N} \frac{\zeta_0 * \mathrm{g} * \mathrm{k}}{\omega} * \frac{\cosh k(z+d)}{\cosh kd} * \cos(\mathrm{kx} - \omega\mathrm{t} + \varphi) \qquad \text{Equation 4.28}$$

Because of time consuming when operating in Matlab, we have chosen to operate in deep water although this is intermediate water depth as shown in chapter 3.2. The consequences of this is very small, but might have an impact on the results. Since we are going to compare our results for theoretical purposes and not for dimensioning a construction those assumptions is accepted. Then the following formula is obtained:

$$V^1(z) = \sum_{n=1}^{N} \frac{\zeta_0 * \mathrm{g} * \mathrm{k}}{\omega} * \cos(\mathrm{kx} - \omega\mathrm{t} + \varphi) * e^{k*z} \qquad \text{Equation 4.29}$$

Where φ is a random number between 0 and 2π to insure random phase and $\omega^2 = g * k$, meaning that we can simplify to:

$$V^1(z) = \sum_{n=1}^{N} \zeta_0 * \omega * \cos(kx - \omega t + \varphi) * e^{k*z}$$

Equation 4.30

To find the horizontal particle velocity profile for the 3-hour surface process in Matlab, one would need to simulate the surface process first and identify the largest crest height of the sequence. When the largest crest height is identified, we chose to find the horizontal particle velocity profile for a 200 second window. Where the largest crest height is in the middle of the window. For more information of how this was done, see Appendix A for details about Matlab files created. An example of the results are shown below. Where figure 4.11 shows a 200-second window of the maximum wave obtained from a 3-hour simulated surface process.

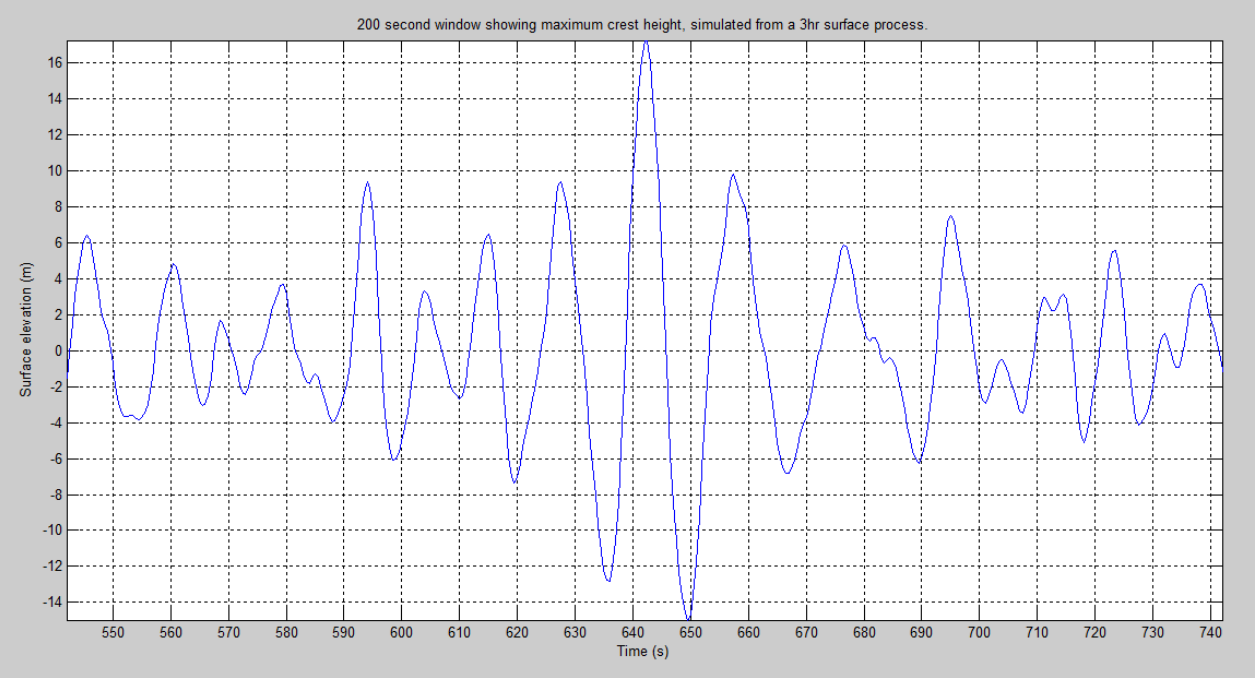

Figure 4.11. 200-second window of a 3-hour linear surface process. Where h_s = 14,9m and t_p = 15.8s.

Figure4.11 show that the maximum crest height obtained from the 3-hour simulated surface process is 17.23m high with a period of 14s. From the horizontal particle velocity formula, one can obtain all the horizontal particle velocity profiles for each 0.5s in the 200s window. This is stored in a matrix in Matlab and one can therefore plot all the values for an example of depth 30m and at mean water level with time as variable. Result of this is shown in figure 4.12-13.

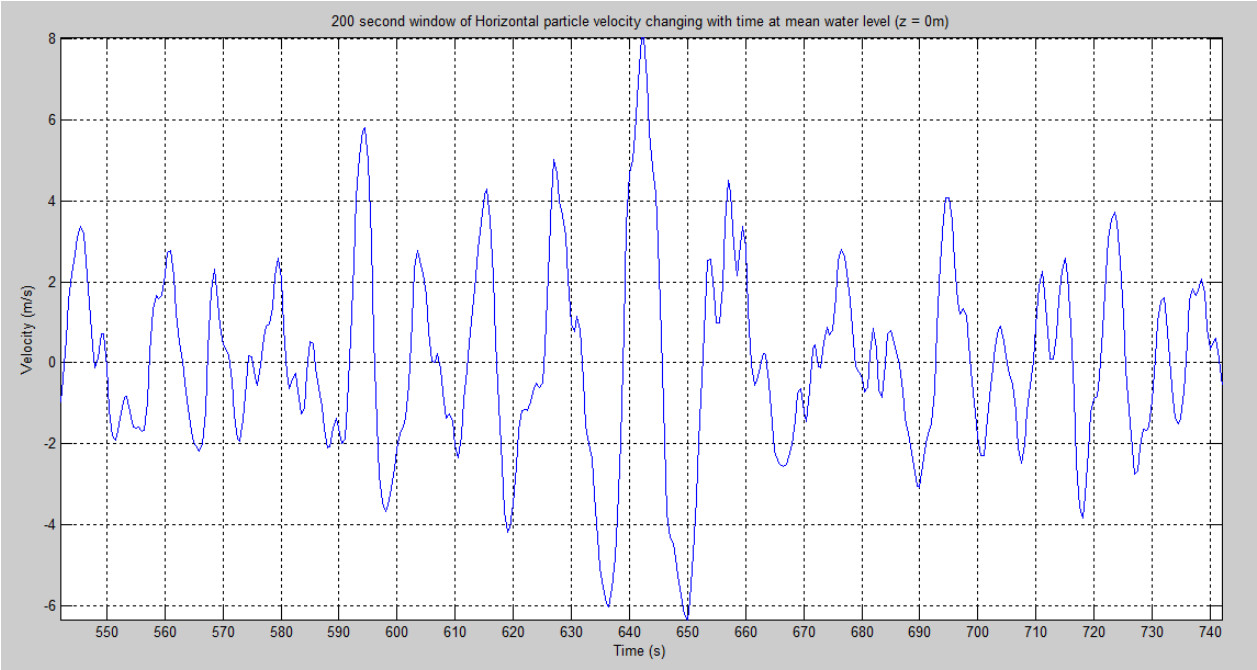

Figure 4.12. 200 second window of horizontal particle velocity changing with time at mean water level (z = 0m).

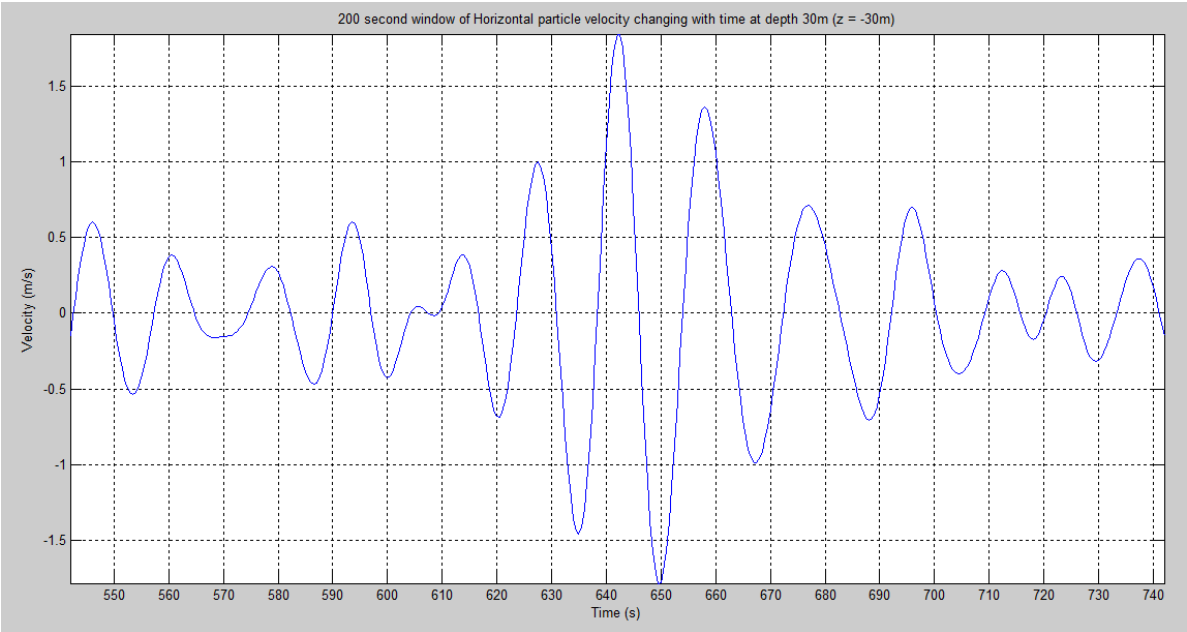

Figure 4.13. 200 second window of horizontal particle velocity changing with time at depth 30m (z = -30m).

Figure 4.12 is only an approximation of the horizontal particle velocity at the mean water level. In real life, there would not be any horizontal particle velocity between the waves, where no water is present. In this estimation, we have extrapolated up to mean water level for illustrative purposes. However, figure 4.13 shows a good estimate of the horizontal particle velocity in a depth of -30m.

By comparing those two figures to the surface process, one can see a very good similarity in shape since they have the same phase angle. Next figure below show us the horizontal particle velocity depending on depth.

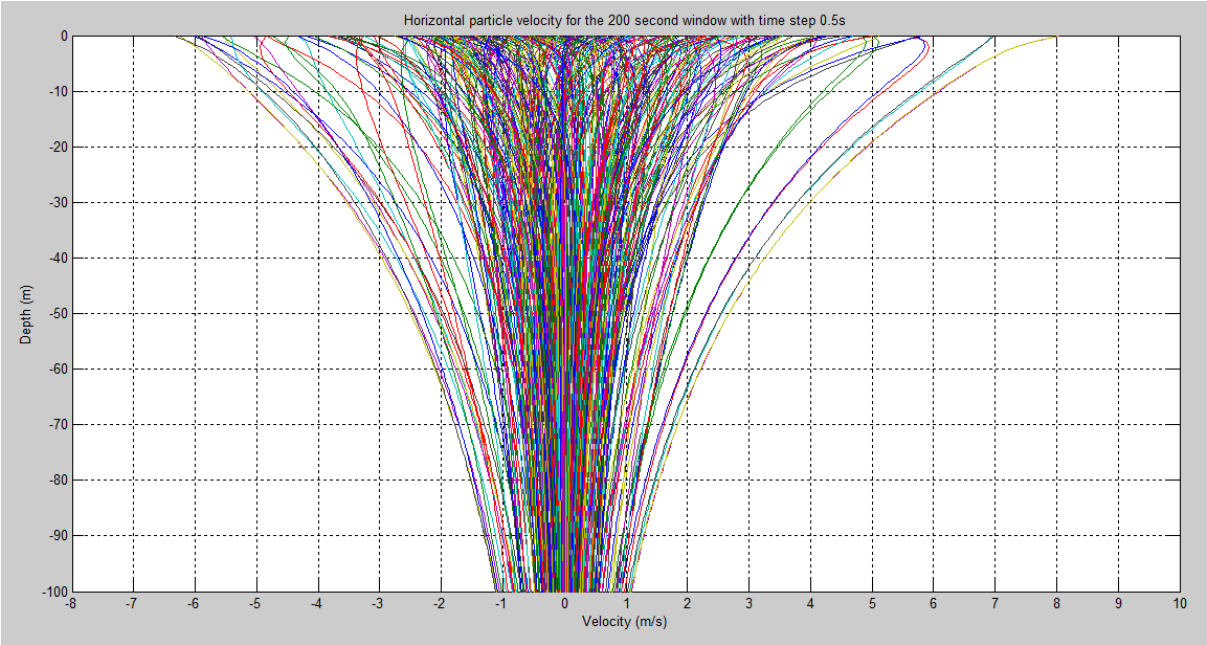

Figure 4.14. 400 horizontal particle velocity profiles created from a 200-second surface process with time step 0.5s.

Figure 4.14 is only used to compare with figure 4.15 to show the horizontal particle velocity profile for the 200s window. Since figure 4.15 shows the horizontal particle velocity under the largest crest, one can compare those results to figure 4.14. This will confirm that the largest horizontal particle velocity is obtained under the largest crest in the time series.

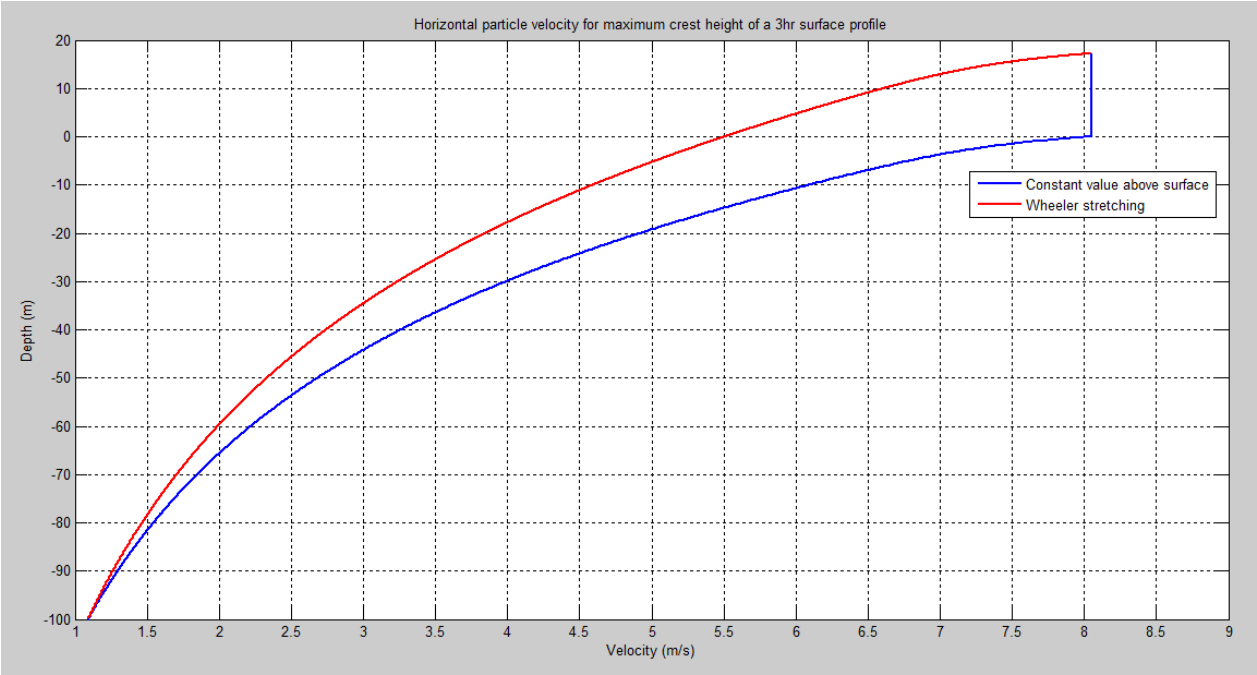

Figure 4.15. Horizontal particle velocity profiles for the largest crest height in the time series. Where crest height = 17,23m and period = 14s.

There are two plots in figure 4.15, where the blue plot represents horizontal particle velocity with extrapolation to mean surface level and constant value above the mean surface level . The red line is Wheeler stretching. By comparing the blue line to the maximum horizontal particle velocity profile in figure 4.14, one can see that those two lines are the same and confirm the statement above.

4.1.6 Verification of linear horizontal particle velocity program

To confirm that the program creates an accurate approximation, one would need to do some calculations outside of Matlab. Those results will be compared with Matlabs results for verification. Excel will be used as the second program to calculate some of the horizontal particle velocity with the same formula as shown above. If the results are the same, one can say that the program runs in a correct manner.

First of all, one would need to confirm that the surface process generates the same values in bout approaches. If the surface process generates the same values, it would mean that bout programs calculate a correct answer. It will also confirm that we have a correct estimate for the generated wave spectrum. To create the same sea state for bout programs the random phase value needs to be saved, and used in bout programs. This has been done and we have used the same phase angle values as the sea state from figure 4.11. To simplify the work in excel, the only wave generated for the surface process is the wave with the largest crest height for the whole 3-hour sea state. Results from Matlab can be seen in figure 4.16 and figure 4.17 shows the results from Excel.

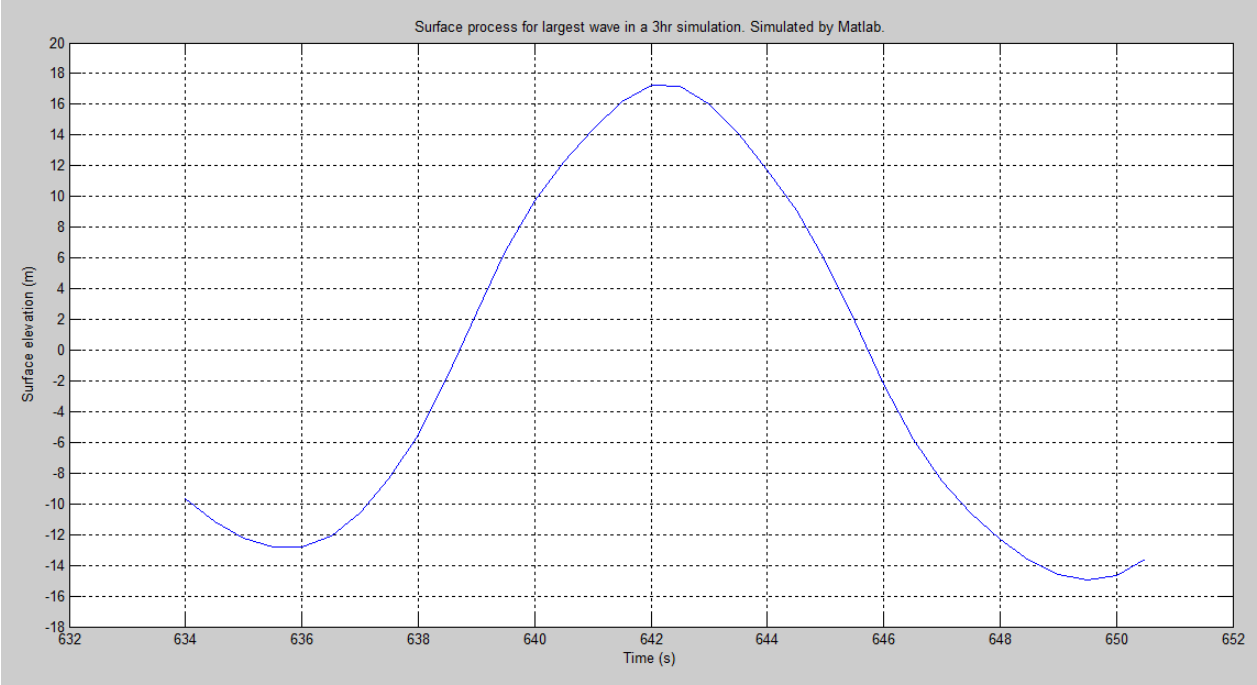

Figure 4.16. Largest wave of a 3-hour linear surface process obtained from the same sea state as figure 4.11. Where h_s = 14,9m and t_p = 15.8s. Simulated from Matlab.

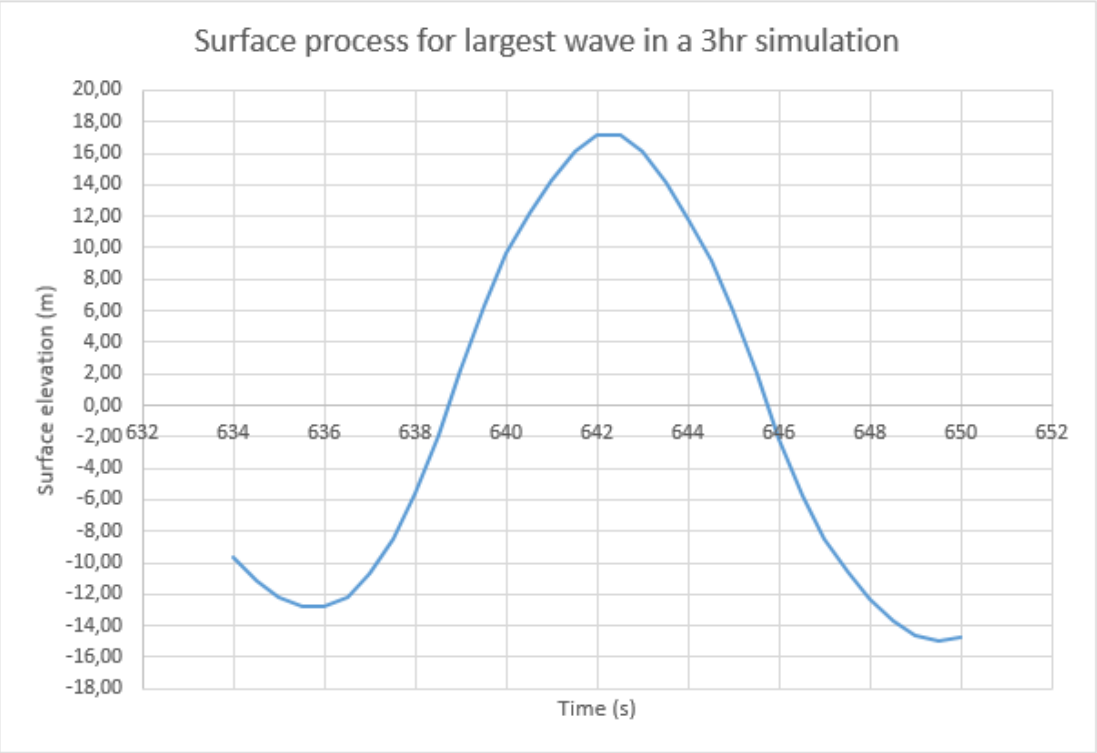

Figure 4.17. Largest wave of a 3-hour linear surface process obtained from the same sea state as figure 4.11. Where h_s = 14,9m and t_p = 15.8s. Calculated from Excel.

From figure 4.16 and 4.17, one can see that Matlab and Excel creates the same values with two different approaches. This means that our process in Matlab generates correct values for the surface process. In Excel I have calculated every number and summarized them with help of Excels commands. To see the calculations done in Matlab, see Matlab file "Verification_of_Matlab_program_linear_Matlab_file" for Excel file, see "Verification of Matlab program Excel file". The same two files are also used to verify the horizontal particle velocity profile. Here we have chosen to generate the horizontal particle velocity profile under the crest at time 642s and at time 641s. The reason I have chosen to investigate at time 641s is since Matlabs generated horizontal particle velocity profile in this time curves in the opposite side as it approaches the mean water level. This can be seen in figure 4.18, which is generated from the Matlab file. Results from the Excel file can be seen in figure 4.19, which is the same result as the Matlab file generates. This means that the curve near the surface is not a wrong approximation. Instead, it is a result from summing up all the waves with different frequency and phases. Where the high frequency waves do a much more impact at the surface and lesser the deeper it gets. Even if the high frequency waves in general provides low impact in the horizontal particle velocity. Results of this might be the cause for the curve. Our program have now been confirmed to provide a correct answerer. For more details about the Excel or Matlab calculations, see the referred files above.

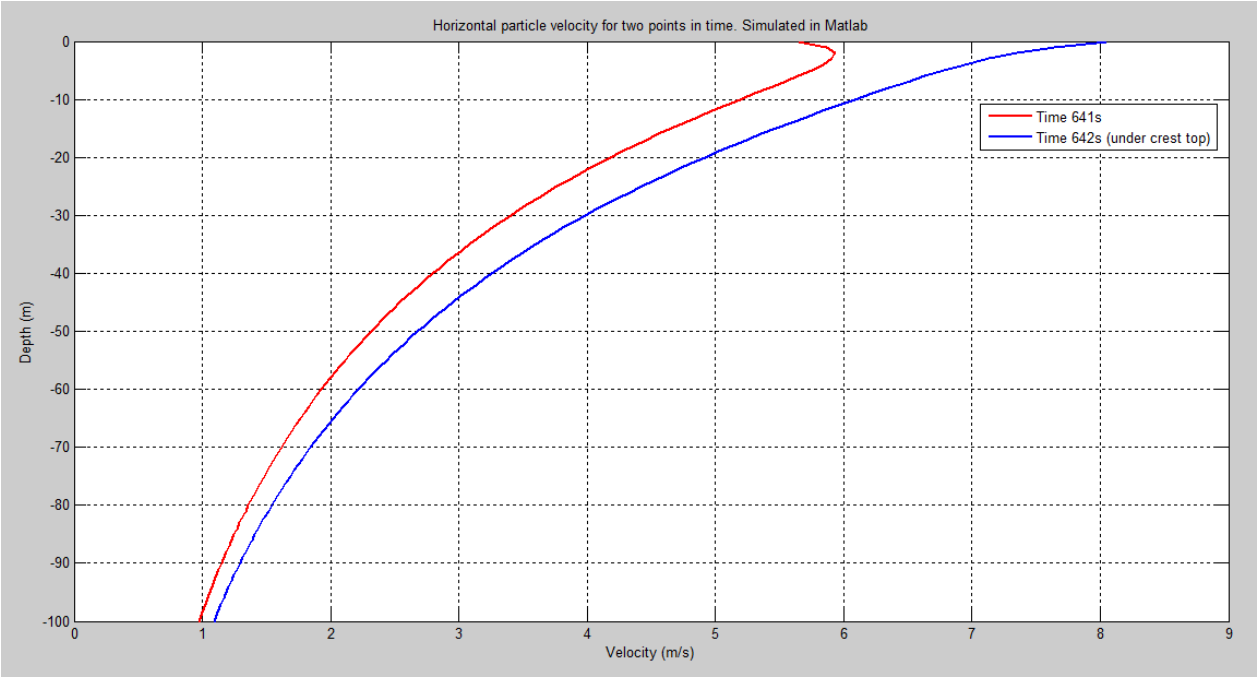

Figure 4.18. Horizontal particle velocity profiles at time 642s (under crest top) and time 641s. Where crest height = 17,23m and period =14s. Simulated from Matlab.

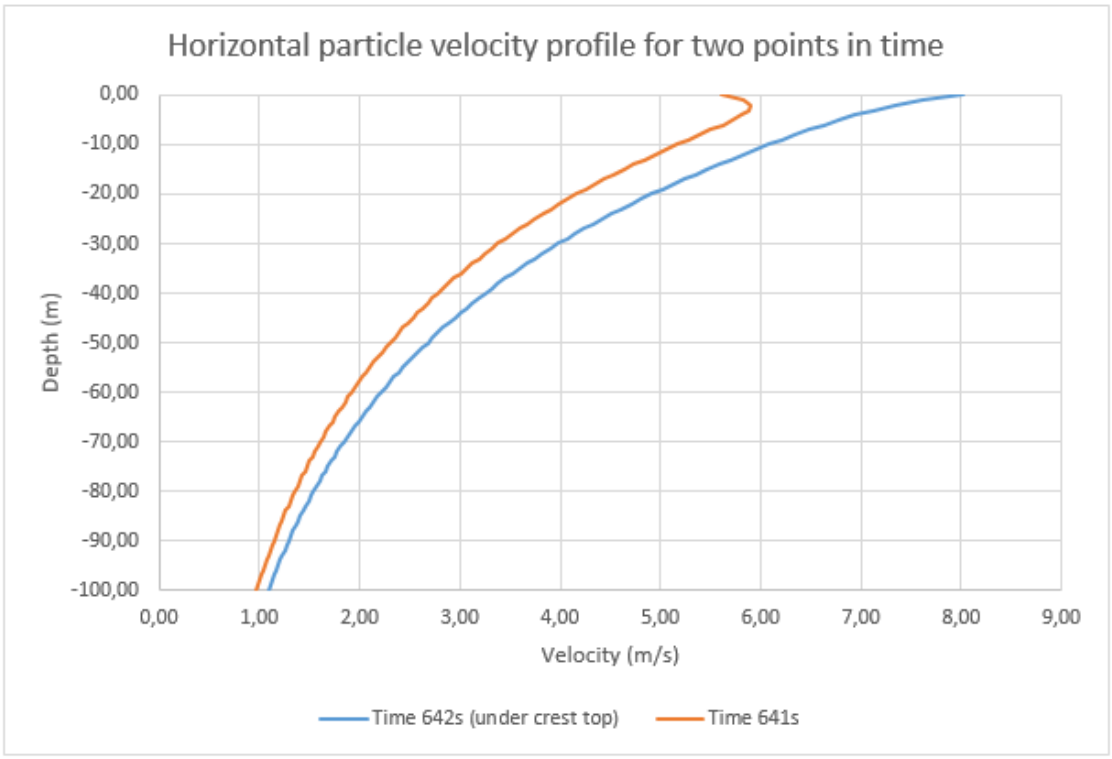

Figure 4.19. Horizontal particle velocity profiles at time 642s (under crest top) and time 641s. Where crest height = 17,23m and period =14s. Calculated from Excel.

4.1.7 Results for horizontal particle velocity compared to Stokes waves

Now that the program used to estimate the horizontal particle velocity has been verified, one can start comparing the results to a Stoke wave. In order to re do the simulations shown in figure 4.20 the different random phase φ values has been stored in an excel file named "Different phases for linear surface process". There are three different 3-hour simulations below showing the horizontal particle velocity profile for each case, where the next chapter calculates loads and loads effects for each case. The first case is the same case as shown above. Where the surface process is shown in figure 4.11 and for the horizontal particle velocity profile, see figure 4.20.

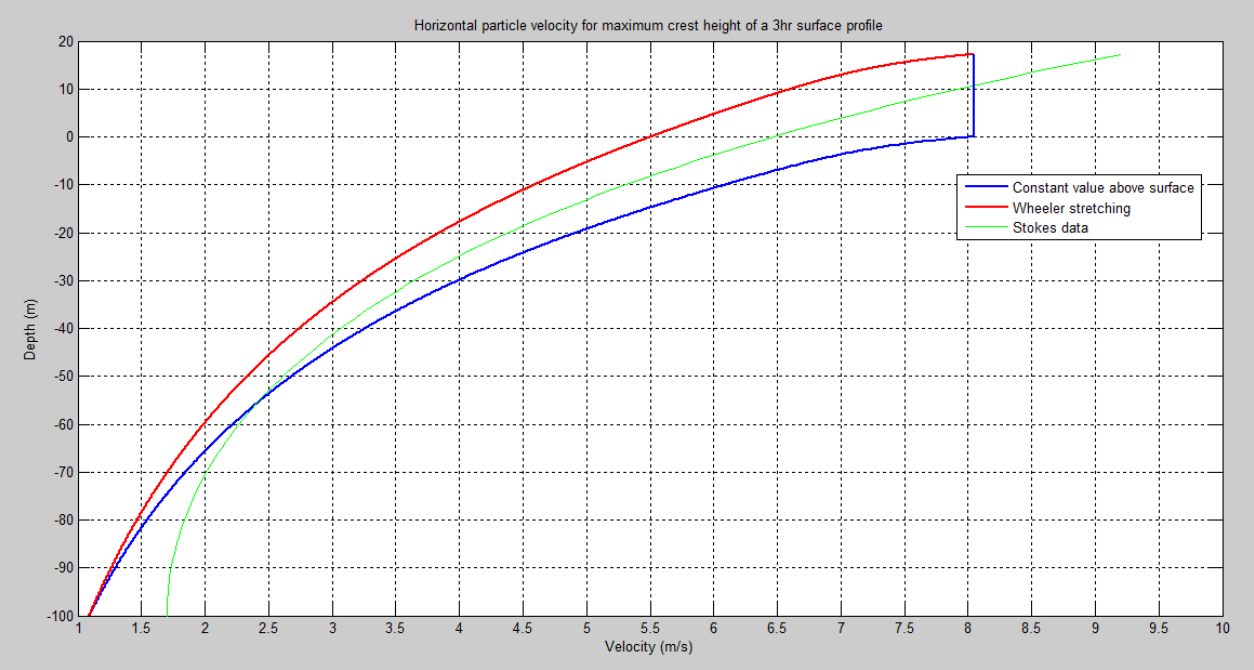

Figure 4.20. Comparison between different methods to obtain the horizontal particle velocity profiles for the largest crest height in a time series. Where maximum crest height = 17,23m and period = 14s.

Figure 4.20 shows the three different plots for the same crest height and period. Where Wheeler stretching might be giving to low value as discussed before. If one assume that a Stokes wave are the most accurate method, since this is a higher order approximation. By look at the third plot, which uses constant value above mean surface level, one can see that it has a much better fit than the Wheeler stretching for a linear approach. It might also be a good estimate for the loads and loads effect that's shown later on.
The second case shows the kinematics of a much lower maximum crest height. See figure 4.21 for surface process and figure 4.22 for the horizontal particle velocity profiles for this case. The third case has a maximum crest height similar to the crest height corresponding to an exceedance probability of 0.1 for the sea states. Where Surface process are shown in figure 4.23 and the horizontal particle velocity profiles can be seen in figure 4.24 for case three.

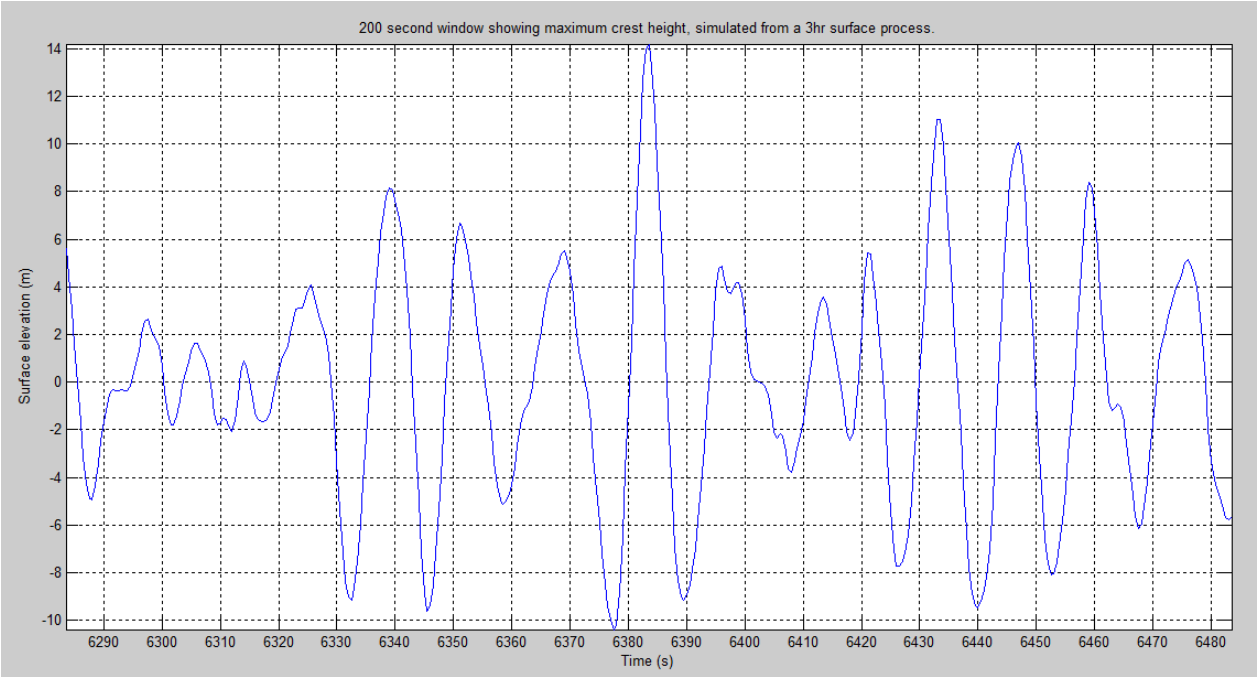

Figure 4.21. 200-second window of a 3-hour linear surface process. Where h_s = 14,9m and t_p = 15.8s. Maximum crest height obtained is 14,21m with a period of 12s and wave height = 24.00m.

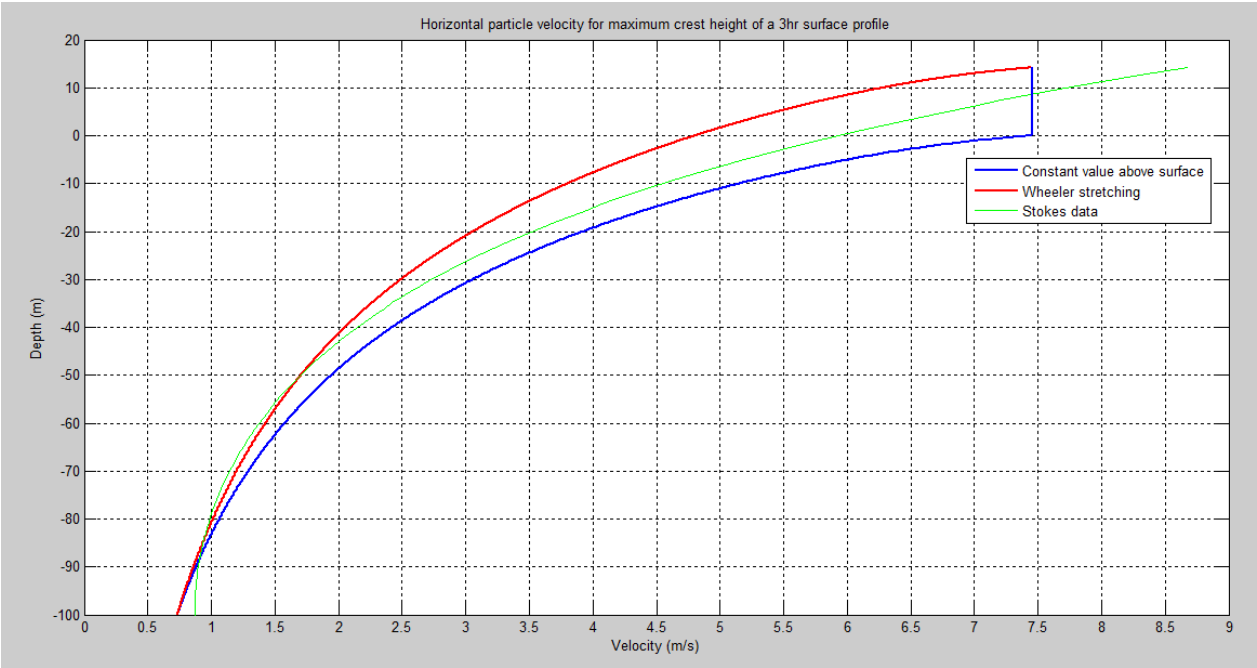

Figure 4.22. Comparison between different methods to obtain the horizontal particle velocity profiles for the largest crest height in a time series. Where maximum crest height = 14,21m and period = 12s with a wave height = 24.00m.

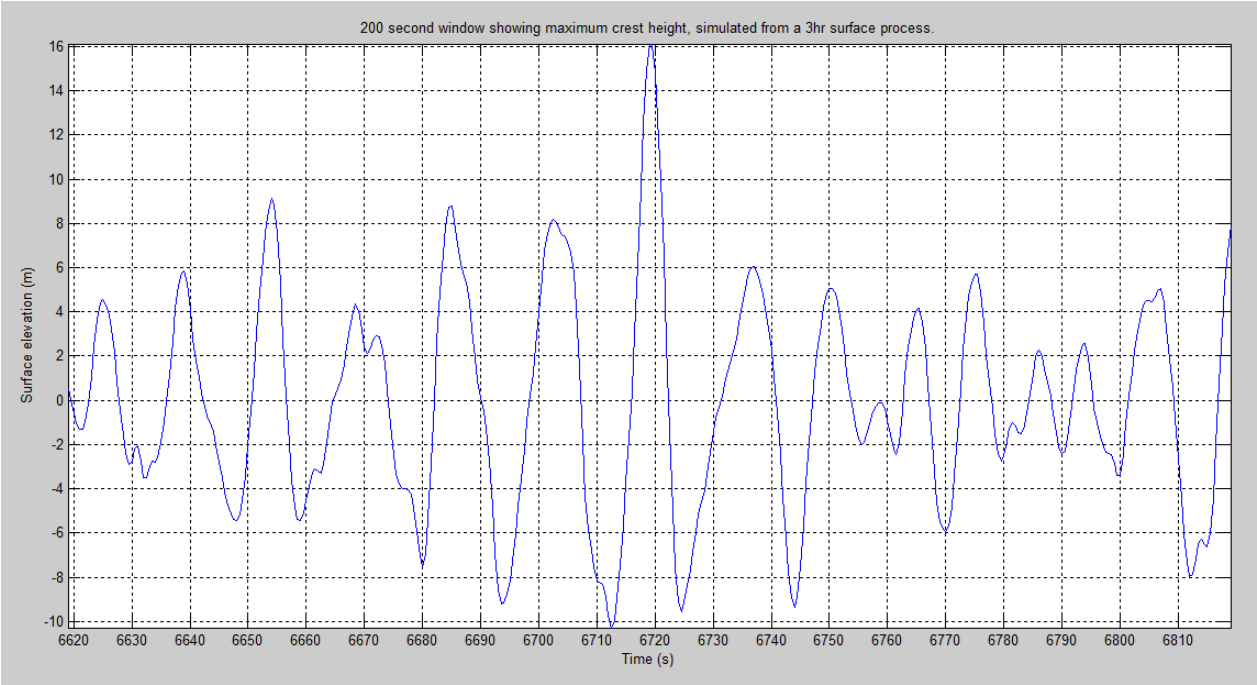

Figure 4.23. 200-second window of a 3-hour linear surface process. Where h_s = 14,9m and t_p = 15.8s. Maximum crest height obtained is 16,11m with a period of 12s and wave height = 26.03m.

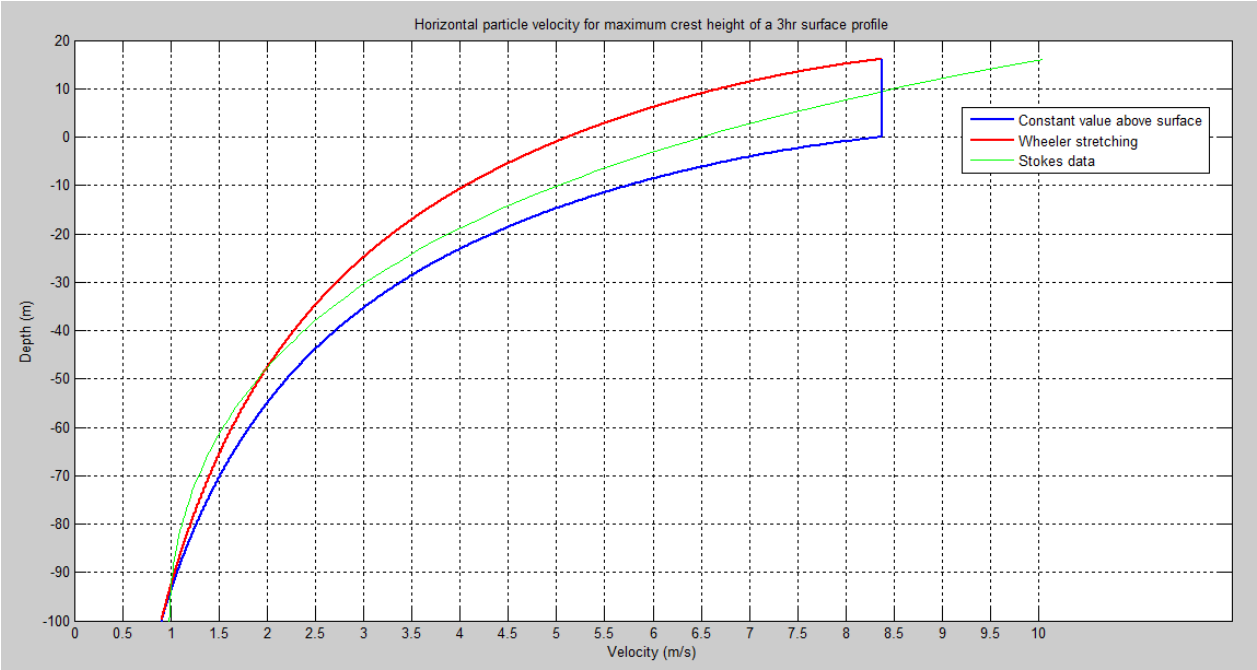

Figure 4.24. Comparison between different methods to obtain the horizontal particle velocity profiles for the largest crest height in a time series. Where maximum crest height = 16,11m and period = 12s with a wave height = 26.03m.

By comparing the three cases to the Stokes data, one can clearly see that the linear surface process may generate similar kinematics as a Stokes waves. This can especial be seen in case two and three, where a very good approximation to the horizontal particle velocity compared to the Stokes data gathered from the Stokes 5th order program is obtained.

4.1.8 Drag dominating forces for simulated maximum crest height compared to Stokes waves

Now that the horizontal particle velocity profiles has been obtained, one can use the Morison equation to estimate the base shear and overturning moment for a drag dominated case. A column diameter of D = 1m will be used further on. The Morison equation has been introduced previously in chapter 3.5.1, but is shown in equation 4.31 for base shear and 4.32 for overturning moment again. Those formulas can only be used to calculate drag dominated cases.

$$F(t) = \int_{-d}^{\xi} f_D(z,t)dz = \int_{d}^{\xi} \left(\frac{1}{2} * \rho * \mathrm{C_D} * \mathrm{D} * V * |V|\right) dz \qquad \text{Equation 4.31}$$

$$M = \int_{-d}^{\xi} (z+d) * f_D(z,t)\, dz \qquad \text{Equation 4.32}$$

Where V is the horizontal particle velocity profile for each of the three cases above. The results is shown in table 4.1.

Table 4.1. Load results for column diameter 1m, drag dominating forces. Where 1GN =10^3 MN = 10^6 kN = 10^9 N. X^o for stokes data instead of time for linear data. Crest top is the x-position when 0^o, mean surface level is approximately 80^o and through is 180^o. Max value obtained at crest top with a first order process.

	Forces on simplified offshore structures according to different wave models where: D=1m (Drag dominating force)						
Case name	Period, T.(s)	Wave height, h.(m)	Amplitude, a.(m)	Height over surface, ξ.(m)	Wave phase (s or ^{o})	Force, F.(MN)	Moment, M.(MNm)
Constant above surface	14	31.12	17.23	17.23	642s	1.13	99.28
Wheeler Stretching	14	31.12	17.23	17.23	642s	0.709	61.23
Stokes data	14	29.13	17.23	17.23	0^o	0.976	84.37
Constant above surface	12	24.00	14.21	14.21	6383,5s	0.771	69.43
Wheeler Stretching	12	24.00	14.21	14.21	6383,5s	0.457	40.29
Stokes data	12	24.06	14.21	14.21	0^o	0.635	57.82
Constant above surface	12	26.03	16.11	16.11	6719s	1.02	92.47
Wheeler Stretching	12	26.03	16.11	16.11	6719s	0.574	51.09
Stokes data	12	26.80	16.11	16.11	0^o	0.838	77.63

Our results show that the constant value above surface approach obtains the most base shear and overturning moment. Where Wheeler stretching obtains very low values compared to the other two cases. This confirm the concern of the new N-003 standard, [2] in recommendation to not use Wheeler stretching since it might give values below the safe zone when designing. The constant value above surface approach might be giving to high value and cause oversizing in the design process. It would therefore be very interesting to create a second order process and compare the results of loads and loads effects from a linear and second order approach.

4.2 Second order approximation for irregular waves

To improve the accuracy of our simulated surface process and the kinematics of the maximum event, one would need to generate a second order process. The new N-003 standard, [2] also state that the surface process and the corresponding kinematics for a time domain simulation, shall be modelled as a second order random process with second order theory, when calculating load and loads effects. Those are the mean reason to generate a second order process also to compare the result with Stokes waves and a first order process. Generating a second order process needs a much higher capacity from Matlab and the computer used. Because of this, we are going to simulate 20-minutes time series instead of a 3-hour sea states for this thesis. To run a second order surface process of 3-hour, a good computer is required and patient since it might take 1 to 12-hours running time. Depending on the computer and Matlab settings.

4.2.1 Simulation of a 20-minutes second order surface process

A second order surface process can be obtained with a second order correction plus the first order equation. This can be seen from equation 4.33. Where the following formulas where obtained from [8], [20] and [21]. [20] is a short presentation of [21].

$$\eta = \eta^{(1)} + \eta^{(2)} \qquad \text{Equation 4.33}$$

Where $\eta^{(1)}$ is the formula for first order surface process used earlier and $\eta^{(2)}$ is the second order correction to achieve a second order surface process, η.

$$\eta^{(1)} = \sum_{n=1}^{N} a_n * \cos(\phi_n) \qquad \text{Equation 4.34}$$

$$\eta^{(2)} = \sum_{n=1}^{N} \frac{1}{2} * a_n^2 * k_n * \cos(2 * \phi_n) + \sum_{n=1}^{N-1} \sum_{m=n+1}^{N} \frac{1}{2} * a_n * a_m * ((k_n + k_m) * \cos(\phi_n + \phi_m) - (k_m - k_n) * \cos(\phi_m - \phi_n)) \qquad \text{Equation 4.35}$$

The second order correction uses a double summation. This is why it requires a high computer capacity and time to simulate a 3-hour sea state. When a double summation is used one obtain N times the number of a first order simulation. Where N is the number of frequency components.

The same wave spectrum generated under chapter 4.1.1 is used here as well, except for a shorter interval of the wave spectrum meaning that:

$\xi_{0,i} = a_n$
$\xi_{0,(i+1)} = a_m$

Which has been explained under chapter 4.1.2. The following formulas, that were not explained is as following:

$$\phi_n = k_n * x - \omega_n * t + \varphi_n \qquad \text{Equation 4.36}$$

Equation 4.36 determine the phase of the wave. Equation 4.36 has been obtained from [20].

$$\omega_n^2 = g * k_n \qquad \text{Equation 4.37}$$

k_n is the wave number described by the frequency in Hz.

$$k_n = \frac{(2\pi * f)^2}{g} \qquad \text{Equation 4.38}$$

The differences on $_n$ and $_m$ is that the $_n$ starts with an $f = \frac{1}{T}$ and $_m$ starts with $= \frac{2}{T}$, if the steepness of the frequency, f are $\frac{1}{T}$. This means that $k_m > k_n$.

For a 20-minutes sea state, one need to have T > 1200s to insure it doesn't repeat itself. In the following 20-minutes simulation, T = (1200 + 50) has been used where $\Delta\omega = 2\pi * 1250$.

Because of the extra second order correction, one obtain a much larger use of the wave spectrum, meaning that the summed up amplitude will be to large if full spectrum are used. This will affect the kinematics and create to high values. To fix this one would need to reduce the use of high frequencies waves. A cut-off frequency has therefore been proposed by Stansberg, C.T. This cut-off frequency has been confirmed to show reasonable values, when comparing calculated wave profiles to measured waves. It is also recommended to use this cut-off frequency from DNV, [8]. Which is obtained from [21] and shown in equation 4.39.

$$\omega_{Cut_S} = \sqrt{\frac{2 * g}{h_s}} = \sqrt{\frac{2 * 9.81}{14.9}} = 1.14 \qquad \text{Equation 4.39}$$

To use frequency in Hz as the spectrum frequency cut-off one can use: $f_{Cut_S} = 1.14 * 2\pi = 0.18\ Hz$. This is the cut-off frequency used for the 20-minute's simulations in this thesis.

From those formulas, we obtain the following results. Shown in figure 4.25-27.

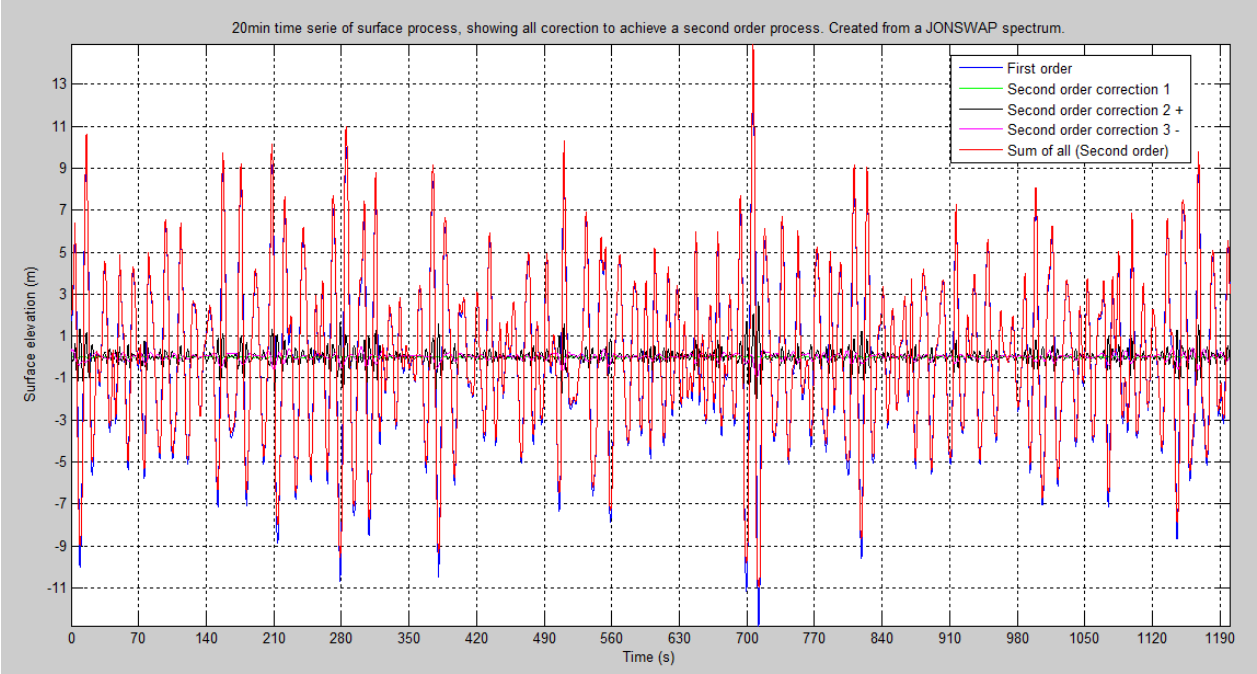

Figure 4.25. 20-minutes second order surface process, created from a JONSWAP spectrum. With h_s = 14.9m and t_p = 15.8s.

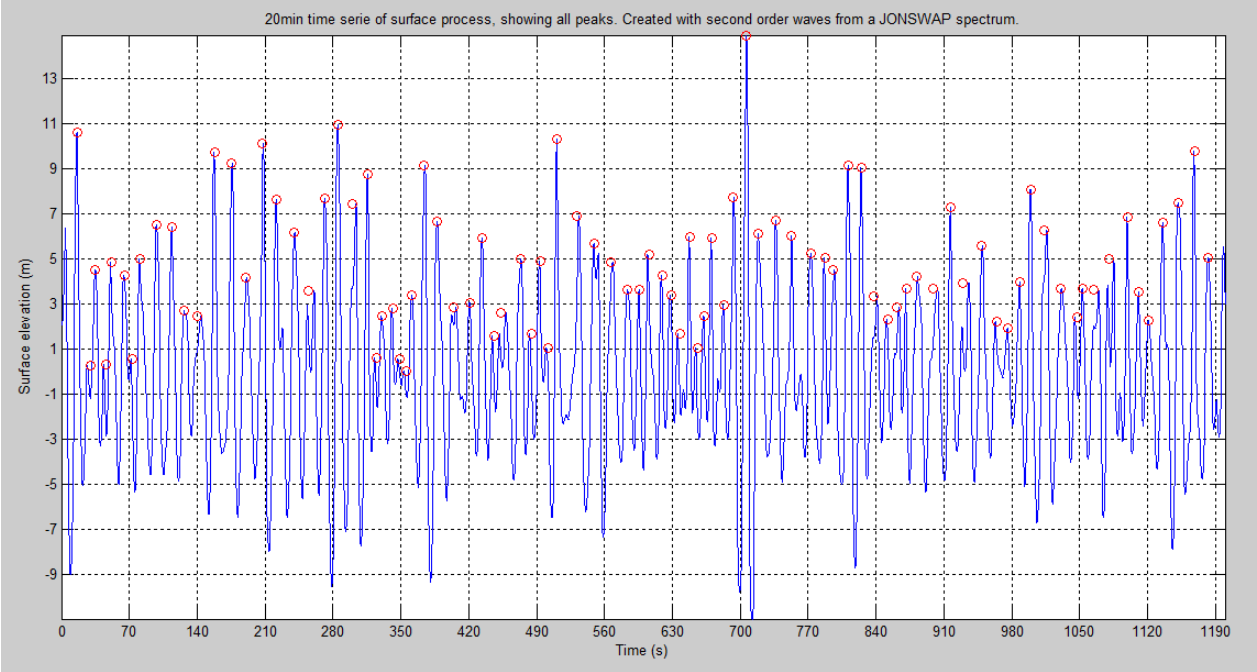

Figure 4.26. 20-minutes second order surface process showing global peaks. Created from a JONSWAP spectrum. With h_s = 14.9m and t_p = 15.8s.

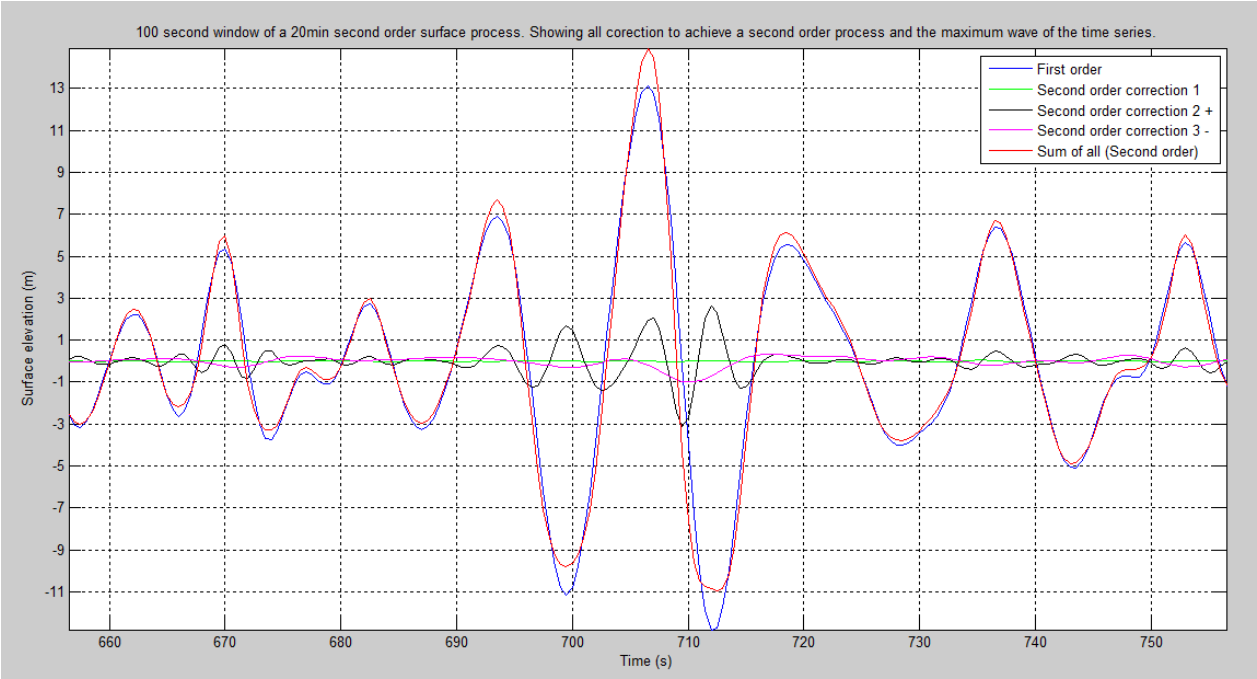

Figure 4.27. 100 seconds window, showing maximum crest height of a 20-minutes second order surface process and corrections to achieve a second order process. Created from a JONSWAP spectrum with h_S = 14.9m and t_P = 15.8s.

From this sea state, one can obtain a maximum crest height of 14,92m with a period of 13s. The difference between the linear and second order surface process can be seen in figure 4.25 and 4.27. Figure 4.27 show the values from a linear process, all the second order corrections and finely the second order surface process, which is the sum of them. Where second order correction 1 uses one summation, second order correction 2 is the positive double summation and second order correction 3 is the negative summation from equation 4.35. From this figure, one can see that the linear process produces shorter crest height and higher trough than a second order process. It is the second order correction that correct those heights to a more realistic wave.

Now that a surface process is established, we can obtain all the peak values that has been pointed out by figure 4.26. Since the simulation is only a 20 minutes series, a maximum crest height distribution cannot be obtained. To do this one would need to simulate 30+ 3-hour simulations and obtain the maximum crest height value for each of those simulations as we did with the first order approach. With the second order approach, it would take too long time and we would therefore suggest that this would be recommended on further work later on. What one can do is to confirm, if the data follows a second order distribution. By comparing the peak data to a 2-parameter Weibull distribution formula set on a Weibull scale. One can observe if the data follows the linearized short term Weibull distribution and goes in a straight line. If it does, one would have confirmed that the second order surface process follows the 2-parameter

Weibull distribution, which has been confirmed by Forristall to follow a second order simulations. This will be an indication that our program has the right output.

The short term 2-parameter Weibull distribution formula have already been introduced in chapter 2.4, when the 10^{-2} annual probability crest height, $C_{0.01}$, was predicted. This means that our expected 10^{-2} annual probability crest height, $C_{0.01}$, in this second order surface process is 17,87 m. The 2-parameter Weibull distribution formula used is:

$$\mathrm{F_{C|H_s,T_1}(c|h_s,T_1,d)} = 1 - \mathrm{e}^{-\left(\frac{\mathrm{c}}{\alpha_F * \mathrm{h_s}}\right)^{\beta_F}} \qquad \text{Equation 4.40}$$

The result for putting this formula to a Weibull scale can be seen in equation 4.41.

$$\ln\left(-\ln\left(1-\mathrm{F(y)}\right)\right) = \beta_F * \ln(\mathrm{c}) - \beta_F * \ln(\alpha_F * \mathrm{h_s}) \qquad \text{Equation 4.41}$$

For obtaining the Fitted Weibull line, equation 4.40 has been used and is shown below:

$$1.88 * \ln(\mathrm{c}) - 1.88 * \ln(0.37 * 14.9) = \mathrm{Cum.Prob}$$

To fit the different crest height data one can used the following formula.

$$\ln\left(-\ln\left(1-\mathrm{F(y)}\right)\right)$$

Where $\mathrm{F(y)} = \frac{C_n}{N+1}$, Empirical distribution. And the X-axes is Ln(crest height).

The result can be seen in figure 4.28, which is the same 20-minutes simulation as figure 4.25.

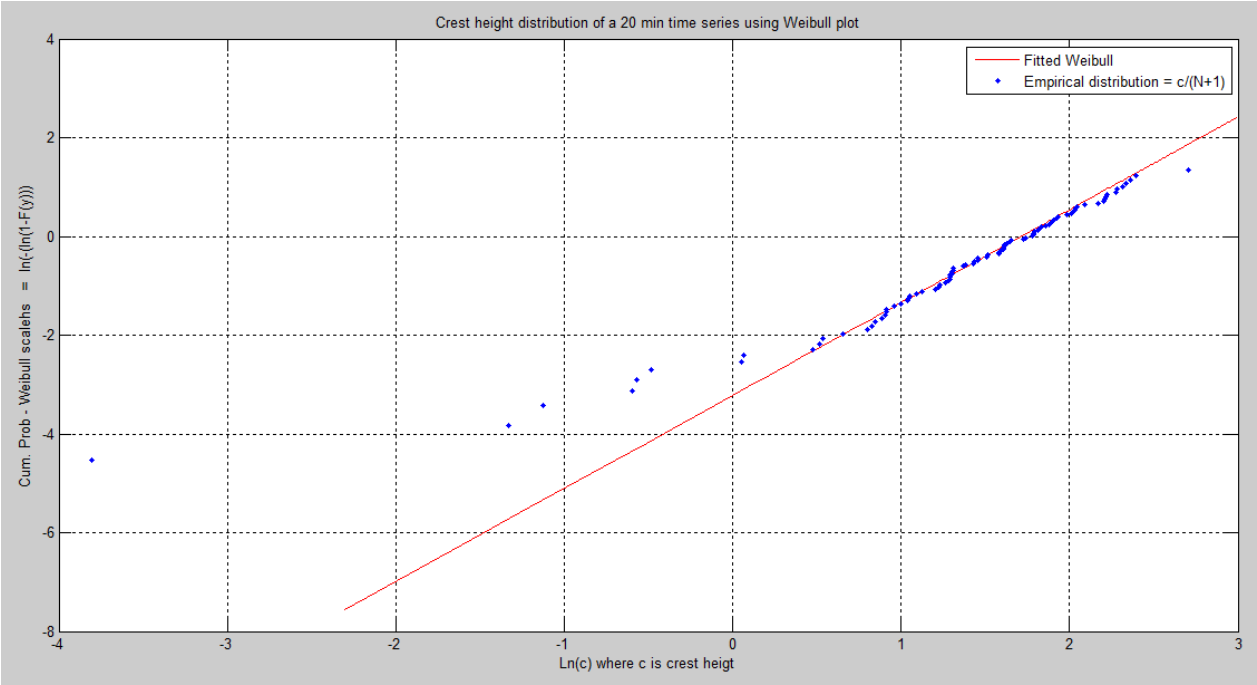

Figure 4.28. Global maxima versus a 2-parameter Weibull distribution (1)

Another result from a random simulation can be observed in figure 4.29 to compare with figure 4.28.

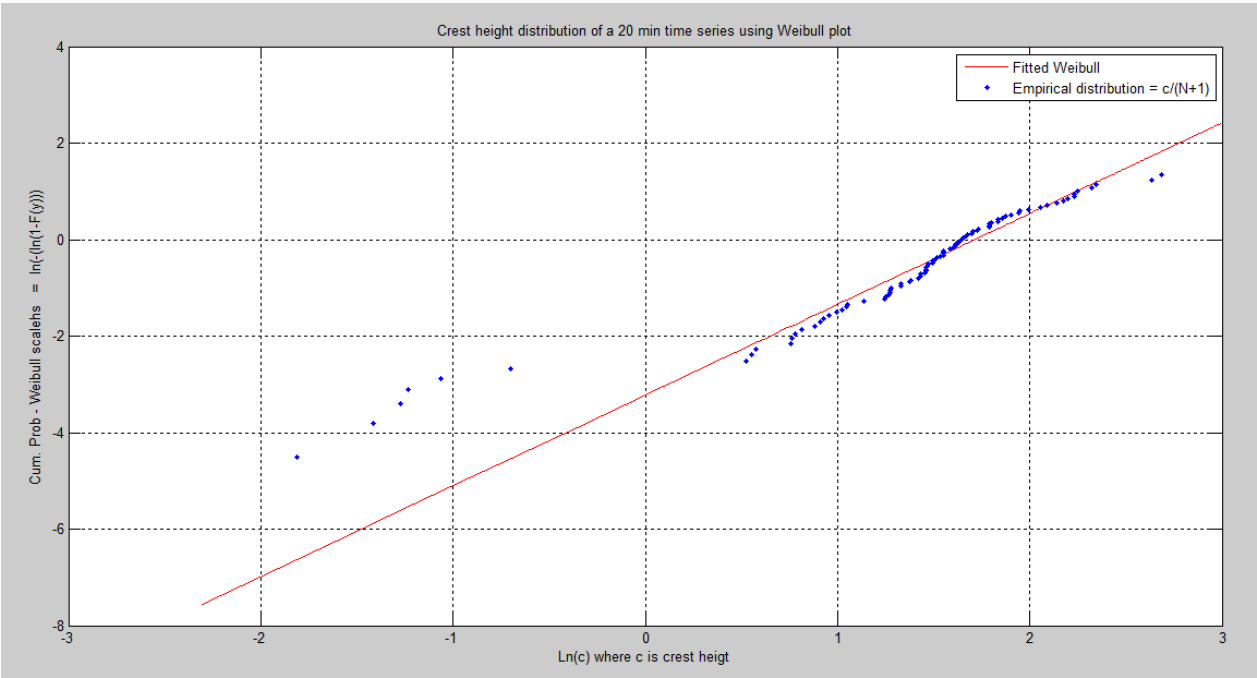

Figure 4.29. Global maxima versus a 2-parameter Weibull distribution (2).

Figure 4.28 and 4.29 show that the main peak data follows the Weibull distribution. The lower part of the peaks below Ln(0), which is at a crest height < 1m can be neglected since a known error of Matlab is known. As mentioned before, this error is caused because of to close zero up crossings. A good example of this error can be seen in figure 4.30, where all the circles are peaks, but the read ones shouldn't have been there. This is the reason for neglecting peaks below 1m. Apart from this, one can clearly see that the crest heights follows a Weibull distribution, meaning that our program is verified to follows a second order distribution.

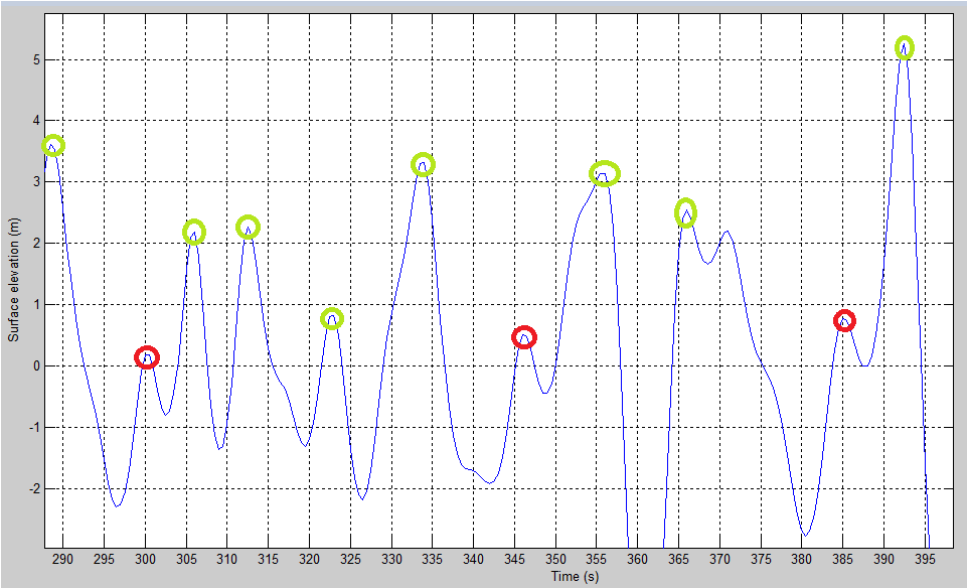

Figure 4.30. Illustrating peaks of a surface process, where green peaks are real peaks and red peaks are not valid.

4.2.2 Second order kinematics

Horizontal particle velocity is the only interesting kinematics for a drag dominated case, as discussed in the linear part for irregular waves. Therefore, a second order correction formula has been obtained from [20], [21]. This formula is only valid at depth below mean water level ($z < 0$). Since the formula will drastically overestimate the velocity above mean water level. A linear Taylor expansion above mean water level is therefore introduced later on. We have also mentioned that a cut-off frequency are needed especially for the kinematics. This was introduced in chapter 4.2.1.

The velocity potential obtained from [20], can be seen in equation 4.42 and 4.43. Where $\phi^{(1)}$ is first order and $\phi^{(2)}$ is the second order correction for velocity potential.

$$\phi^{(1)} = \sum_{n=1}^{N} \frac{a_n * \omega_n}{k_n} * \sin(\phi_n) * e^{k_n * z} \qquad \text{Equation 4.42}$$

$$\phi^{(2)} = -\sum_{n=1}^{N-1} \sum_{m=n+1}^{N} a_n * a_m * \omega_m * \sin(\phi_m - \phi_n) * e^{(k_m - k_n) * z} \qquad \text{Equation 4.43}$$

The second order velocity potential correction doesn't include all the subsection for the surface process. This is because the two first subsection of the surface process becomes zero in the velocity potential when summed up according to [22].

The horizontal particle velocity is found through the derivative of velocity potential in x direction and can be seen in equation 4.44 and 4.45. Where the formula for a second order horizontal particle velocity is shown in equation 4.46, which is only for $z < 0$.

$$\phi_x^{(1)} = \sum_{n=1}^{N} a_n * \omega_n * \cos(\phi_n) * e^{k_n * z} \qquad \text{Equation 4.44}$$

$$\phi_x^{(2)} = -\sum_{n=1}^{N-1} \sum_{m=n+1}^{N} a_n * a_m * \omega_m * (k_m - k_n) * \cos(\phi_m - \phi_n) * e^{(k_m - k_n) * z} \qquad \text{Equation 4.45}$$

$$\phi_x \Big|_{z<=0} = \phi_x^{(1)} + \phi_x^{(2)} \Big|, \quad for \quad z <= 0 \qquad \text{Equation 4.46}$$

All the parameters and variables has been explained in chapter 4.2.1 and the result for using those formulas in Matlab is as following:

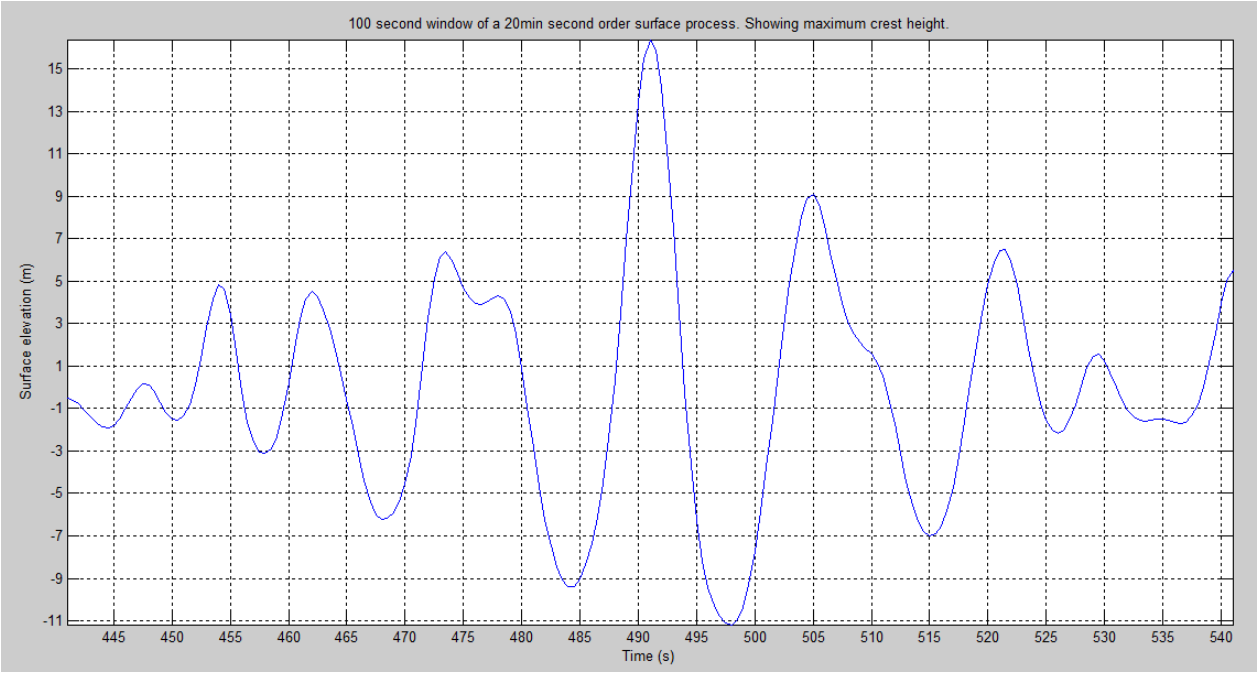

Figure 4.31. 100-second window of a 20-minuts second order surface process. Where h_s = 14,9m and t_p = 15.8s. Maximum crest height obtained is 16,38m with a period of 14s and a wave height = 26.67m.

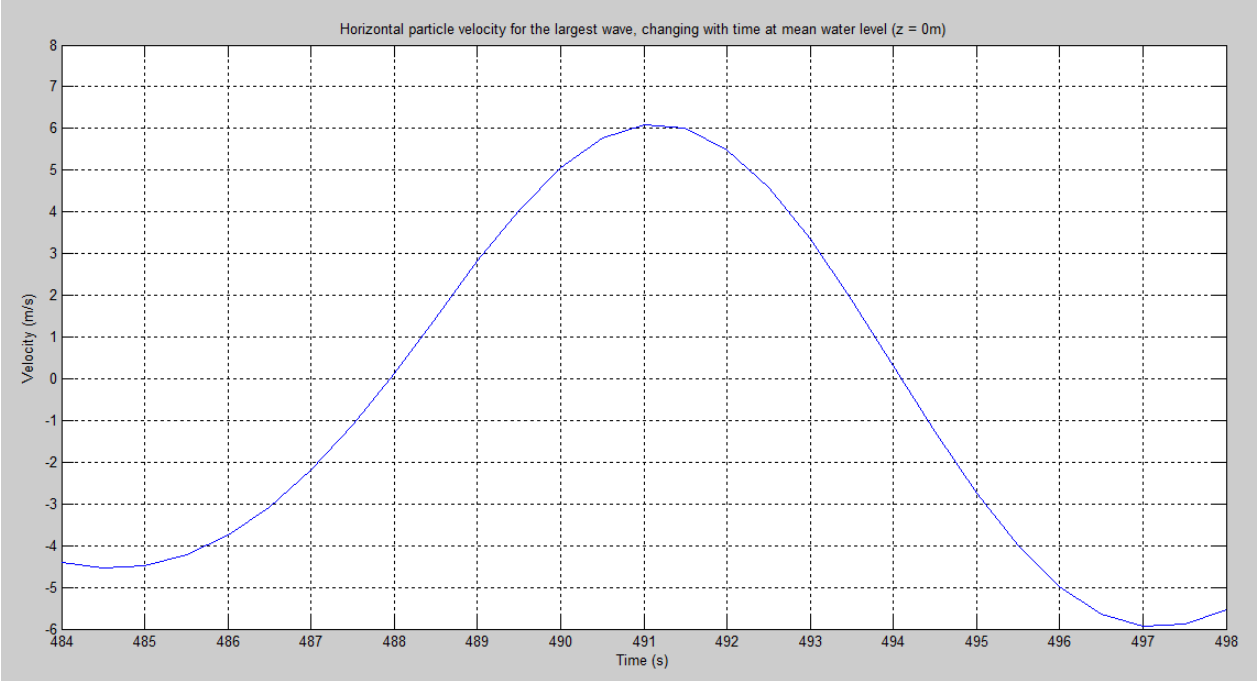

Figure 4.32. Horizontal particle velocity changing with time at mean surface level (z = 0m). For the largest wave in a 20-minuts surface process.

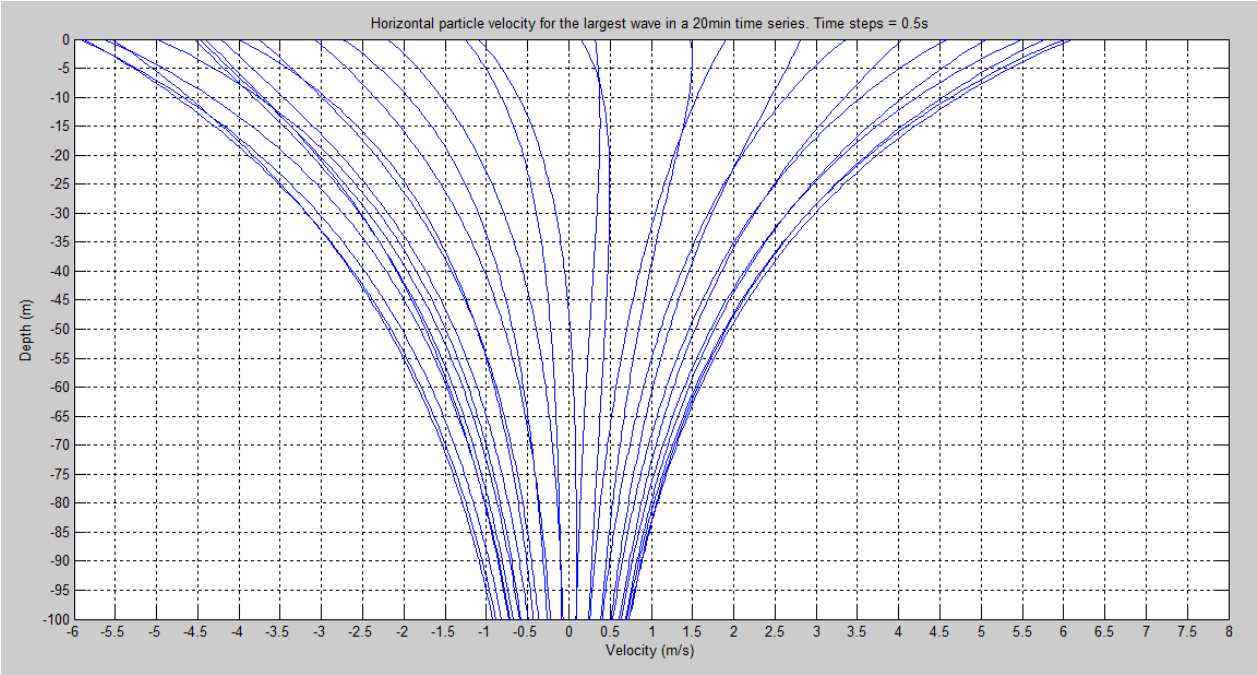

Figure 4.33. Horizontal particle velocity profiles for the largest wave in the 20-minutes surface process, where time step = 0.5s.

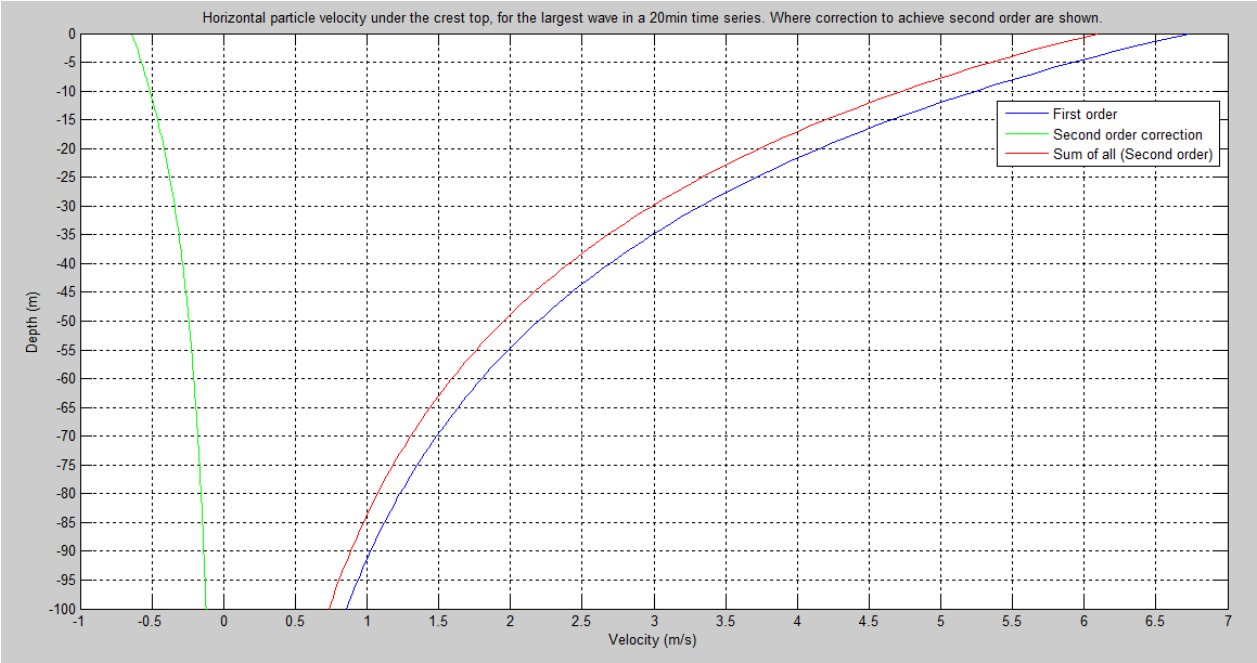

Figure 4.34. Horizontal particle velocity profile for the largest crest height in the time series, where crest height = 16,38m and period = 14s. Showing first order and second order correction to achieve a second order profile.

Figure 4.31-34 is the result of the same simulation for a 20-minutes surface process. In figure 4.32, one can see how the horizontal particle velocity for the largest wave changes with time at mean surface level, bear in mind that this is just an approximation. All the horizontal particle velocity profiles for the largest wave can also be seen in figure 4.33, where the horizontal particle velocity profile under the crest top for this wave is shown in figure 4.34. This is the largest horizontal particle velocity obtained for the time series, but the kinematics only goes up to mean surface level (z = 0). Finding the horizontal particle velocity above mean surface level can be done with different approaches. In this thesis, we have chosen to use Stansbergs approach. His method is a linear Taylor expansion above mean surface level. This formula can be seen in equation 4.47 and is obtained from [20]. Figure 4.34 also shows that the second order correction has a negative value meaning that it reduces the first order equation when obtaining the second order horizontal particle velocity profile.

$$\phi_x \Big|_z = \phi_x^{(1)} + \phi_x^{(2)} + z * \phi_{xz}^{(1)} \Big|_{z=0}, \quad for \quad z > 0 \qquad \text{Equation 4.47}$$

Where $\phi_{xz}^{(1)}$ is the derivative of horizontal particle velocity in z direction. Shown in equation 4.48

$$\phi_{xz}^{(1)} = \sum_{n=1}^{N} a_n * \omega_n * k_n * \cos(\phi_n) * e^{k_n * z} \qquad \text{Equation 4.48}$$

The result of this is can be observed in figure 4.35. From this figure, one can approximate that the maximum horizontal particle velocity at the crest top is 8.9 m/s.

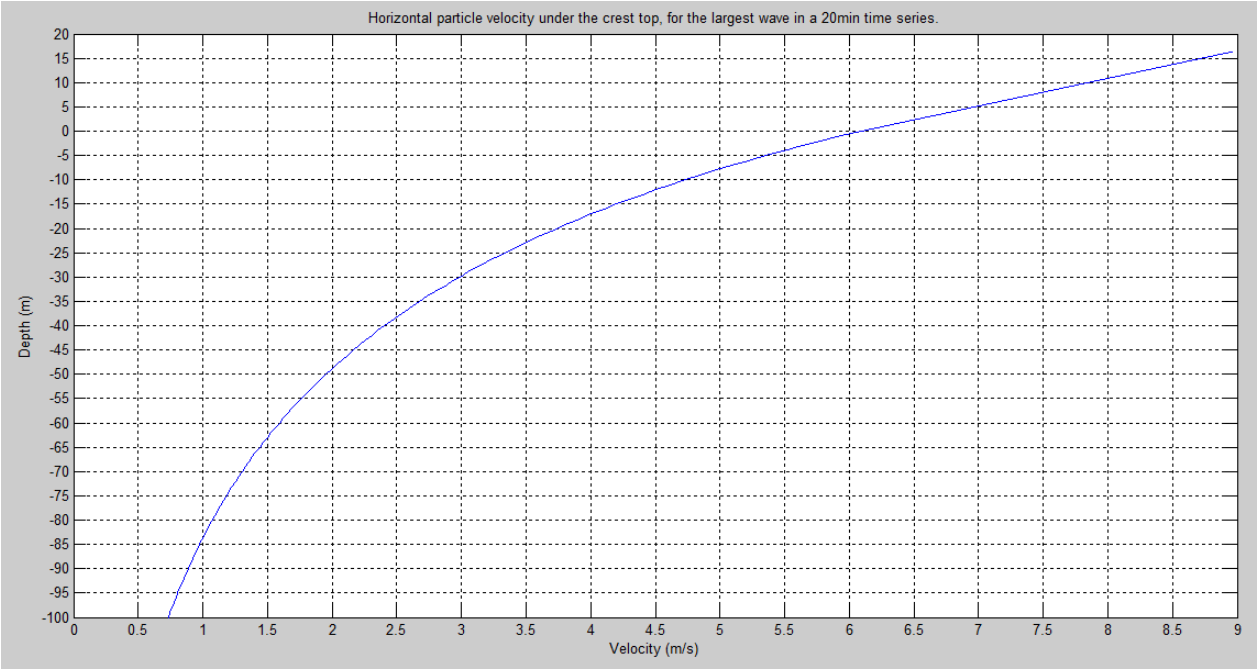

Figure 4.35. Horizontal particle velocity profile for the largest crest height in the time series, where crest height = 16,38m and period = 14s. With linear Taylor expansion above mean water level (z > 0).

4.2.3 Results for Second order horizontal particle velocity compared to Stokes waves

The next step will be to compare the horizontal particle velocity profile of the Matlab file to the Stokes data obtained from Stokes program. In the Stokes program, we have iterated the wave height to obtain the same crest height as the simulated maximum crest height obtained. The same period has also been used in Stokes program and the result of this is shown in figure 4.36.

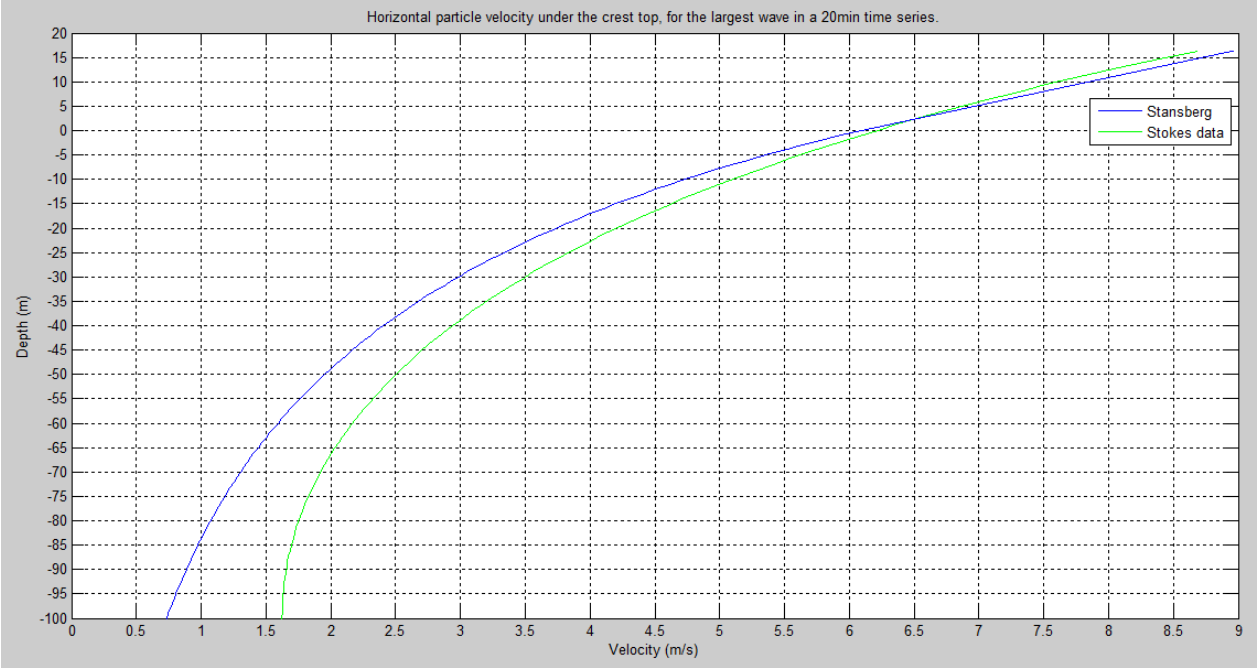

Figure 4.36. Horizontal particle velocity profile for the largest crest height in the time series, where crest height = 16,38m and period = 14s. Compared to a Stokes wave.

From figure 4.36, one can see that the Stokes wave and the simulated wave produces almost the same horizontal particle velocity above mean surface level, which is the most important area. At a deeper depth, there are a deferens where Stokes wave have a larger value than the simulated waves. This may give a small reduction for the second order process when calculating the forces but not that critical. To confirm the results two more simulations have been preformed. One with a lower crest height and one closer to the $C_{0.01}$ crest height and mean period. Result for those can be seen in figure 4.37 to 4.40.

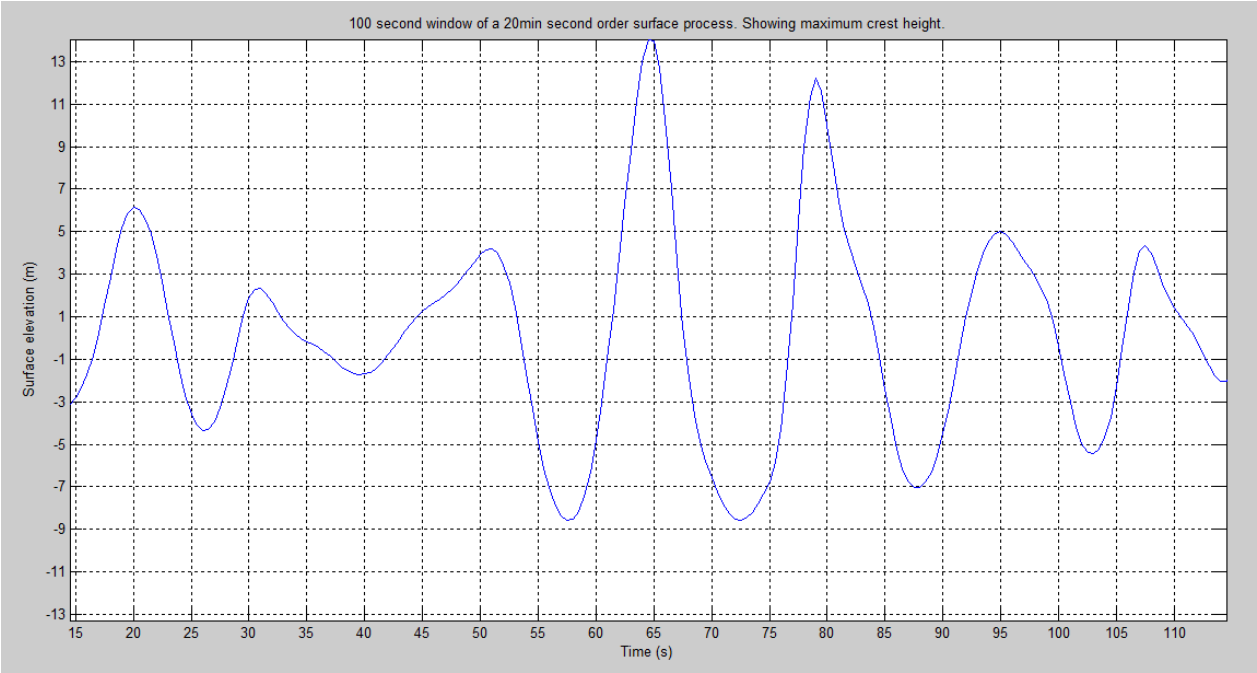

Figure 4.37. 100-second window of a 20-minutes second order surface process. Where h_s = 14,9m and t_p = 15.8s. Maximum crest height obtained is 14,05m with a period of 15s. Where the wave height is 22.65m.

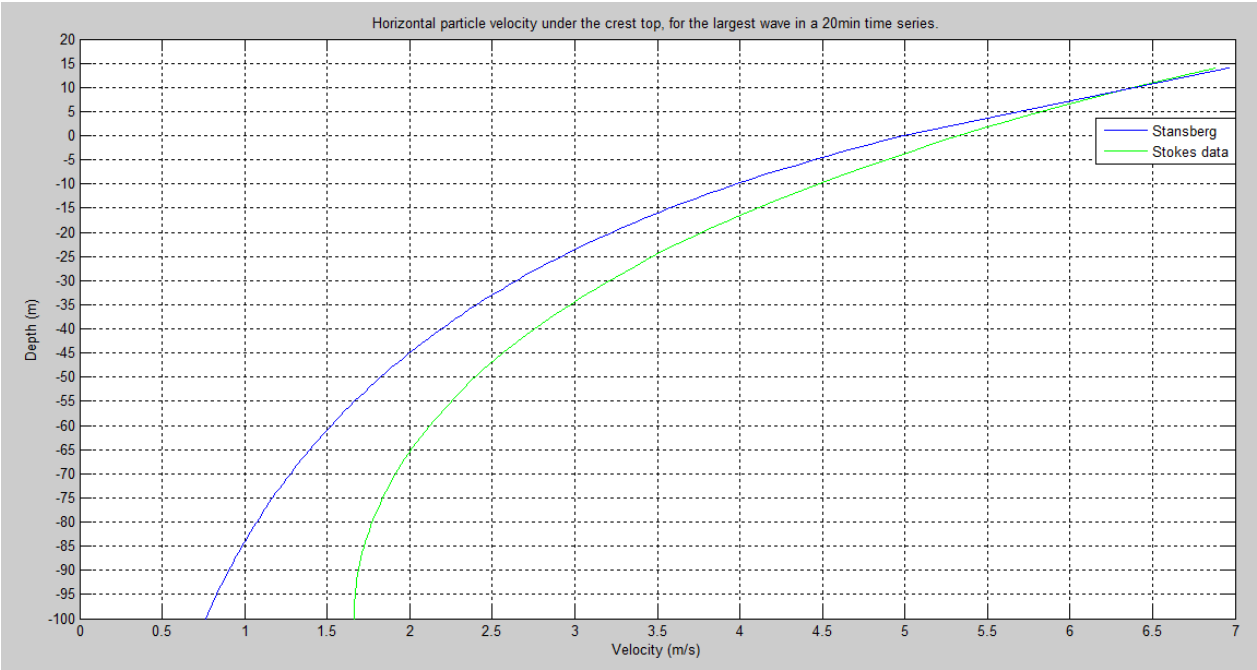

Figure 4.38. Horizontal particle velocity profile for the largest crest height in figure 4.37 time series, where crest height = 14,05m and period = 15s. Compared to a Stokes wave.

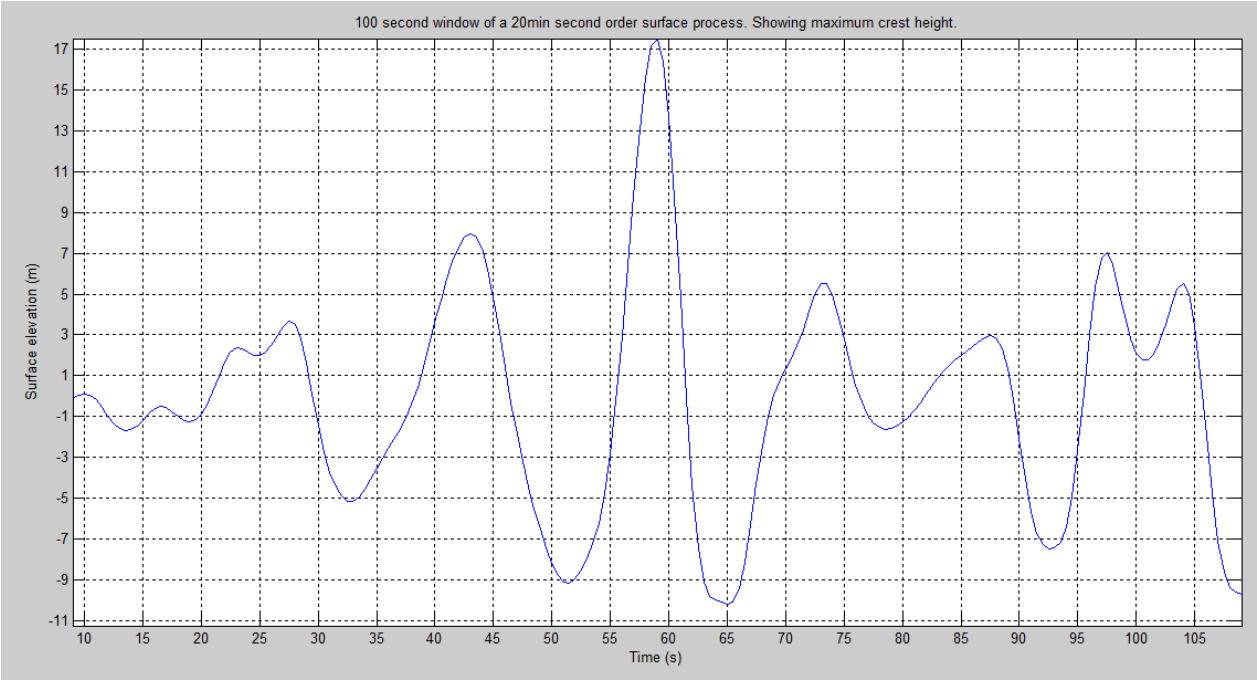

Figure 4.39. 100-second window of a 20.minutes second order surface process. Where h_s = 14,9m and t_p = 15.8s. Maximum crest height obtained is 17,52m with a period of 13,5s. Where the wave height is 27.19m.

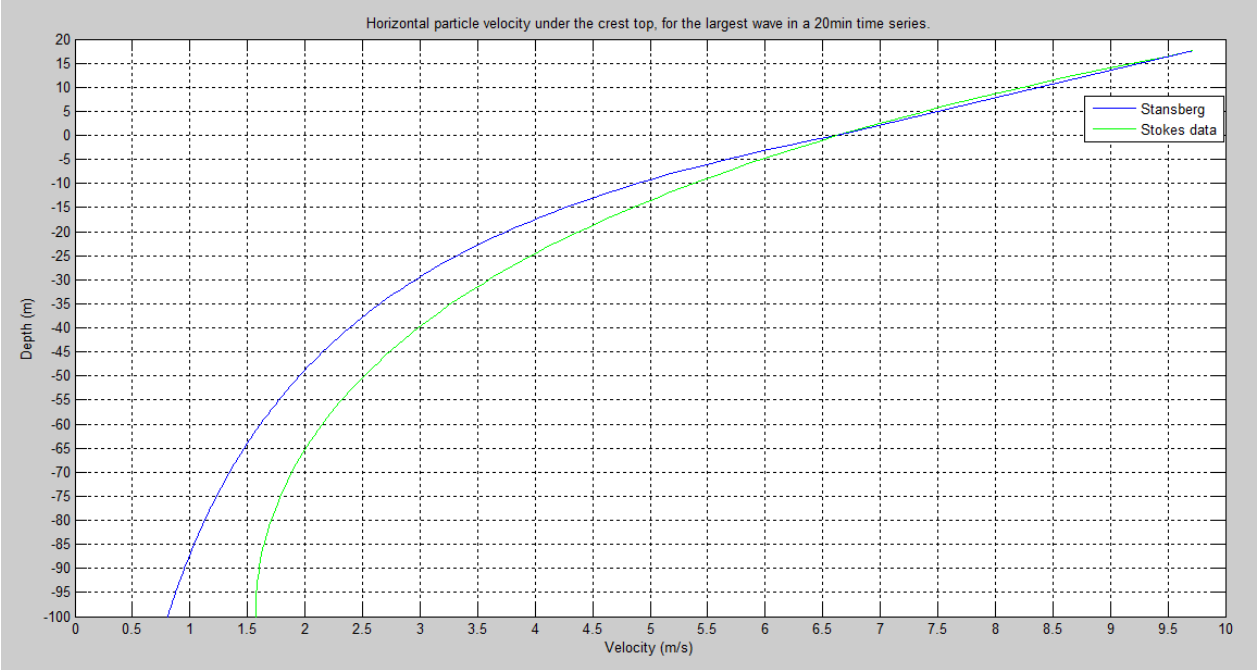

Figure 4.40. Horizontal particle velocity profile for the largest crest height in figure 4.39 time series, where crest height = 17,52m and period = 13,5s. Compared to a Stokes wave.

Figure 4.38 and 4.40 confirm that the Stokes wave produces almost the same horizontal particle velocity above mean surface level, and a higher value below mean surface level compared to the simulated maximum wave. To understand the deferens more, one would need to calculate the forces for all the horizontal particle velocity profiles.

4.2.4 Verification of second order horizontal particle velocity program

There will not be any comparison between Excel and Matlab files for a second order process. This is too time consuming and have therefore chosen to neglect this part. Another option is to obtain the results from another article, but one would also need to obtain the phase angles used and this may not be possible to find. Instead, we have chosen to obtain the results from this article, [21], which has compared their second order process to a Stokes 5th order wave. By assuming that our Stokes 5th order program generate the same wave data as their Stokes 5th order wave, one can compare the results from both articles to see if the second order process and Stokes 5th order wave interact in the same manner. The imported figures from, [21] can be seen in figure 4.41-44.

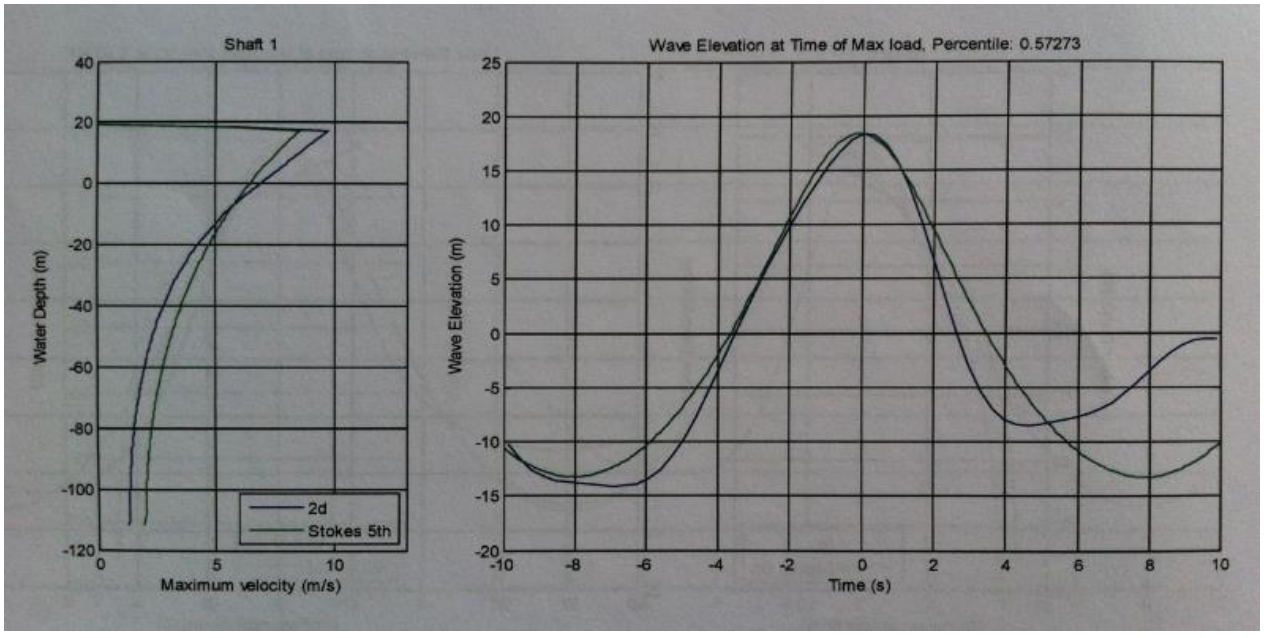

Figure 4.41. Example 1, comparison between second order process and Stokes 5th order process. Obtained from, [21].

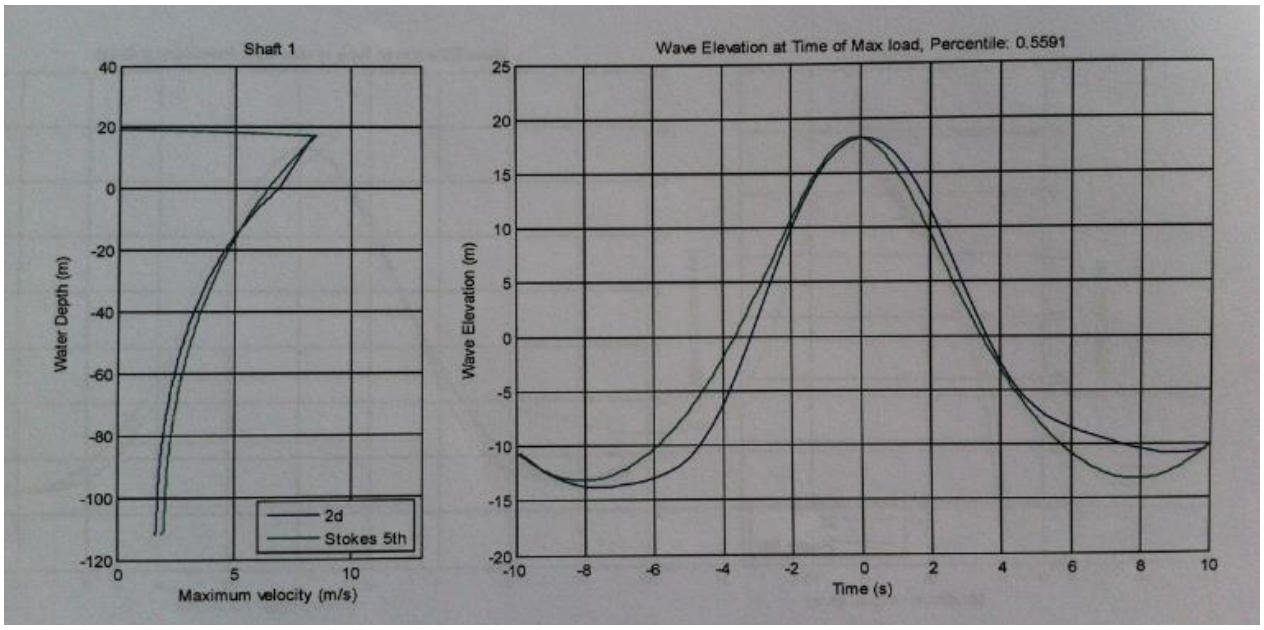

Figure 4.42. Example 2, comparison between second order process and Stokes 5th order process. Obtained from, [21].

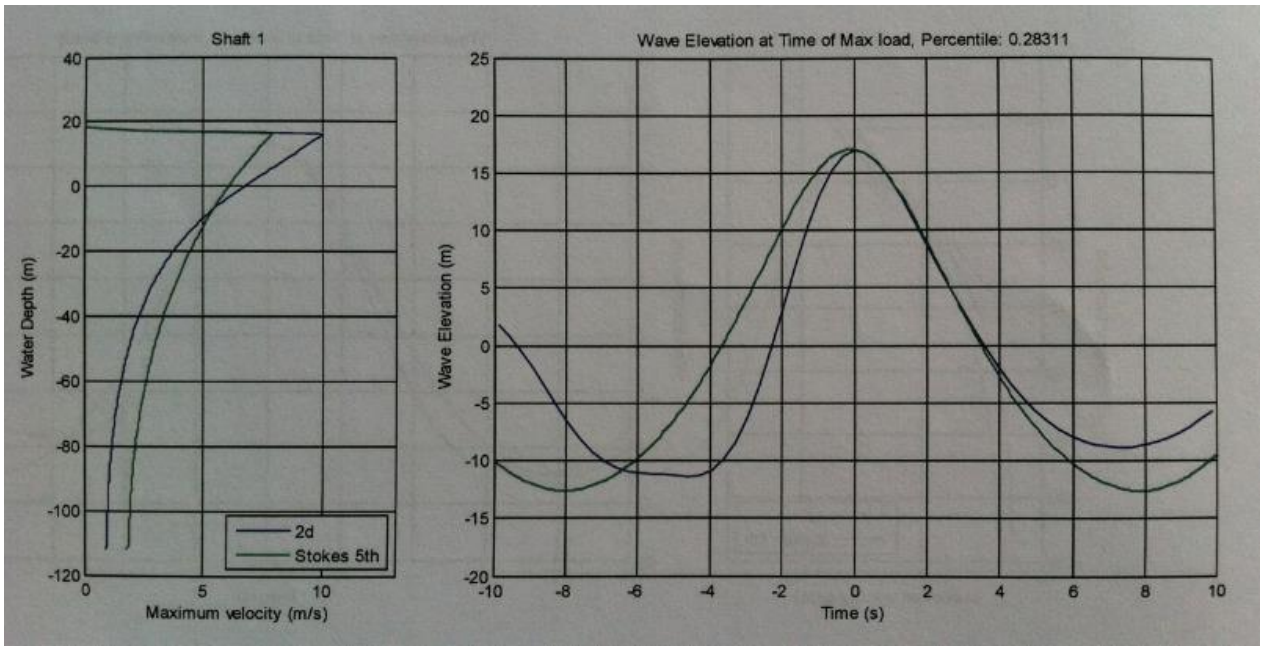

Figure 4.43. Example 3, comparison between second order process and Stokes 5th order process. Obtained from, [21].

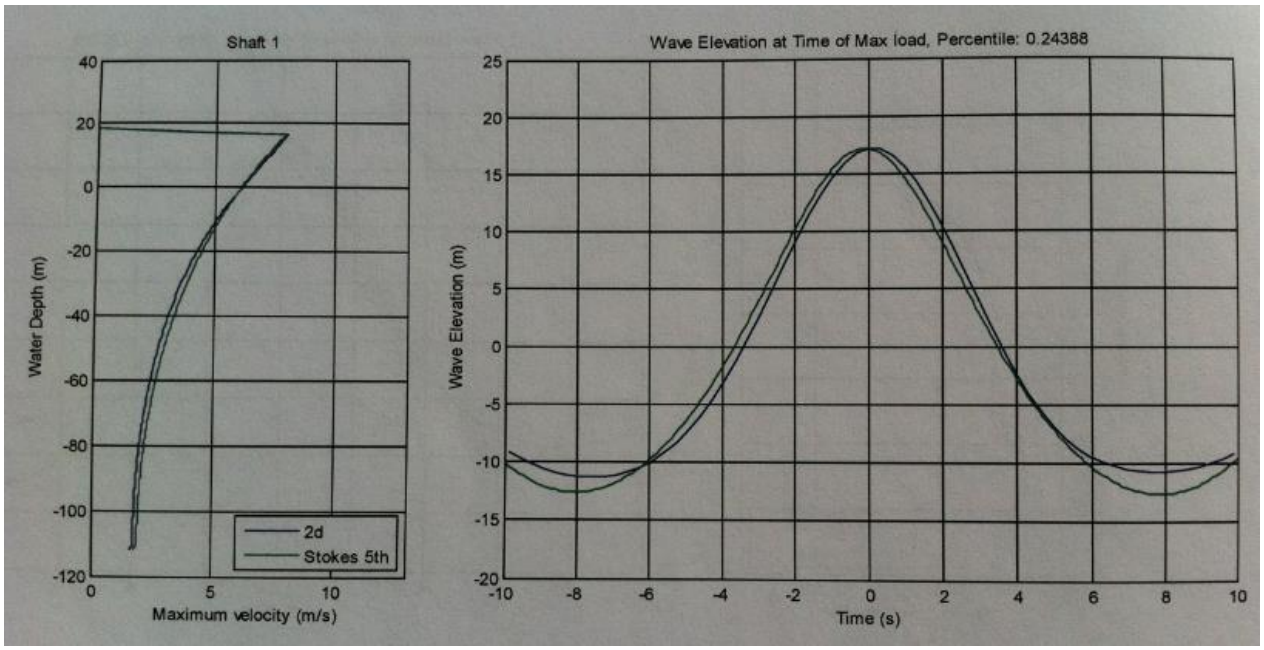

Figure 4.44. Example 4, comparison between second order process and Stokes 5th order process. Obtained from, [21].

By comparing figure 4.41-44 with our data in figure 4.36, 4.38 and 4.40, one can see that the horizontal particle velocity profile for the second order process interacts with Stokes waves in the same manner for all figures. Where a higher horizontal particle velocity is obtained from a Stokes wave below mean surface level compared to a second order wave. Meaning that the second order process has a higher horizontal particle velocity above mean surface level compared to a Stokes wave. This is of course in different magnitudes for each wave. The position of the change in the largest horizontal particle velocity between the second order process and Stokes wave, also changes around mean surface level for each wave. This implies that our second order process runs in an acceptable manner. For more comparison figures, one can see, [21].

4.2.5 Drag dominating forces for second order simulated maximum crest height, compared to Stokes waves.

As mentioned before, one can use Morison equation to estimate the base shear and overturning moment for a drag dominated case. Where a column diameter as D = 1m has been used. Morison equation was introduced in chapter 3.5.1 and mentioned again in chapter 4.1.8. See those chapters for more information about the formula used to calculate the loads and loads effects shown in table 4.2.

Table 4.2. Load results for column diameter 1m, drag dominating forces. Where 1MN = 10^3 kN = 10^6 N. X^o for stokes data instead of time for linear data. Crest top is the x-position when 0^o, mean surface level is approximately 80^o and through is 180^o. Max value obtained at crest top with a second order process.

	Forces on simplified offshore structures according to different wave models where: D=1m (Drag dominating force). Second order irregular waves.						
Case name	Period, T.(s)	Wave height, h.(m)	Amplitude, a.(m)	Height over surface, ξ.(m)	Wave phase (s or ^{o})	Force, F.(MN)	Moment, M.(MNm)
Stansberg	15	22.65	14.05	14.05	64.5s	0.498	43.55
Stokes data	15	24.55	14.05	14.05	0^o	0.650	52.42
Stansberg	14	26.67	16.38	16.38	491s	0.751	68.90
Stokes data	14	27.89	16.38	16.38	0^o	0.881	75.63
Stansberg	13.5	27.19	17.52	17.52	59s	0.859	80.43
Stokes data	13.5	29.41	17.52	17.52	0^o	1.01	89.07

Our results from table 4.2, show that the differences on the Stokes wave and Standsbergs second order approach is small, but Standsbergs approach obtain smaller values than a 5^{th} order Stokes waves. From table 4.2, one can see that the irregular surface process produces smaller wave heights than the Stokes regular waves when they have the same crest height. This might of course change for different phase angles, but it is real for those three cases. To confirm this, more simulations have to be performed. This will not be done in this thesis, instead we are going to compare the first and second order simulation and see the differences obtained with the same phase angle. Bear in mind that the second order process has a cut-off frequency. Meaning that the wave spectrum from 0 to 0.18 Hz has only been used in the second order process. The second order correction is used to obtain the same magnitude of the full wave spectrum as the first order process uses. In the first order process, we will use the wave spectrum from 0 to 0.8 meaning that, one would only have the same phase angle from 0 to 0.18 and from 0.18 to 0.8 it would be random for each simulation. This may case some differences in the result, but the largest values comes from the wave spectrum area 0 to 0.18 and therefore it would be a good approximation to understand the differences of first and second order process. This has been performed in chapter 4.3.

4.3 Comparison between a 20-minutes simulated first and second order process.

The same sea state as figure 4.39 has been used to simulate the comparison below. Where the first order process may have different values for each simulation because of the high frequency waves. The differences are not large and therefore it is still a good comparison. First of all, a comparison of the surface process and the distribution of peak values can be found in figure 4.45 and 4.46.

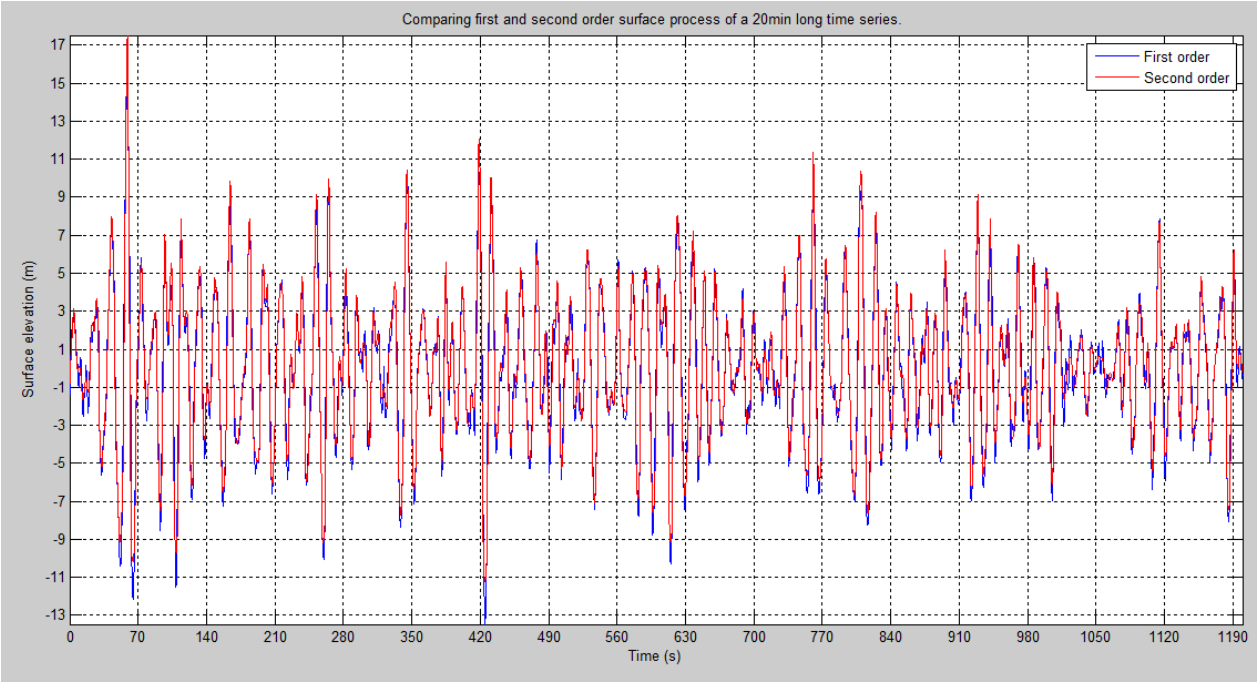

Figure 4.45. 20-minutes first and second order surface process, created from a JONSWAP spectrum. Where h_s = 14.9m and t_p = 15.8s.

By comparing the surface process in figure 4.45, one can clearly see that a second order process produces higher crest heights, but lower trough than a first order surface process. This is as expected since a higher order process take this in to account as discussed in regular waves. By knowing this, one can expect higher global peaks from the second order process than the first order process with same cumulative probabilities. This can be seen in figure 4.46, which confirm that the first order follows a Rayleigh distribution and produces lower crest height than a second order process, which follows a Weibull distribution. For a better view of the surface process, a 200-second window is shown in figure 4.47. In this figure, a straighter line can be seen for the second order process where the first order process has more noise.

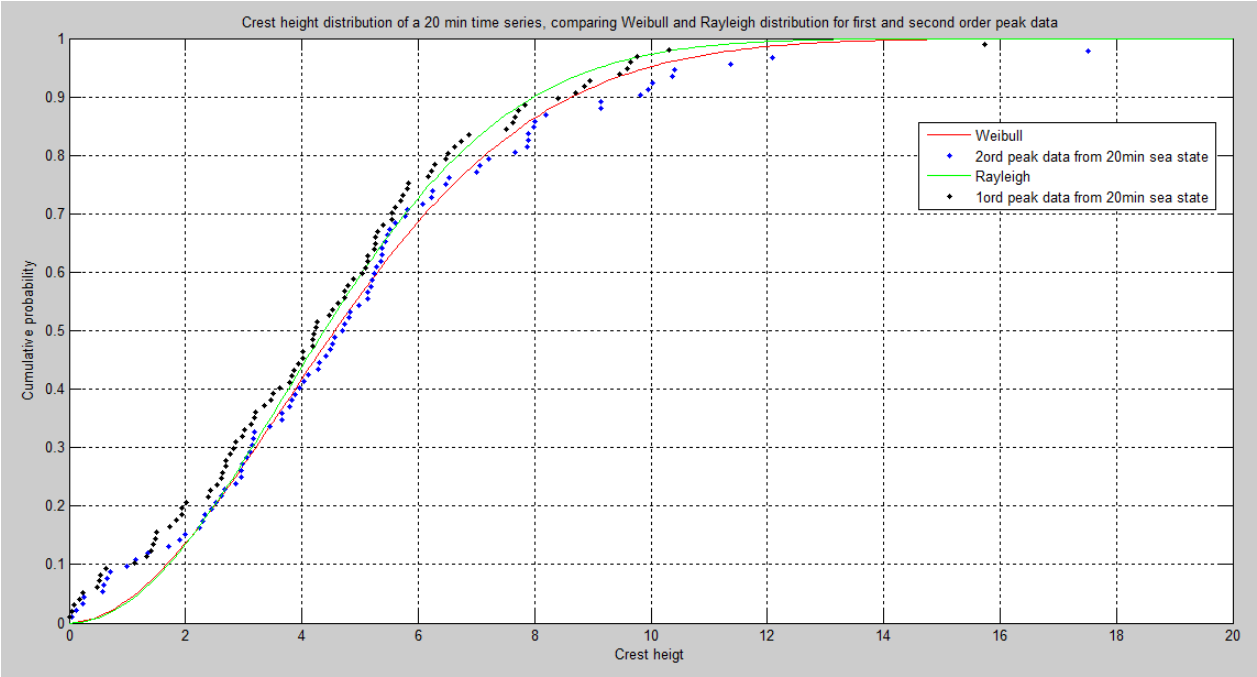

Figure 4.46. Global maxima from a first and second order surface process versus a Weibull and Rayleigh distribution.

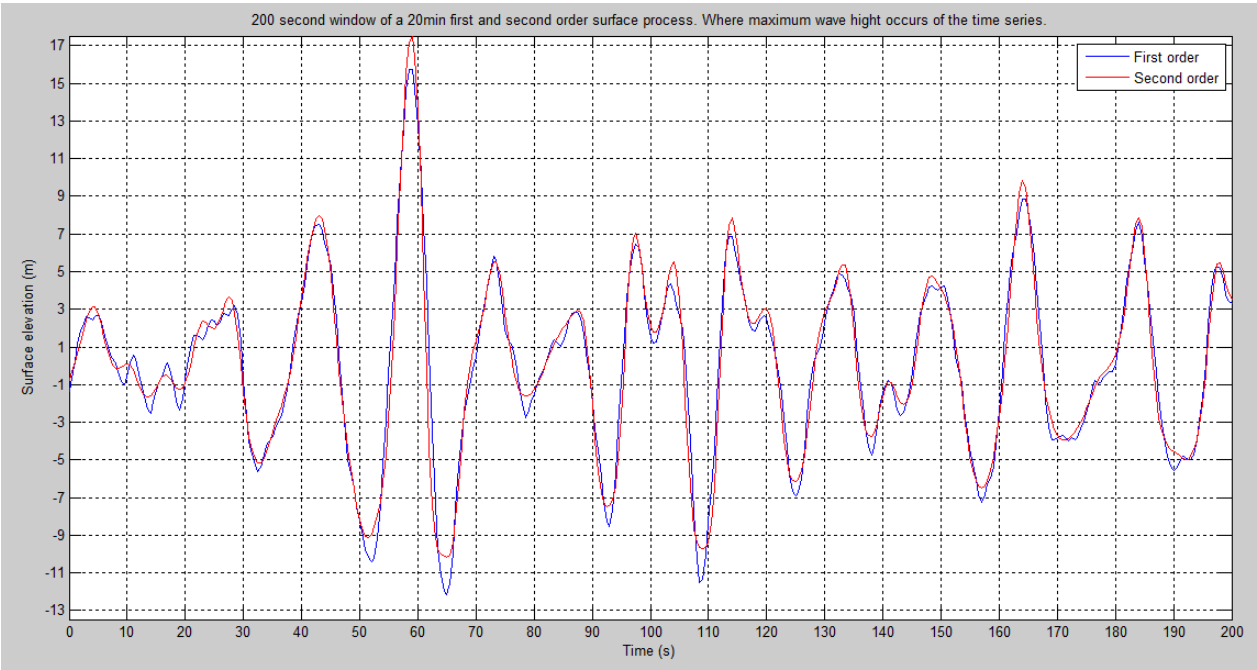

Figure 4.47. 200-second window of a 20-minutes first and second order surface process. Where h_s = 14,9m and t_p = 15.8s. Maximum crest height obtained 17,52m with a period of 13,5s.

The last part is to compare the horizontal particle velocity, which can be found in figure 4.48. In regular waves, we found out that a linear approach overestimate the kinematics by using the same crest height as to the higher order wave. In that situation a best fit was the Wheeler stretching. Here in irregular waves the first order crest height is almost 2 meters smaller than the second order crest height, and Stokes wave that have been tuned up to the same crest height as the second order wave. Result of this is a good fit for a first and second order approach to the Stokes wave. Where wheeler stretching might be giving to low values compared to the rest.

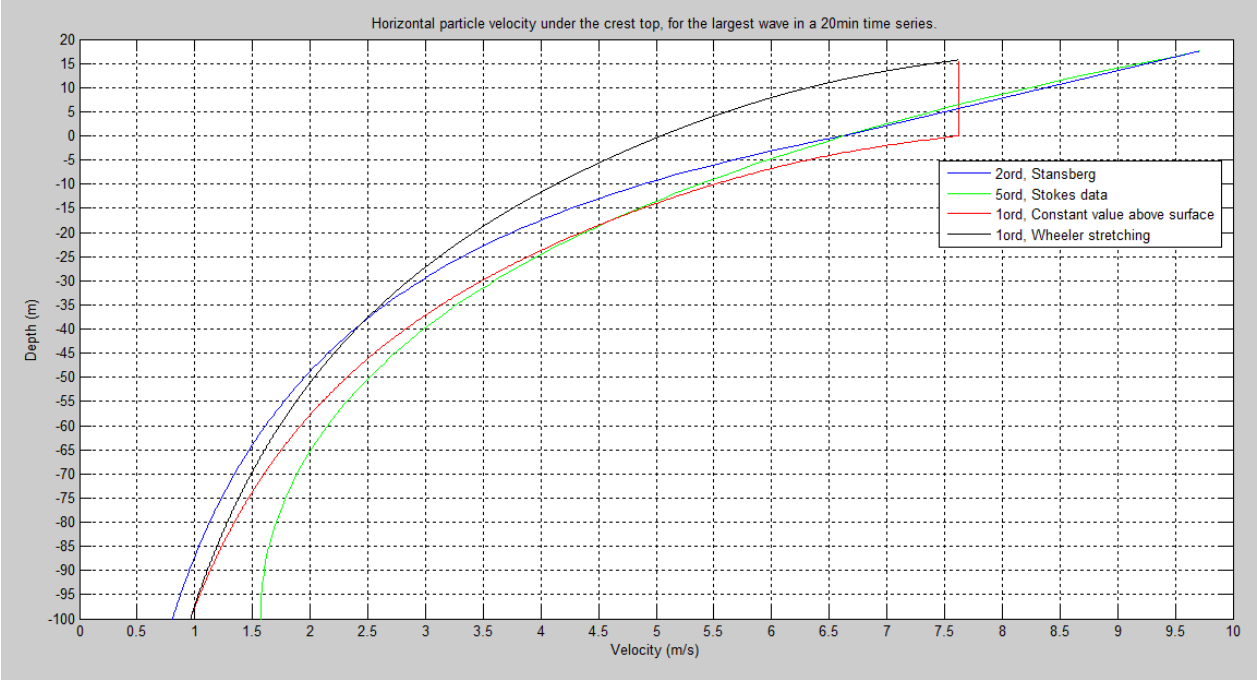

Figure 4.48. Horizontal particle velocity profile for the largest crest height in figure 4.47 time series, where crest height = 17,52m and period = 13,5 for second and fifth order. First order has a crest height = 15.74m and period = 13s.

To confirm that this isn't a rare case, a second comparison have been created. Where, we are looking at the same simulation history as figure 4.31. Compared it with the same method as above. Result of this is shown in figure 4.49 and 4.50.

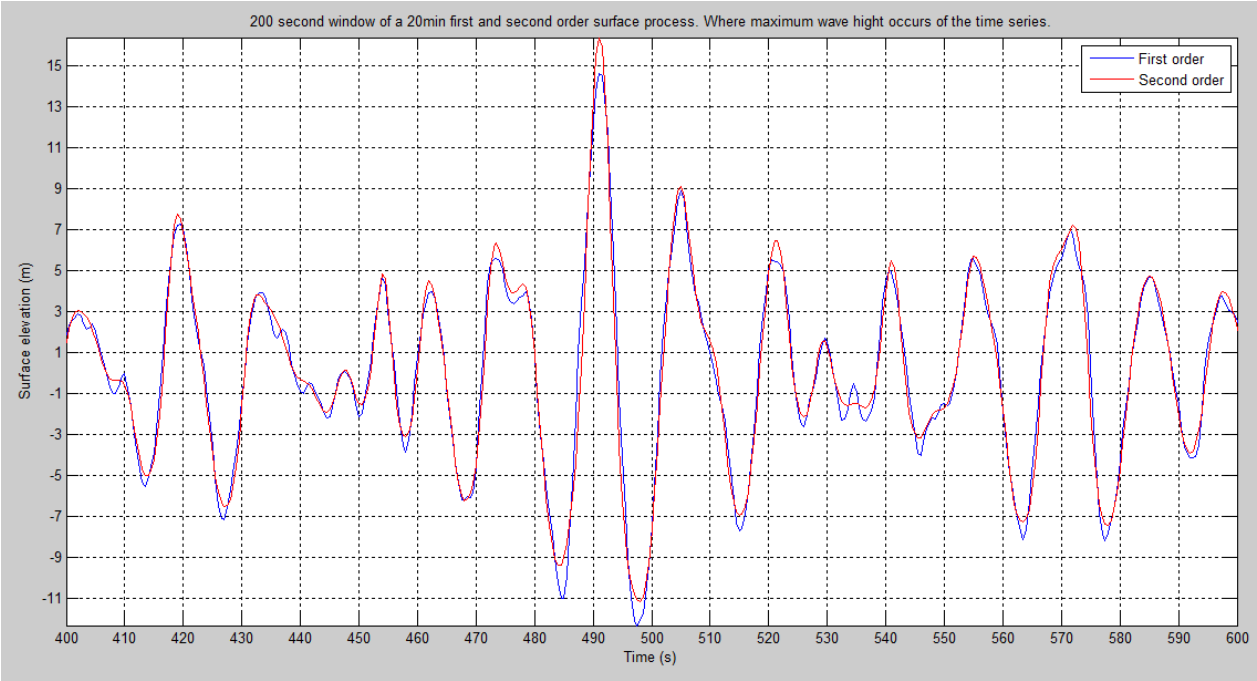

Figure 4.49. 200-second window of a 20-minutes first and second order surface process. Where h_s = 14,9m and t_p = 15.8s. Maximum crest height obtained is 14,05m with a period of 15s.

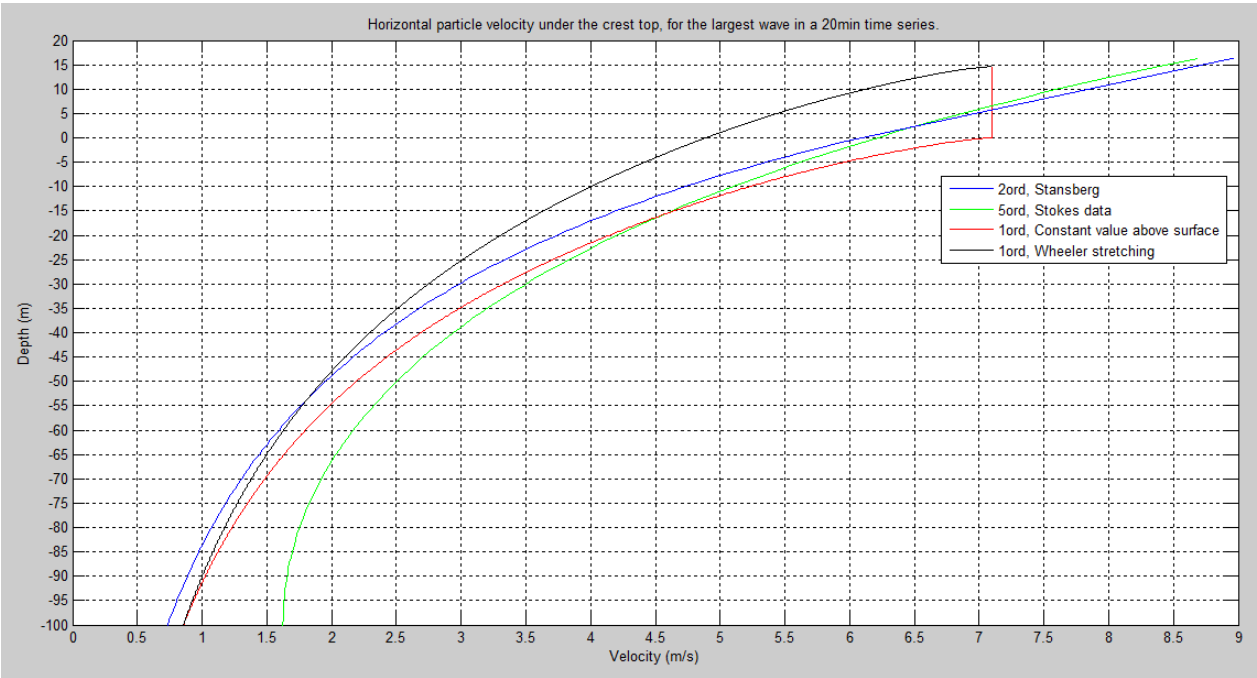

Figure 4.50. Horizontal particle velocity profile for the largest crest height in figure 4.49 time series, where crest height = 14,05m and period = 15s for second and fifth order. First order has a crest height = 14.64m and period = 13s.

Figure 4.49 shows the same results as obtained in figure 4.47. Where a second order process has higher crest and lower trough with a smoother line than a first order surface process. Horizontal particle velocity in this case can be observed in figure 4.50 and has a very similar result as figure 4.48. Where the linear and second order are a good comparison to a Stokes 5th order wave except for Wheeler stretching.

For a better comparison the base shear and overturning moment has been obtained for those two cases for each horizontal particle velocity model. Those forces is drag dominating forces since the column diameter is 1m. For calculating the loads and loads effects, Morison equation has been used. Results of this can be seen in table 4.3.

Table 4.3. Load results for column diameter 1m, drag dominating forces. Where 1MN = 10^3 kN = 10^6 N. X^o for stokes data instead of time for linear and second order data. Crest top is the x-position when 0^o, mean surface level is approximately 80^o and through is 180^o. Max value obtained at crest top.

	Forces on simplified offshore structures according to different wave models where: D=1m (Drag dominating force). Comparison of irregular waves.						
Case name	Period, T.(s)	Wave height, h.(m)	Amplitude, a.(m)	Height over surface, ξ.(m)	Wave phase (s or ^{o})	Force, F.(MN)	Moment, M.(MNm)
Stansberg	13.5	27.19	17.52	17.52	59s	0.859	80.43
Stokes data	13.5	29.41	17.52	17.52	0^o	1.01	89.07
Wheeler Stretching	13	27.03	15.74	15.74	58.5s	0.654	48.96
Constant above surface	13	27.03	15.74	15.74	58.5s	0.918	81.34
Stansberg	14	26.67	16.38	16.38	491s	0.751	68.90
Stokes data	14	27.89	16.38	16.38	0^o	0.881	75.63
Wheeler Stretching	13	26.33	14.64	14.64	491s	0.505	43.51
Constant above surface	13	26.33	14.64	14.64	491s	0.792	69.62

Table 4.3 shows that a Stokes wave still generates the most base shear and overturning moments. Where Wheeler stretching is way off. For the second order Stansberg approach and the linear constant value above mean surface level a very interesting result is shown. Bout those approaches gives very similar results for the same phase angle value, but still the high frequency waves might change this for rare cases. This just confirm that the linear process produces lower crest heights but overestimates the kinematics and end up very close to a second order approach this way. But of course in some cases this might deviate from the second order results. Another observation can be seen in the wave heights and periods, where the period and wave height is smaller for a linear approach than a second order approach. This might repeat itself but to confirm this more comparison would be needed. As discussed in regular waves, a wave with lower period creates larger velocity at surface and therefore higher forces. This may also be the reason for a linear process obtain almost the same values as a second order process.

4.4 Summary for irregular Waves

In irregular waves, one have chosen to use a JONSWAP spectrum, because it is similar to the North Sea. By this spectrum, a first and second order process has been generated in Matlab. Those processes can simulate a 3-hour or a 20-minutes sea state for the first order process and a 20-minuts sea state for the second order process.

The first order process has been verified by Excel to run in a correct manner. Even with out the random amplitude, which where neglected in this thesis. First order process still generates a random sea state with the random phase value. The reason for neglecting a random amplitude where because of the large set of components. By obtaining the peak values (crest heights) from the first order surface process created in Matlab, we confirmed that the distribution of the peaks follows a Rayleigh distribution, which is a distribution for first order approach. After words, the extreme crest height distribution where obtained and confirmed to follow a Rayleigh distribution as well. With those data, bootstrapping where preformed to find the interval of the crest height corresponding to an 10^{-2} annual probability. The interval for the, $c_{0.01}$, crest height is between 15,2m to 17,4m. Next step taken for the first order process where to compare the loads and loads effects results with Stokes waves. By doing this, one found out that a constant value above surface approach obtains the most base shear and overturning moment. Where Wheeler stretching obtains very low values compared to the Stokes and linear constant value above surface approach.

The second order process has not been verified by Excel but has been compared to another article and shown good comparison for this. One have also compared the crest height data (peak data) from a 20-minutes simulation to a Weibull distribution, which is a distribution for second order waves. This has confirmed that our second order process follows the Weibull distribution. To obtain the kinematics above mean surface level Standsbergs method was used. The loads and load effects obtained from this approach compared to a Stokes wave can be seen in table 4.2. The differences on the Stokes wave and Standsbergs second order approach is small, but Standsbergs approach obtain a little smaller base shear and overturning moment than a 5^{th} order Stokes waves.

An extreme crest height distribution where not obtained for the second order process, because a 3-hour sea state was not created. Instead a comparison between a first and second order process where done with a 20-minutes simulations by using the same wave spectrum from 0 to 0.18 Hz . This comparison shows that a Stokes wave still generates the most base shear and overturning moments. Where Wheeler stretching is way off. For the second order Stansbergs approach and the linear constant value above mean surface level a very similar results can be obtained by using the same phase angle for wave spectrum 0 to 0.18 Hz. The second order process also generates higher crest heights and lower trough than a first order process.

5 Conclusion and suggestion for further work

Throughout this thesis, a comparison between the old and new NORSOK N-003 standard has been performed. Where this thesis have been divided in to two main parts. The first part revolves around regular waves, where a comparison between the old and new methods of calculating the ULS design wave have been discussed. The old method uses a Stokes wave profile defined by the 10^{-2} annual probability wave height, $h_{0.01}$, where the new method uses the 10^{-2} annual probability crest height, $c_{0.01}$ to define the ULS design wave. With the same defined wave profile as the new and old recommendation, one have also compared the Stokes wave with a first order approach.

The main conclusions for part one are as following:

- Having half the wave height as the amplitude for a linear approach, one would need to use extrapolation above mean surface level to obtain the most accurate kinematics compared to a Stokes wave. If the crest height were used as the amplitude instead, one would have to use wheeler stretching to obtain an accurate kinematics value.
- Finding the unfavorable period associated with a wave height equal to, $h_{0.01}$ cannot be obtained before the loads effects are calculated for all periods used. It is therefore a time consuming method with possibility's to choose wrong period.
- The new method using Stokes wave with $c_{0.01}$ as the amplitude results in a little larger base share and overturning moments for all cases except for a mass dominated case, which obtains a little larger overturning moment by using $h_{0.01}$as the wave height and T_{min} as period.
- The final conclusion for regular waves is therefore that the new N-003 standard is more efficient with time and describe the waves in a more accurate manner.

For the second part of this thesis, one have disgusted irregular wave, where the old N-003 standard suggests a first order process to find the corresponding kinematics of a time simulation. Where the new N-003 standard in other hand require a second order process to describe the surface process and a second order theory to obtain the kinematics of the time history. By comparing those two methods, one have reaching the following main conclusions for part two:

- The formula used to create the first order irregular surface process follows a Rayleigh distribution for crest heights and the second order surface process follows a Weibull distribution for crest heights.
- A second order surface process describes the wave history more like a real ocean by increasing the crest height and lower the trough height.

- Wheeler stretching for a first order process underestimates the kinematics, but a constant value above mean surface level is a very good approximation to a second order process using Standsbergs approached.
- First order process underestimates the crest heights but overestimates the kinematics, which achieves almost the same result as second order process.
- The second order process is more reliable than a first order process, because it simulates a sea state closer to a real ocean, but it is more time consuming.
- Second order process with Standsbergs approach is manageable to do for command people and does not require advanced programs to run, but a certain knowledge in programming is required to achieve a 3-hour second order simulation.

Final conclusion for irregular waves is therefore that the new N-003 standard has the most reliable approach to estimate the sea state, but a first order approach may actually be sufficient enough and more time efficient. More comparison between a first and second order process would be required to understand this fully.

We would therefore suggest the following for further work:

- Optimize the program used to simulate the irregular second order process to run a 3-hour simulation.
- Find the extreme crest height distribution and confirm if it follows a Weibull distribution. After words one can obtain the crest height with an annual probability of 10^{-2}.
- Comparison between a first and second order process, which can simulate in 3-hour. To obtain the differences between the two approaches.
- Compare the first and second order process to real measured wave data to confirm the kinematics are generated in a correct manner.
- By having more comparison of a first and second order process, one can confirm the need of a second order process or disprove it.
- For regular waves, one can suggest to investigate if extrapolation really is the best approximation with half the wave height as amplitude, and Wheeler stretching when crest height is used as amplitude.

6 References

[1] "NORSOK STANDARD N-003 (2007): Actions and action effects, Edition 2," NORSOK Standard, September 2007.

[2] "NORSOK STANDARD N-003 (2015): Actions and action effects, Edition 3," NORSOK Standard, XXX 2015.

[3] J. D. Fenton, "The steadily-progressing wave problem," 2015. [Online]. Available: http://johndfenton.com/Steady-waves/Fourier.html. [Accessed 26 February 2015].

[4] Unknown, "Metocean," Wikipedia, 2015. [Online]. Available: http://en.wikipedia.org/wiki/Metocean. [Accessed 5 February 2015].

[5] "Glossary of Coastal Engineering Terms," Ocean Engineering Research Group, 2015. [Online]. Available: http://cdip.ucsd.edu/?sub=faq&nav=documents&xitem=glossary. [Accessed 7 February 2015].

[6] K. J. Eik and E. Nygaard, "Statfjord Late Life Metocean Design Basis," *Statoil,* pp. 22-41, 22 October 2003.

[7] S. Haver, "On the prediction of extreme wave crest heights," *7th Int. Workshop on wave hindcasting and forcasting,* pp. 1-4, October 2002.

[8] *DNV-RP-C205: ENVIRONMENTAL CONDITIONS AND ENVIRONMENTAL LOADS,* Det Norske Veritas, October 2010.

[9] O. T. Gudmestad, "CHAPTER 2 LINEAR WAVE THEORY," in *Marine Technology and Operations*, University of Stavanger, 2014, pp. 27-76.

[10] V. Riazi and H. Rahmati, Writers, *Linear and Nonlinear Wave theories and applications.* [Performance]. University of Stavanger, 2014.

[11] H. E. KROGSTAD and Ø. A. ARNTSEN, "LINEAR WAVE THEORY PART A," *NORWEGIAN UNIVERSITY OF SCIENCE AND TECHNOLOGY,* pp. 5-9, 5 March February 2000.

[12] E. Bækkedal, "Alternative methods of realizing the sea spectrum for time-domain simulations of marine structures in irregular seas," *University of Science and Technology,* pp. 17-21, June 2014.

[13] J. D. Fenton, "Use of the programs FOURIER, CNOIDAL and STOKES for steady waves," 7 February 2014. [Online]. Available: http://johndfenton.com/Steady-waves/Instructions.pdf. [Accessed 5 February 2015].

[14] O. T. Gudmestad, "Chapter 4. Wave Loads," in *Marine Technology and Operations*, University of Stavanger, 2014, pp. 85-125.

[15] Unknown, "Morison equation," Wikipedia, 2015. [Online]. Available: http://en.wikipedia.org/wiki/Morison_equation. [Accessed 15 March 2015].

[16] J. Zhang, "Chapter VII Wave Statistics & Wave Spectra," [Online]. Available: https://ceprofs.civil.tamu.edu/jzhang/oe671class/statistics-Spectrum.pdf. [Accessed 3 April 2015].

[17] S. Haver, "Description of Metocean Characteristics for Planning of Marine Operations," University of Stavanger, Stavanger, November 2014.

[18] S. Haver, "Prediction of Characteristic Response for Design Purposes Rev 5," Statoil, February 2013.

[19] S. Haver, Writer, *Bootstrapping – an example.* [Performance]. Statoil, 2012.

[20] Ø. Lande, Writer, *Second order Wave Kinematics: Comparative Studies..* [Performance]. Det Norske Veritas AS, April 8th, 2013.

[21] Ø. Lande, "Assessment of second order wave kinematics," Det Norske Veritas, Rev 0, May 30, 2013.

[22] C. T. Stansberg, O. T. Gudmestad and S. K. Haver, "Kinematics Under Extreme Waves," May, 2008.

Appendix A. Attached Matlab and Excel files

All Matlab and Excel files created for this thesis, has been stored in different folders and named for their purposes. Below is a collection of files where "•" stands for folder and "-" for files. To see the deferens of a Matlab file or Excel file a code can be seen at the end of the file name. For Excel files, the end name is ".xlsx". A Matlab file has two different end names, where Matlab scripts has ".m" and saved Matlab data (workspace data) has ".mat".

- 1. Metocean contour method
  - Extreme_WaveHeight_and_CrestHeight.m
  - Worst_Hs_Tp_along_the_contour_line.m

- 2. Horizontal particle velocity and acceleration for regular waves
  - Acceleration_data_Stokes.mat
  - All_Stokes_data_Sp_Vel_Acc.mat
  - Comparison_between_linear_and_Stokes.m
  - Linear_surface_Profile.m
  - Linear_wave_Intermediate_Crest_height.m
  - Linear_wave_Intermediate_Wave_height.m
  - Stokes_5th_wave_data_plots.m
  - Surface_Profile_data_Stokes.mat
  - Velocity_data_Stokes.mat

- 2-3. Stokes data for regular waves
  Containing many Stokes data files for different cases, which has been transformed to .mat files under 2. and 3.. For those phase data used in this thesis.

- 3. Loads and load effects for regular waves
  - Acceleration for stokes 5th order1.xlsx
  - All_load_data_where_D_1m.m
  - All_load_data_where_D_5m.m
  - All_load_data_where_D_20m.m
  - Velocity and Acceleration for stokes 5th order1.xlsx
  - Velocity for stokes 5th order1.xlsx
  - Wave_Loads_Stokes_D_1m.m
  - Wave_Loads_Stokes_D_5m.m
  - Wave_Loads_Stokes_D_20m.m

- 4. Kinematics, loads and load effects for linear irregular waves
  - Different phases for linear surface process.xlsx
  - Highest amplitude of a 3 hr sea state.xlsx
  - Linear_Bootstraping_and_more.m
  - Linear_Kinametics.m
  - Linear_wave_spectrum.m
  - Velocity for stokes 5th.xlsx
  - Verification of Matlab program Excel file.xlsx
  - Verification_of_Matlab_program_linear_Matlab_file.m

- 5. Kinematics, loads and load effects for second order irregular waves
  - 100 genereted second order simulations.xlsx
  - Comparison data between second and first order.xlsx
  - Comparison_of_surface_process.m
  - Different phases for second order surface process.xlsx
  - Secund_order_kinametics.m
  - Secund_order_wave_spectrum.m
  - Velocity for stokes 5th second order.xlsx

Stokes 5^{th} order program used can be found in:

- Stoke 5th order Program
  - Fourier Program.zip
  - Stokes Program.zip